AN ABSTRACT OF THE THESIS OF

KENNETH DWIGHT DOBBIN for the degree of MASTER OF SCIENCE
(Name of Student) (Degree)

in Nuclear Engineering presented on July 18, 1974
(Major Dept.) (Date)

Title: CONSTRUCTION AND CALIBRATION OF A FAST NEUTRON SPECTRUM GENERATOR

Redacted for privacy

Abstract approved by: _____
Dr. B. I. Spinrad

A standard fast reactor spectrum can be created by the partial moderation of the U-235 fission spectrum in an air cavity. Spherical natural uranium shells are driven by thermal neutrons from a thermal column. The uranium is placed at the center of a spherical graphite hohlraum to reduce the anisotropic effect of a planar source of thermal neutrons.

The Oregon State University (OSU) fast neutron spectrum facility design employs this method which is being used by Albert Fabry in Mol, Belgium and the NISUS assembly in London, United Kingdom, to create a fast neutron spectrum. The OSU facility uses the thermalizing column of a TRIGA Mark II reactor for a thermal neutron source. The mechanical design is presented showing the location of the facility, the aluminum container and internals, and the transport assembly. Two computer codes are introduced in the nuclear design.

SLAB is a first approximation diffusion theory code which justifies the use of one foot of graphite backed with water in place of "infinite graphite." FASTSPEC is a diffusion theory approximation code in spherical geometry which shows that the design will produce a spectrum characteristic of a fast reactor.

Phase I operation is a mechanical test, health physics evaluation, and a thermal neutron calibration of the facility with a thermal neutron absorber in place of the uranium. The data for phase I is included. Phase II operation will be the insertion of an uranium driver shell and the calibration of the fast spectrum. Only phase I is complete at this time.

Construction and Calibration of a Fast Neutron Spectrum Generator

by

Kenneth Dwight Dobbin

A THESIS

submitted to

Oregon State University

in partial fulfillment of
the requirements for the
degree of

Master of Science

Completed July 1974

Commencement June 1975

APPROVED:

Redacted for privacy

Professor of Nuclear Engineering
in charge of major

Redacted for privacy

Head of the Department of Nuclear Engineering

Redacted for privacy

Dean of Graduate School

Date thesis is presented July 18, 1974

Typed by Illa W. Atwood for Kenneth Dwight Dobbin

ACKNOWLEDGEMENTS

I wish to express my thanks to the many people who helped in the construction of the fast spectrum generator. The Gulf Oil Foundation supplied the fellowship funds to finance the construction and Dr. B. I. Spinrad and Dr. C. Wang supplied the graphite blocks for the assembly and additional funds for cost overruns. Dr. B. I. Spinrad and Dr. S. Binney guided the project and gave advice on the facility design and experimental apparatus. Helpful design suggestions were contributed from Dr. Albert Fabry's experience with the $\Sigma\Sigma$ facility in Mol, Belgium.

My dad, Vincent Dobbin, added suggestions on the mechanical design of the aluminum box and welded part of the transport rigging when certain steel components could not be obtained. Professor D. Bucy contributed hints on modeling the structural calculations. Kelley Cox assisted the machining of the graphite blocks and Mike Shay helped transport them after irradiation.

I wish to thank the Radiation Center Health Physicist, Art Johnson, and the reactor operations personnel, Terry Anderson, Bill Carpenter, Dick Spence, and Steve Bennett for their help conducting the experiment and for their patience during construction and graphite machining.

I also want to express a note of thanks to Nancy Petrowicz for proofreading the manuscript.

TABLE OF CONTENTS

LIST OF ILLUSTRATIONS

CONSTRUCTION AND CALIBRATION OF A FAST NEUTRON SPECTRUM GENERATOR

I. INTRODUCTION

Standard neutron fields can be very useful tools for the study of nuclear parameters. For example, the standard pile has contributed greatly to the study of thermal reactors. It is similarly desirable for the development of fast breeder reactors to develop a standard fast neutron spectrum (7).

The fast reactor designer must be able to predict the behavior of the reactor accurately (4), (17). The kinetics of a fast reactor depend upon the various core-constituent reaction rates, which depend upon the energy spectrum and vary with temperature, change of state, and core composition (17). It is hard to specify the accuracy of calculated reaction rates because of uncertainties in the microscopic cross section data, especially for inelastic scattering, fission of U-238, and capture in U-238, which are integral functions of the neutron energy spectrum. Also, most existing computer codes assume that the neutron spectrum is the same for large regions of the reactor (9).

Presently, the procedure to get a more realistic representation than theory can give is to build a critical mock-up. However, these assemblies are expensive and require thousands of kilograms of

fuel (2), (17). To decrease the cost, exponential or subcritical assemblies are used in place of the criticals. However, the subcriticals are also expensive and the exponential assemblies often suffer from serious flux gradients, anisotropies, and unwanted low energy neutrons returning to the system.

Other ways of creating a fast reactor spectrum are being used and the purpose of this work is to look at one of them. This method of creating a fast neutron spectrum which resembles that in fast reactors is the partial moderation of the U-235 fission spectrum with spherical shells of natural uranium used both as the fission source and the moderating material. The uranium is driven by thermal neutrons from a thermal column of a thermal reactor. Fissions occur primarily in the outer layer of uranium, while the inner layers partially moderate the spectrum by inelastic scattering (7). Spherical geometry is used to facilitate the calculational representation and the whole uranium assembly is placed at the center of a cavity (hohlraum) to reduce anisotropic effects associated with the planar source of thermal neutrons (6), (16).

This type of system is simple, inexpensive, and its spectrum is independent of the source provided that the source is reasonably free of fast neutrons. Therefore, any laboratory having a thermal reactor and a thermal column can create a fast spectrum (5), (10), (12). The thickness of natural uranium can be varied to change the

moderation of the fission spectrum so as to accurately simulate the spectrum of a given fast reactor, or to vary the hardness of the spectrum corresponding to different core compositions (5), (7), (10), (12). The size of the spherical assembly can be designed to be large enough to accommodate practical detectors (10), (12).

The fast spectrum produced can be useful in the development of reliable spectrum measuring techniques, the study of the safety and economic performance of a fast reactor, and it can aid in the improvement of nuclear data files. Also, a standard fast spectrum will aid the development of more accurate reactor physics codes over the life of the reactor core by studying core heterogeneity effects, flux gradients, spectrum distortions in blankets, and void and Doppler coefficients (5).

The Oregon State University (OSU) fast spectrum facility is modeled after the design of Albert Fabry in Mol, Belgium, and the NISUS (neutron intermediate spectrum uranium source) assembly in London, United Kingdom. However, the OSU design has several modifications which will enable greater experimental flexibility.

The thermalizing column of the OSU TRIGA Mark II reactor is the source of thermal neutrons. Core neutrons are thermalized as they are led through this column to the water-filled bulk irradiation tank. A water-tight aluminum box of dimensions $45\frac{1}{2}$" x $45\frac{1}{2}$" x $45\frac{1}{2}$" is lowered into the tank and centered next to the thermalizing column.

Inside the box graphite is stacked to form a cube $44\frac{1}{2}$" on an edge with a hollow air cavity in the center (see Figure 1). This cavity, called the outer cavity, is a 14-sided polyhedron created by filling each corner of the cubic cavity with graphite. If a sphere of diameter 52 cm (20.5") is inscribed inside the outer cavity, then the sphere would touch each of the sides at only one point. At the center of the cavity will be a spherical fission source assembly of natural uranium with a diameter of 24.5 cm (9.65") mounted on an aluminum stand.

The outer cavity, which to the neutrons seems like a spherical cavity (5), causes the thermal neutrons to scatter around, reducing flux gradients in the graphite, and produces more uniform fissioning in the uranium (2), (4). If the outer diameter of the uranium is 24.5 cm, then the minimum diameter of the cavity should be 50 cm (5), (14). A smaller cavity would decrease the total fission rate in the uranium and increase the number of fission neutrons reflected off the walls of the cavity (wall return component of the fast spectrum) (5), which varies more from one assembly to another than does the fission neutrons which travel directly through to the center of the uranium sphere after fissioning (direct component of the fast spectrum) (2), (4).

For good reproduction of the spectrum in various labs, the thickness of the graphite around the outer cavity should be essentially infinite, that is, at least 35 cm (13.78") of graphite (2), (4).

However, it is calculated that 30.5 cm (12") of graphite backed with water is equivalent to infinite graphite. So, one difference in the OSU design is the use of graphite backed with water.

The uranium sphere assembly is composed of a five centimeter thick shell of uranium to create the fission neutrons and degrade their energies into a characteristic fast reactor spectrum. It also serves to attenuate the gamma radiation which may affect certain spectrometers and sandwich foils used for spectral index measurements (7). Inside the uranium is a 3.5 cm thick shell of B_4C to keep out unwanted thermal neutrons and to shape the spectrum below 10 keV, where the inelastic scatter of the uranium no longer moderates the neutrons (2), (4). Inside the B_4C shell there is an air volume about 11 cm in diameter, called the inner cavity, where the fast reactor spectrum will be produced (5), (14).

An uranium thickness of five centimeters is sufficient to attenuate the gammas and create a characteristic fast reactor spectrum (2). However, since the fission is mainly in the outer 1.5 cm of the shell (2), and since it is difficult to handle an uranium shell five centimeters thick and 24.5 cm in diameter (6), the OSU design uses three shells. The outside shell is natural uranium 1.5 cm thick while the two inside shells are depleted uranium, one also 1.5 cm thick and the other 2 cm. The depleted uranium will degrade the spectrum and attenuate the gammas essentially the same as natural

uranium. The shells will be machined as hemispheres plated with nickel or chrome, and keyed together.

This geometry creates a spectrum inside the inner cavity composed of a direct component above 50 keV and a wall return component below 50 keV (2), (4), which is uniform within one to two percent in all directions over a volume four centimeters in diameter (6). The spectrum is independent of the thermal neutron source if the cadmium ratio in the outer cavity is at least 500 (6), so that there is insignificant fast neutron background from the core of the thermal reactor used as the thermal neutron source.

Easy access to this inner cavity is essential for the economic use of the fast spectrum facility (2), (4). Because it is immersed in a pool of water and is accessible from overhead, the OSU facility has the unique opportunity to use a "snorkel" assembly. An aluminum pipe coupler is welded into the top of the box which contains the facility. Above the box, an aluminum pipe extends to above the surface of the water. Inside the box, a pipe extends down through a hole drilled in the graphite to the top of the uranium sphere. There extends down through the uranium and B_4C shells a hole one centimeter in diameter to the inner cavity. Thus, samples can be lowered down through the pipe into the inner cavity from above the water level of the irradiation tank without removing the assembly. Foil samples will be hung from beneath plugs that fill the holes in the B_4C and uranium shells

in order to keep out unwanted thermal neutrons and keep the uniformity of the fission source. The pipe also allows for the possibility of extracting a beam for time of flight studies of the low energy end of the spectrum, which will be discussed later (16). Being perpendicular to the thermal column, the vertical access direction also reduces the anisotropic effects associated with the flux gradients present, possibly extending the four centimeter diameter over which the central spectrum is isotropic.

In order not to have the uranium shells fissioning when the fast spectrum assembly is not in use but the TRIGA reactor is being run, a boral shutter is placed between the aluminum box and the thermalizing column. The shutter, which is 1/8" thick, reduces the thermal flux by at least 99.9%.

There are numerous experiments which are possible on the OSU fast spectrum facility. Some of them are:

Calibration of neutron spectrometers
Spectral index measurements
Differential and integral measurements of microscopic cross sections
Spherical shell transmission experiments
Doppler effects
Microassemblies
Time-of-flight measurements (5), (7).

However, effort will be directed toward the last three groups of experiments. Determination of Doppler effects by the activation technique looks interesting since there now exists large uncertainties

in the Doppler coefficients of fast reactors (9). Obtaining sodium data by use of microassemblies would also be very useful (6), (16). Sodium's three keV resonance is of extreme importance to reactor designers since the loss of this absorption in sodium voiding causes a reactivity insertion tending to make the reactor unstable. Also, the fast spectrum below three keV is very poorly known (6). The OSU design is particularly well suited for an extraction of a beam for time-of-flight study of this low energy end of the spectrum (16).

The OSU fast spectrum facility will be operated in two phases. Phase I will be the thermal neutron calibration phase. The facility will be constructed, leak tested, and then irradiated in the bulk irradiation pool of the TRIGA reactor. The first phase irradiation uses the spherical bottom of a 5000 ml Pyrex boiling flask in place of the uranium sphere since the uranium will not arrive in time. The flask is a borosilicate glass containing about 13% boric oxide which will simulate the absorption of the uranium. The object of phase I is to map the thermal flux and determine the degree of anisotropy present around the spherical absorber.

Under phase II operation, the flask will be replaced with the uranium sphere. The fast spectrum will be established and then compared with the theoretical calculations. Only phase I operation will be handled at this time. Later work will include phase II operation plus various experiments.

II. MECHANICAL DESIGN

Location of the Facility

The OSU fast spectrum facility rests next to the thermalizing column in the bulk shielding tank of the TRIGA Mark II reactor (see Figure 1). The facility consists of a $45\frac{1}{2}$" x $45\frac{1}{2}$" x $45\frac{1}{2}$" aluminum box centered in front of the thermalizing column and sitting on top of a base support assembly. Inside the box is a liner of graphite one foot thick and a glass sphere (phase I operation) or an uranium sphere (phase II operation) located in an air cavity at the centroid of the box. A "snorkel" allows access to the air cavity from the top of the bulk shielding tank. Water in the tank completely surrounds the box.

A water space of about one inch is left between the column and the box to allow for the 5/8" aluminum column cover and bolts and for a boral curtain. The curtain isolates the box, when not in use, from the thermal neutrons coming from the core.

Boral Curtain

Calculations appearing in Appendix A show that 1/8" of boral will stop over 99.9% of the thermal neutrons emerging from the thermalizing column. Therefore, a boral curtain consisting of a sheet of boral 30" x 30" x 1/8" is suspended from a wood support

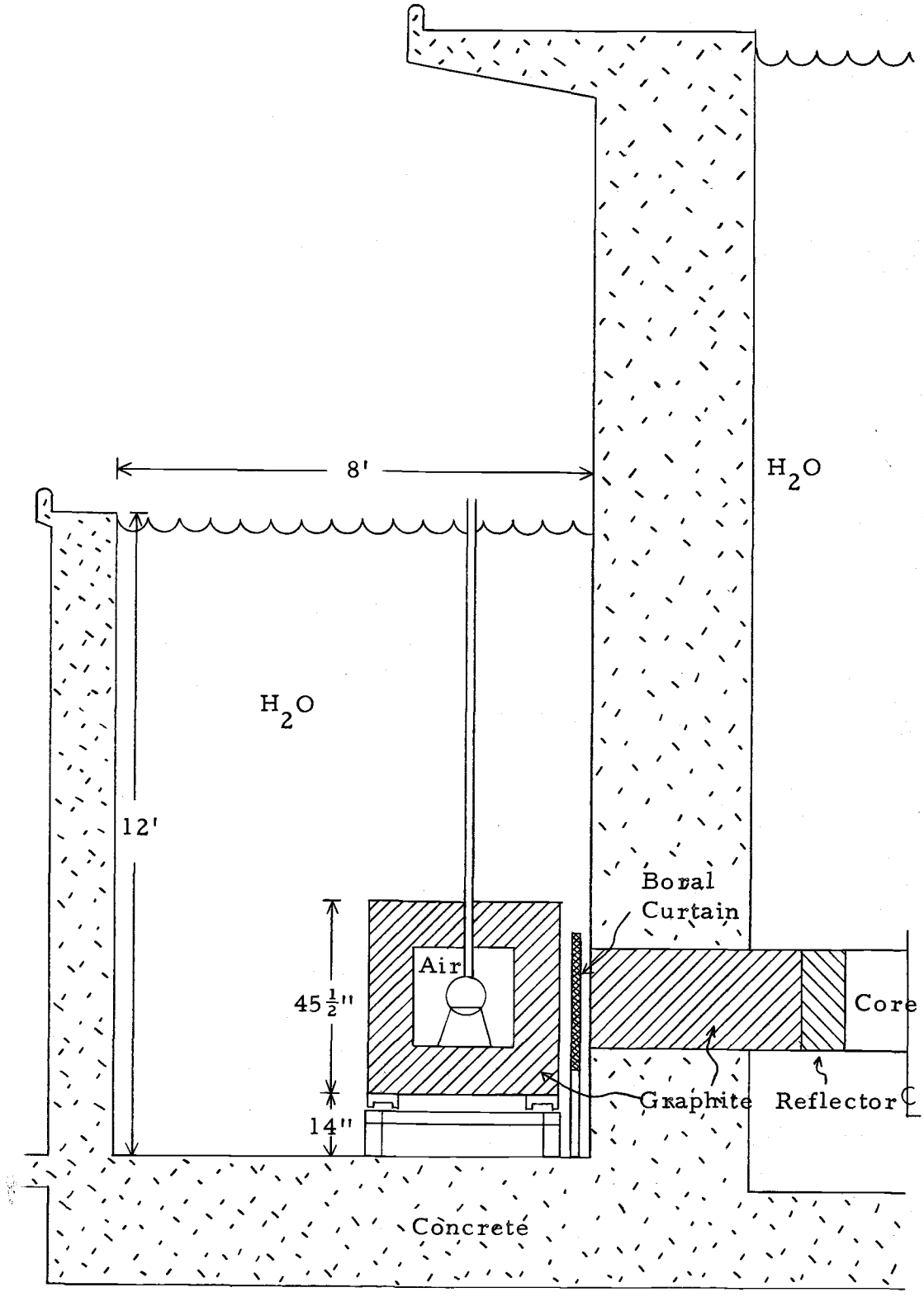

Figure 1. Location of fast spectrum facility.

assembly in the design shown in Figure 2. When the facility is not in use, the boral sheet is lowered down between the aluminum box and the thermal column. The support chains can be very light since the boral sheet has little mass. The pulleys in the support assembly will align the boral sheet in the lateral direction and the box will keep the sheet aligned fore and aft. When in the closed position, a 30" x 22" x 1/8" aluminum sheet attached to the lower edge of the boral sheet rests on the floor of the bulk shield tank and keeps the boral curtain centered in front of the thermalizing column. Upon exceeding this year's budget, the boral curtain was not built. The fast spectrum facility will be removed from the bulk shield tank after phase I operation and the curtain will be built before the first irradiation under phase II.

General Description of Box and Base

The aluminum box sits on top of a transport base fabricated from mild steel channels. The base is lifted by chains from eye bolts on the ends of the channels (see Figure 3). The chains are attached to an I-beam separator bar twelve feet above the base so that the crane hook connected to the I-beam remains out of the water of the bulk shield tank. The lift is from the base only to prevent strain on the welds of the aluminum box which could cause possible leaks.

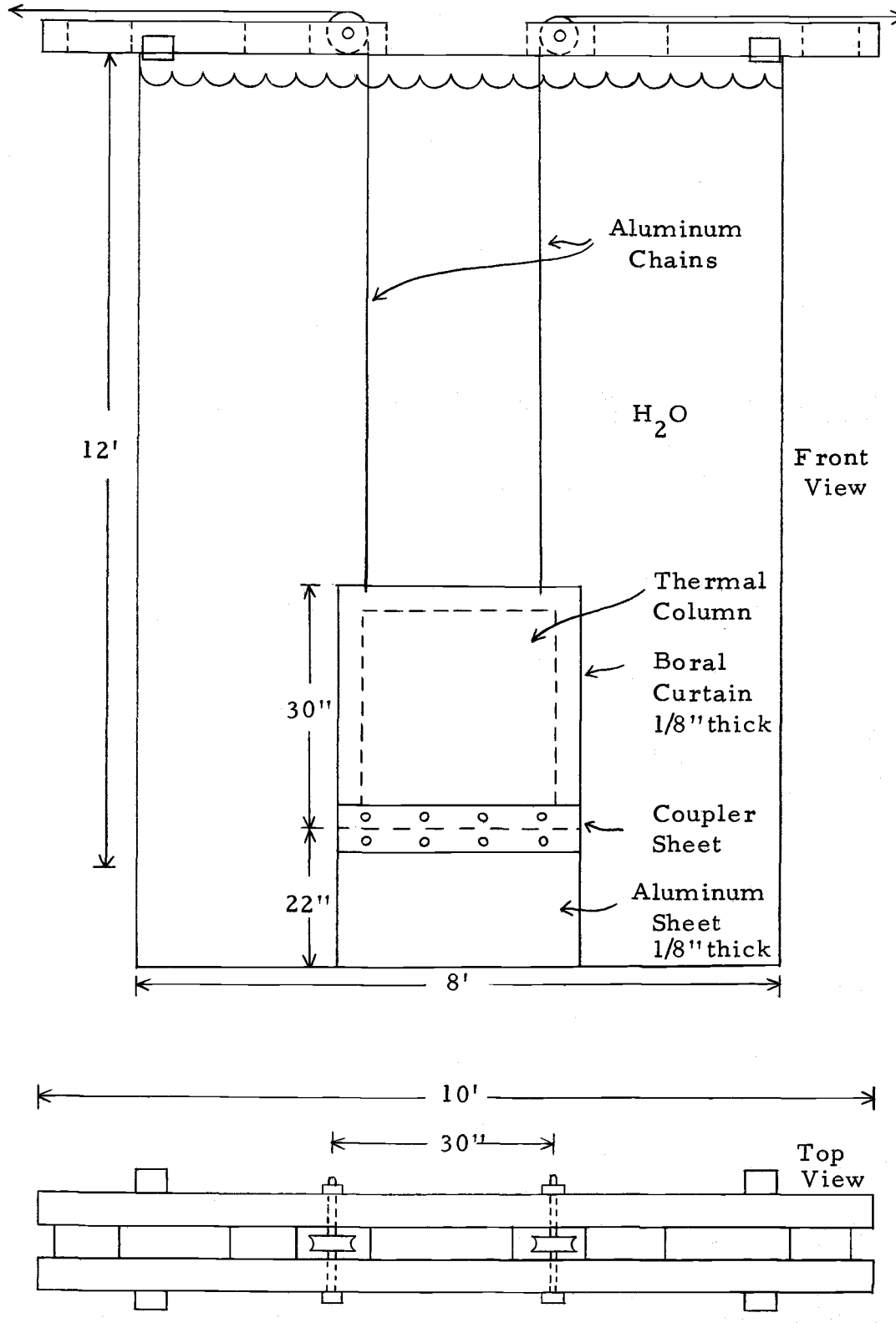

Figure 2. Boral curtain assembly.

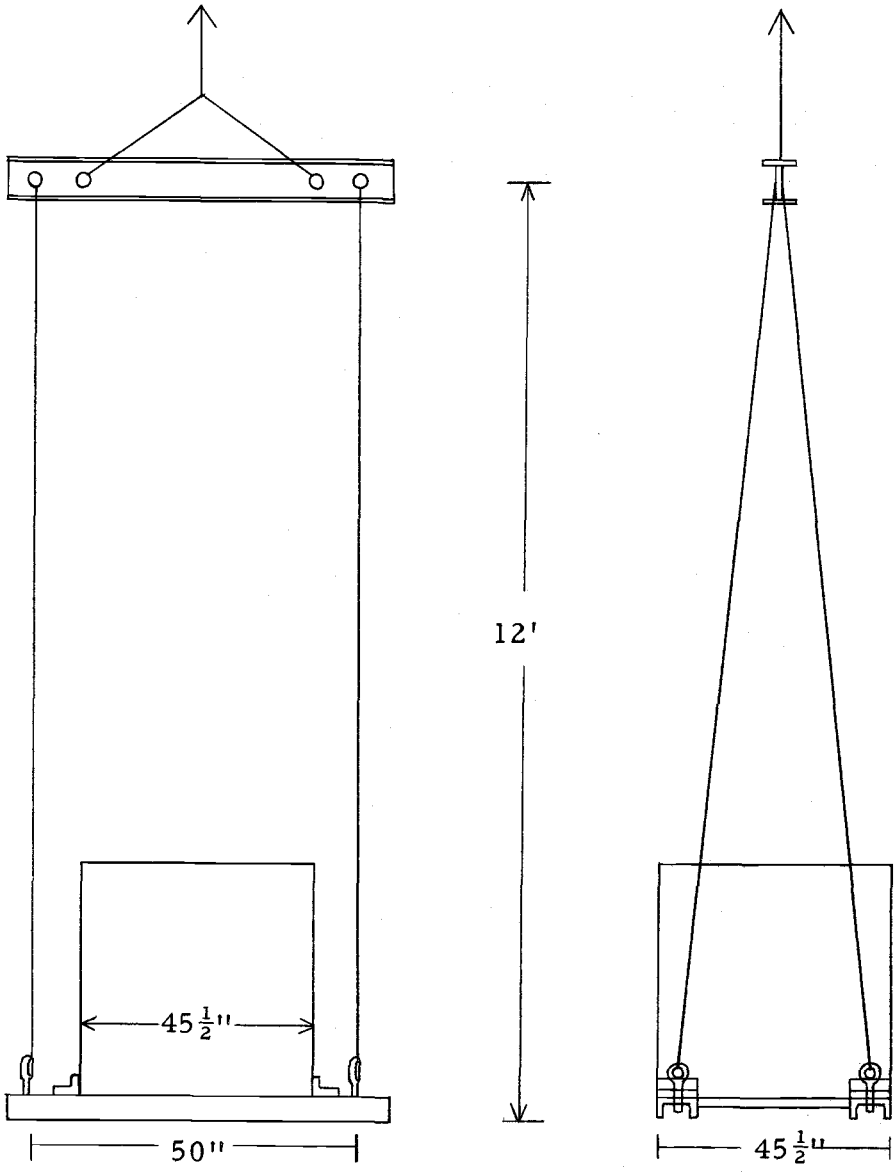

Figure 3. Transport assembly.

When lowered into position in the bulk shield tank, the box and base rest on a base stand. The function of the stand is to position the center of the aluminum box at the same height as the centerline of the thermal column. Horizontal positioning parallel to the column face is done by lining up a mark on the center of the aluminum box with the center bolt of the aluminum plate covering the end of the column. Horizontal positioning perpendicular to the column face is accomplished with aluminum spacers bolted to the base assembly and holding the box one inch from the wall of the tank. It is important to be able to get the box close to the thermalizing column to keep the thermal neutron current entering the box as large as possible but still leave room for the boral curtain.

Four aluminum bolts, one at the end of each channel, allow the box to be leveled. (For sketches of the base and base stand, see the base and base stand design section.) We must first determine the weight of the aluminum box with its contents before the base can be designed. The next section will consider the box design.

Box Design

Aluminum is used as the container material because of its low thermal-neutron absorption, its workability, and its corrosion resistance to extended exposure under water. Also, the activation products of the aluminum and its alloy elements decay to safe activity

levels after short cooling periods.

The container ("box") must hold the $44\frac{1}{2}$" x $44\frac{1}{2}$" x $44\frac{1}{2}$" (outer dimensions) stack of graphite which surrounds the outer cavity. The maximum deflection of any one side of the box must not exceed one half inch, so the box has inside dimensions of $45\frac{1}{2}$" x $45\frac{1}{2}$" x $45\frac{1}{2}$". The sides and bottom are five plates seam-welded together to form a water-tight seal. Angle stiffeners are added on the inside along each seam so that the edges can be considered rigid, and also along the span of each plate in order to keep the deflection of the plates from exceeding one half inch. These angles are welded on the inside so that the water pressure presses the plates against the angles rather than away from them. Along three of the top edges of the box, the angles are welded along the outside of the plates and flanged out so that the top cover plate can be easily bolted onto the box. The angle along the top edge on the side of the box next to the thermal column is welded on the inside of the box and flanged in to allow movement of the boral curtain. The bolts to attach the top cover on the flanged-in side are tapped through the top angles and into a $\frac{1}{2}$" x 1" bar welded on the underneath side of the angle. The top cover is a plate similar to the sides of the container. A 1" aluminum pipe coupling is welded into the center of the top cover in order to accommodate the "snorkel" assembly.

The thickness of the plate and the size of angle needed are

determined assuming that the whole box is subject to a pressure of 5.2 psi due to the pressure of water at a 12 foot depth. Since much of the box is subject to less pressure, this assumption is quite conservative and is used to give a factor of safety and to facilitate the calculations. Each plate is assumed to be divided into strips parallel to and including one angle stiffener. These strips are considered as beams and the maximum deflection, fiber stress, and shear stress are calculated for plates of various thicknesses and angles of various dimensions. This procedure is then repeated for a strip of the plate from one angle stiffener to the next perpendicular to the first strip. The deflections from the first strip and the second set of strips are added together to get the total deflection. Then the design which minimizes the weight of the aluminum needed but still does not violate the maximum total deflection specification or exceed the yield stress for the type of aluminum considered is chosen. The calculations for the optimum design appear in Appendix B. They are conservative in that the strips of the sides do not act independently, so the total deflection will be less than that calculated.

The results from Appendix B indicate that the optimum design is to use plates 1/8" thick. There are $1\frac{1}{2}$" x $1\frac{1}{2}$" x $\frac{1}{4}$" angles stiffening the joints of the sheets at the edge seam welds. The edges of the box are then considered rigid. Stiffening of the plates is accomplished by placing 2" x $1\frac{1}{2}$" x $\frac{1}{4}$" angles vertically at 14" intervals.

The bottom plate must withstand less water pressure, because the weight of the graphite opposes the force of the water. However, the bottom plate must withstand the weight of the graphite during transport. The graphite exerts a pressure of 2.8 psi, which is much less than the design pressure. Also, the base is designed to support with very small downward vertical deflections all the angle stiffeners of the base (see Figures 4 through 6).

Aluminum types 5052-H32 for the plate and 6061-T6 for the angles are chosen for their good weldability, nuclear properties of alloy elements, corrosion resistance, and commercial availability.

The snorkel, which allows the insertion and retrieval of samples without the removal of the entire fast spectrum facility, consists of an eight-foot long 1" aluminum pipe. It extends from the top of the aluminum box to about a foot above the water level in the bulk shield tank. The pipe is screwed into a coupler welded into the box. Teflon tape is used to seal the threads to keep water from leaking into the box. The pipe is held steady by four aluminum wires extending from the corners of the box up to a point four feet higher than the top of the box (see Figure 7).

Base Assembly Design

The base assembly consists of two parts, the base and the base stand. The aluminum box sits on the base which is used for transport

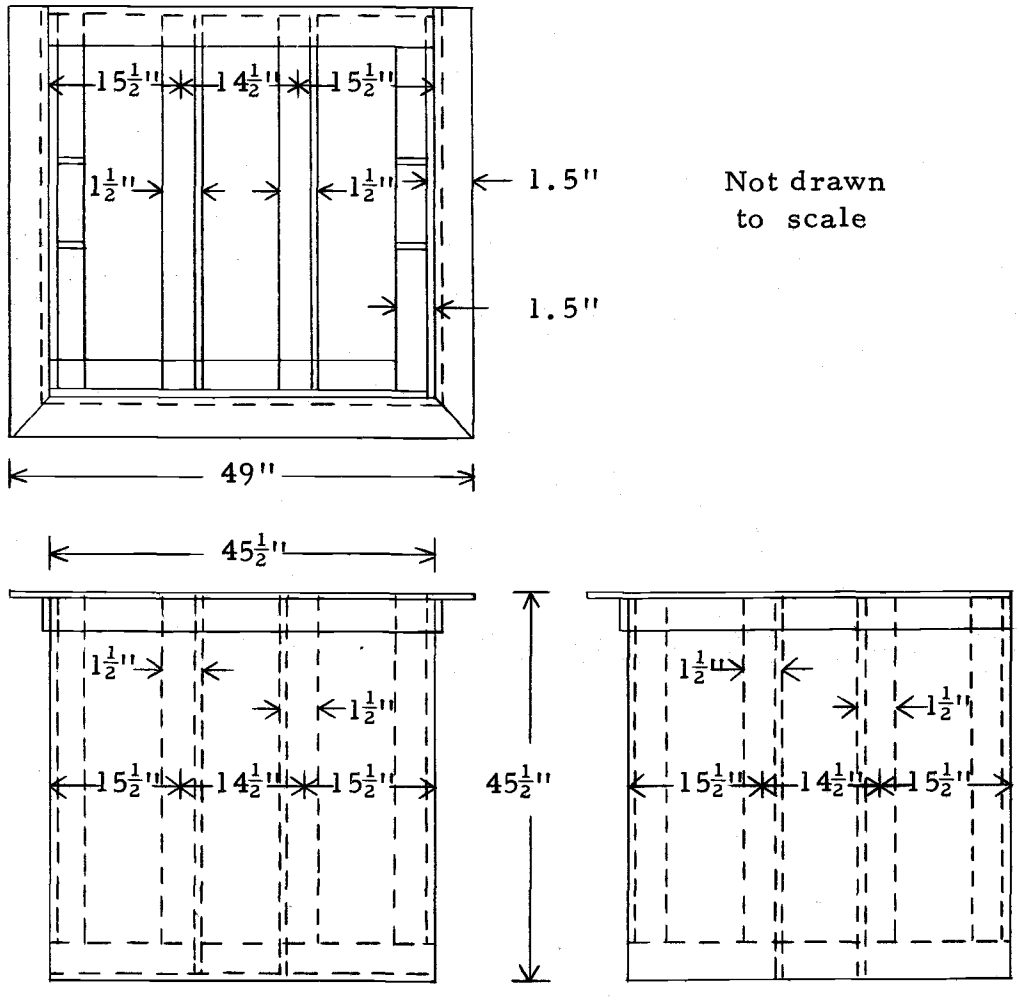

Figure 4. Aluminum box.

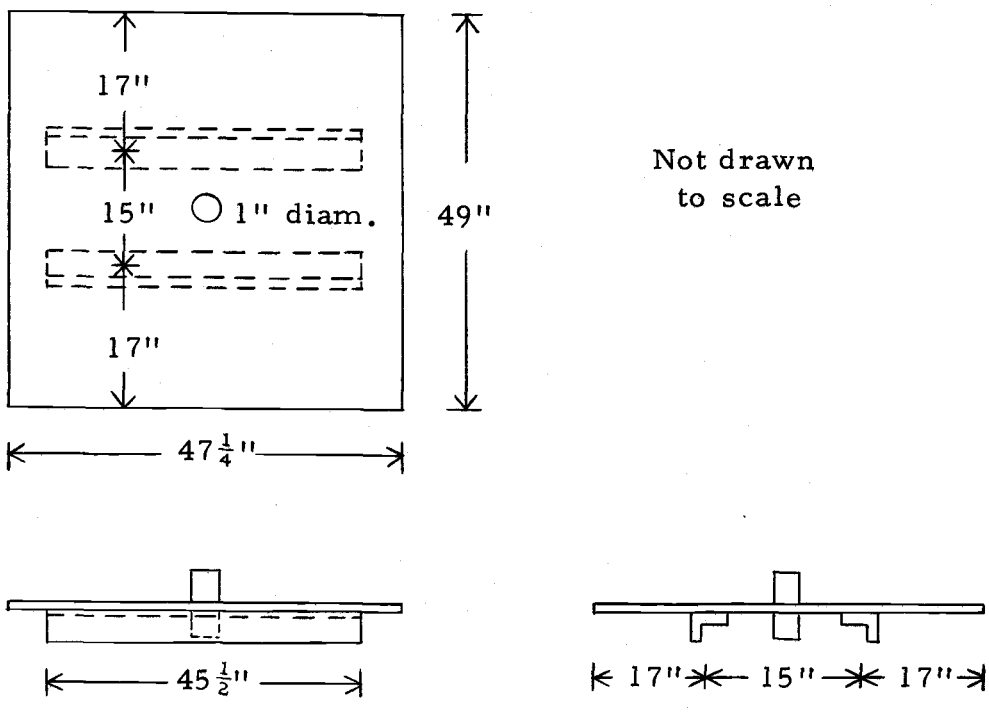

Figure 5. Top of aluminum box.

Lower corner:

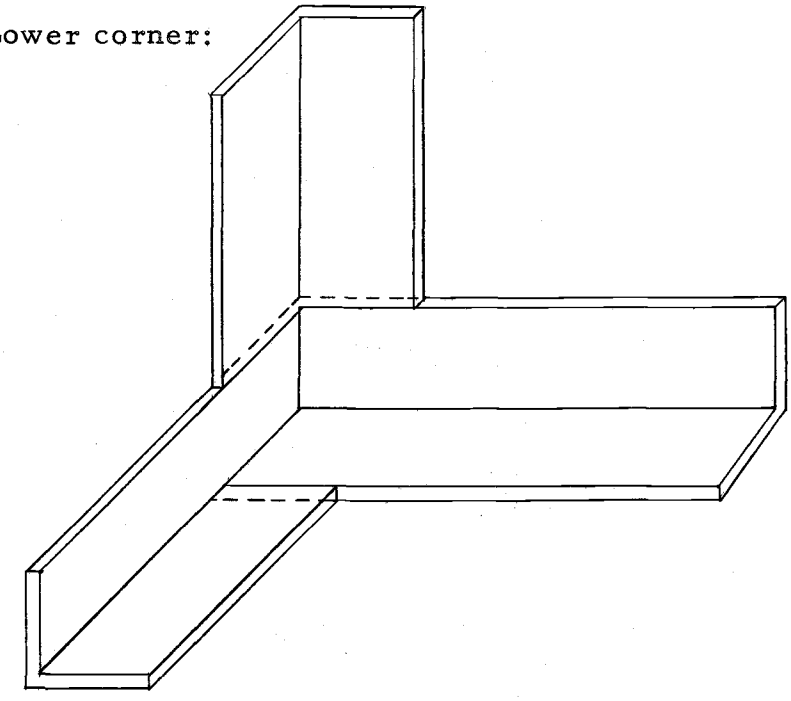

Side stiffener joining bottom stiffener and edge angle:

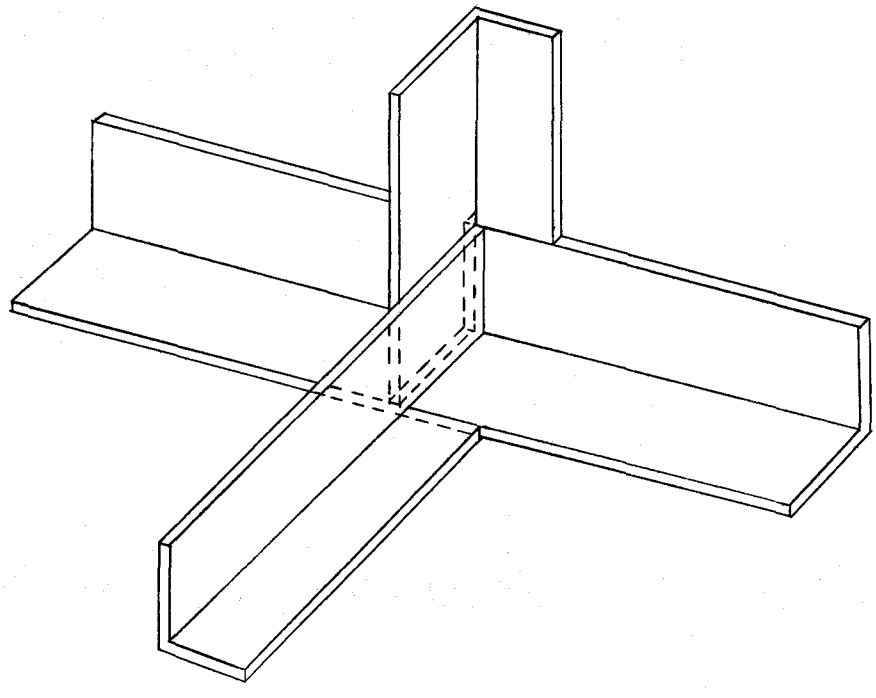

Figure 6. Angle welds.

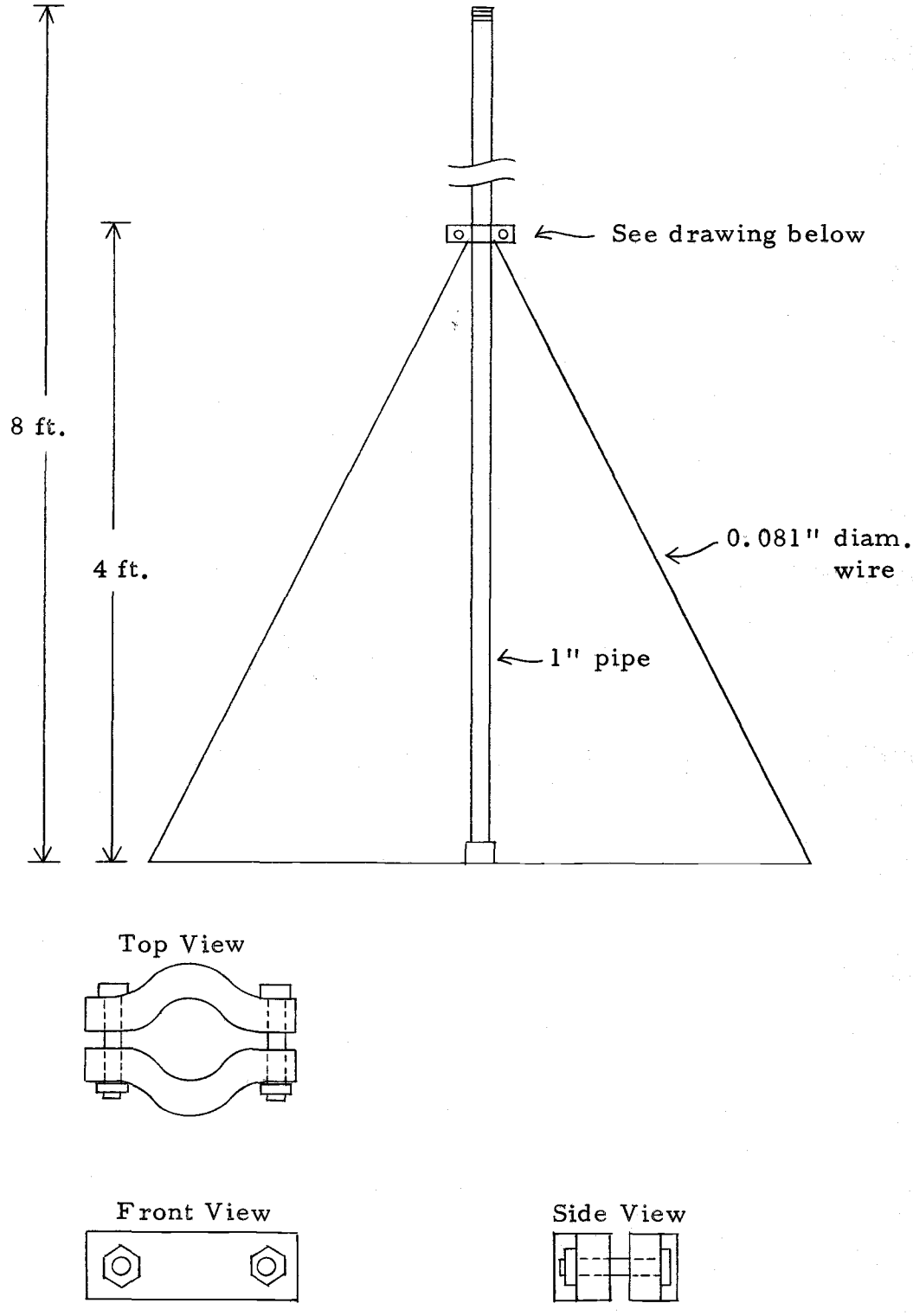

Figure 7. Snorkel assembly.

and final positioning. It must be designed to lift the 5800 pound box and contents. The base is fabricated from seven inch channel beams and three inch channel cross members to give it sufficient strength, as is determined in Appendix C. Eye bolts are bolted onto the end of each channel and are used to lift the facility. The leveler bolts at the end of each channel are $\frac{1}{2}$" x 3" stainless steel bolts adjustable through threaded holes in the channel (see Figures 8 and 9).

The base stand is constructed using 2" x 2" x $\frac{1}{4}$" angles for the legs, and $1\frac{1}{2}$" x $1\frac{1}{2}$" x 1/8" angles for the connecting members. Three-eighth inch pads are used to distribute the weight of the facility to meet the design specifications of 2000 psi for the floor of the bulk shield tank (see Figures 10 through 12). Calculations appearing in Appendix C show that this design gives the base stand sufficient strength.

Both the base and the base stand are painted with special chlorinated rubber paint to prevent rusting under the prolonged exposure under water.

Aluminum Container Seal

The top of the aluminum box is bolted onto the sides using $1\frac{1}{2}$" x 5/16" aluminum bolts spaced every three inches. Three sides of the box have the $1\frac{1}{2}$" x $1\frac{1}{2}$" x $\frac{1}{4}$" angles flanged out, so the bolts can be easily pushed through a 5/16" hole in the top and angle and a nut is

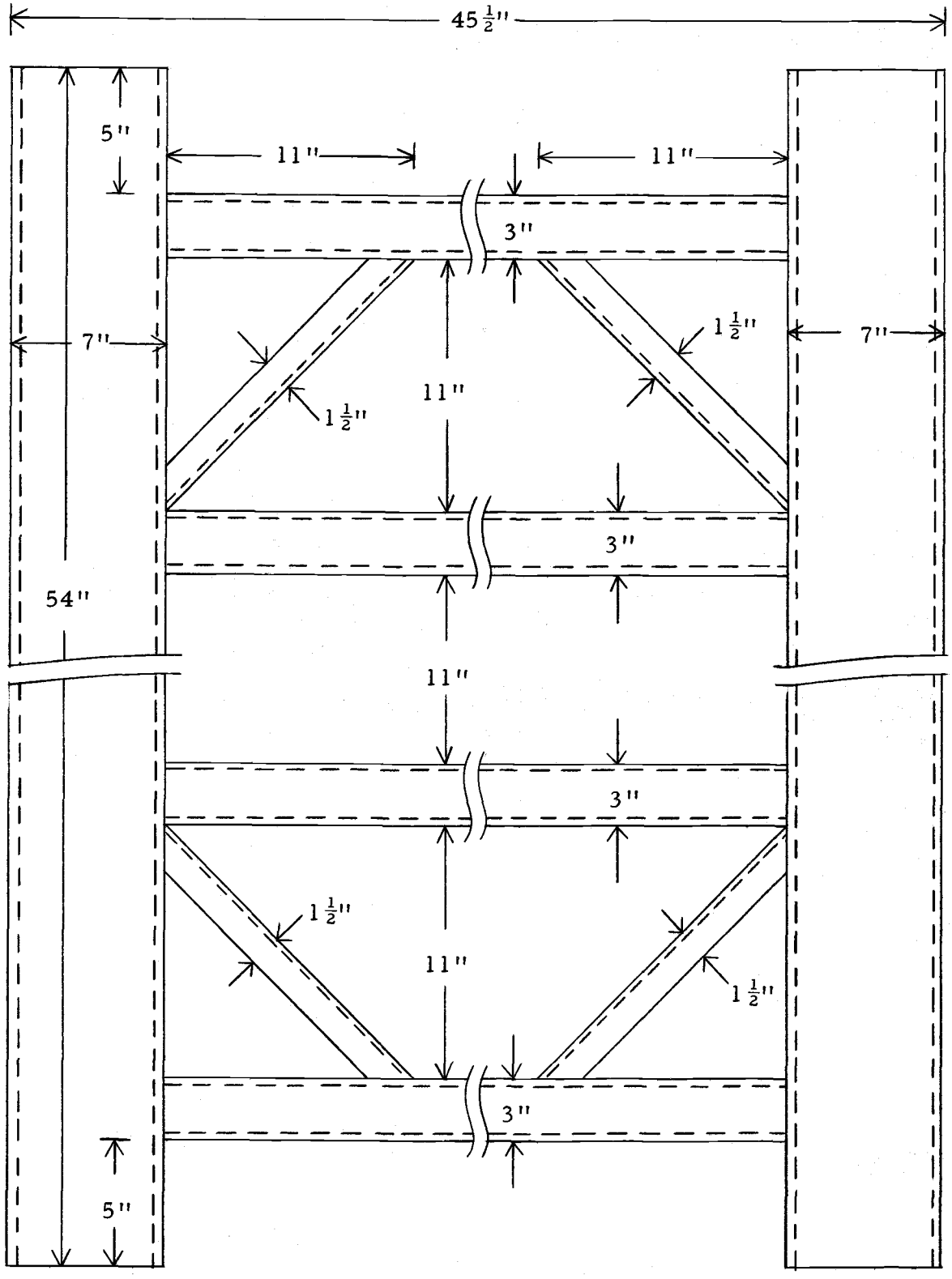

Figure 8. Base (top view).

Side View:

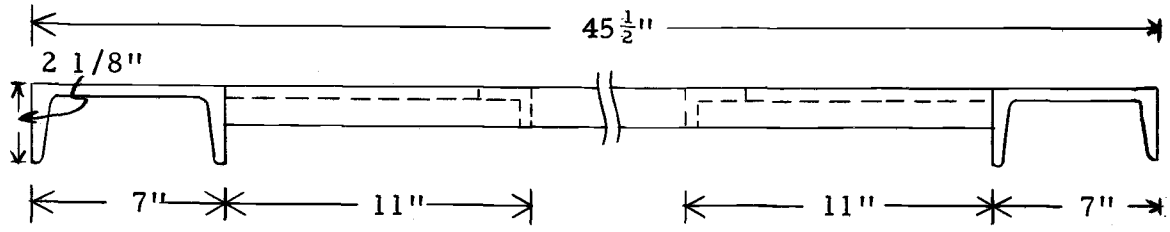

Front View:

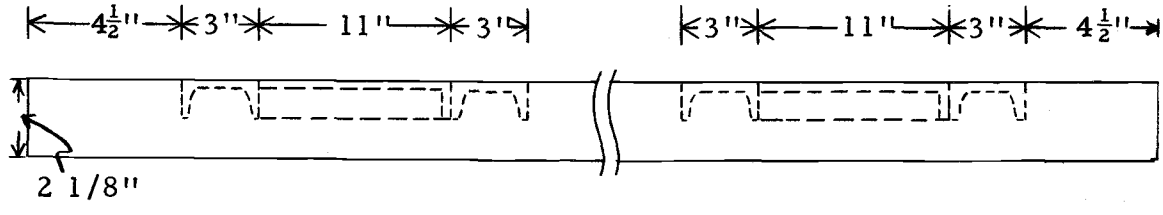

Figure 9. Base (front and side views).

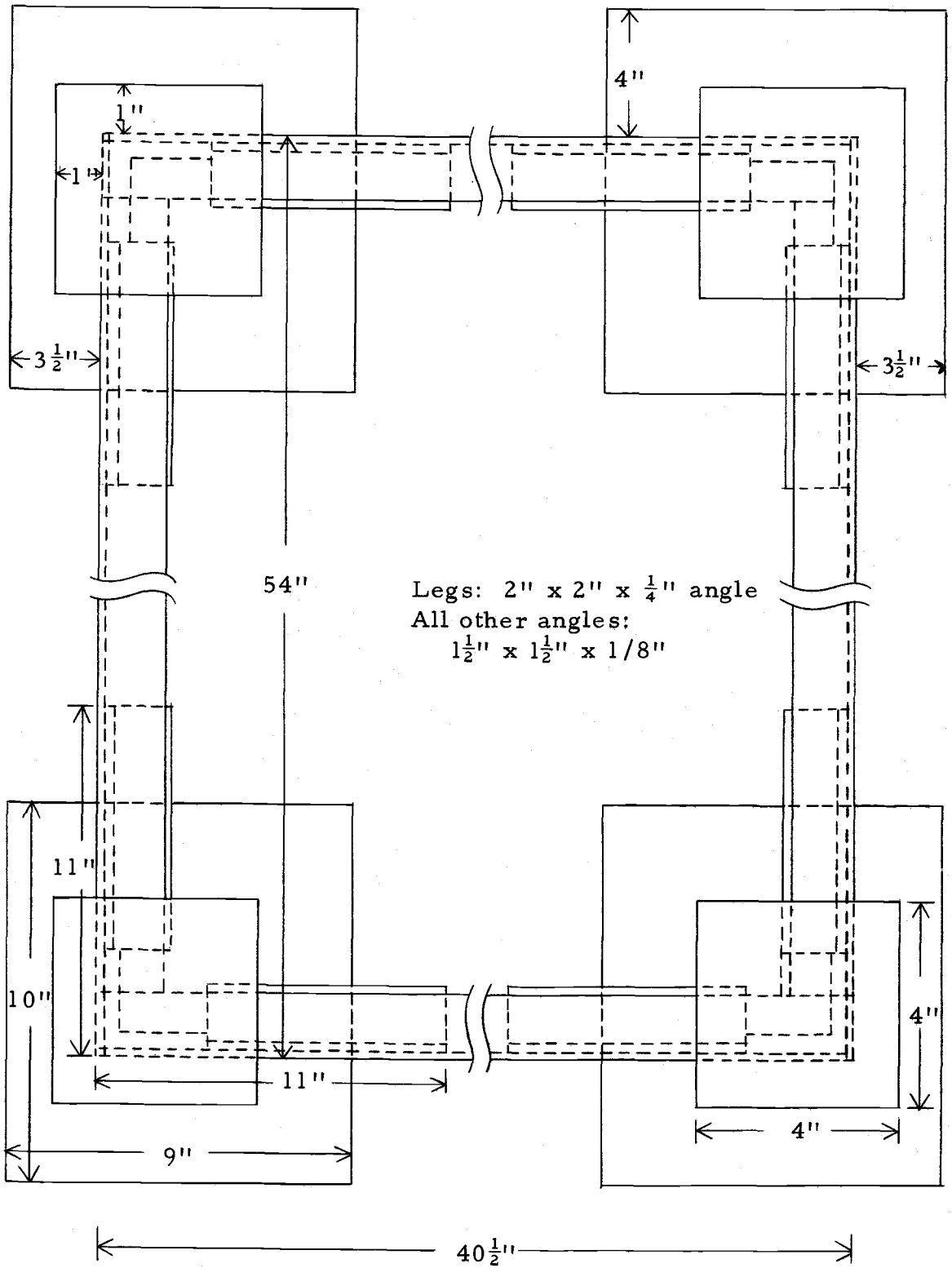

Figure 10. Base stand (top view).

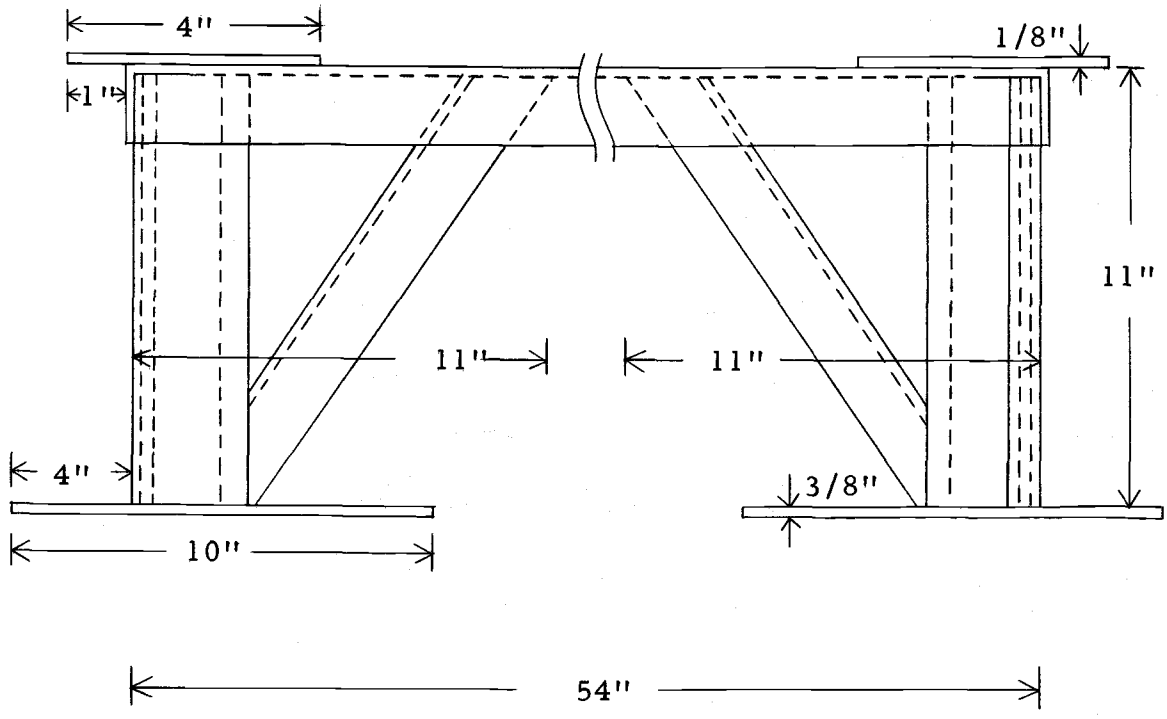

Legs: 2" x 2" x $\frac{1}{4}$" angle

All other angle: $1\frac{1}{2}$" x $1\frac{1}{2}$" x 1/8"

Figure 11. Base stand (front view).

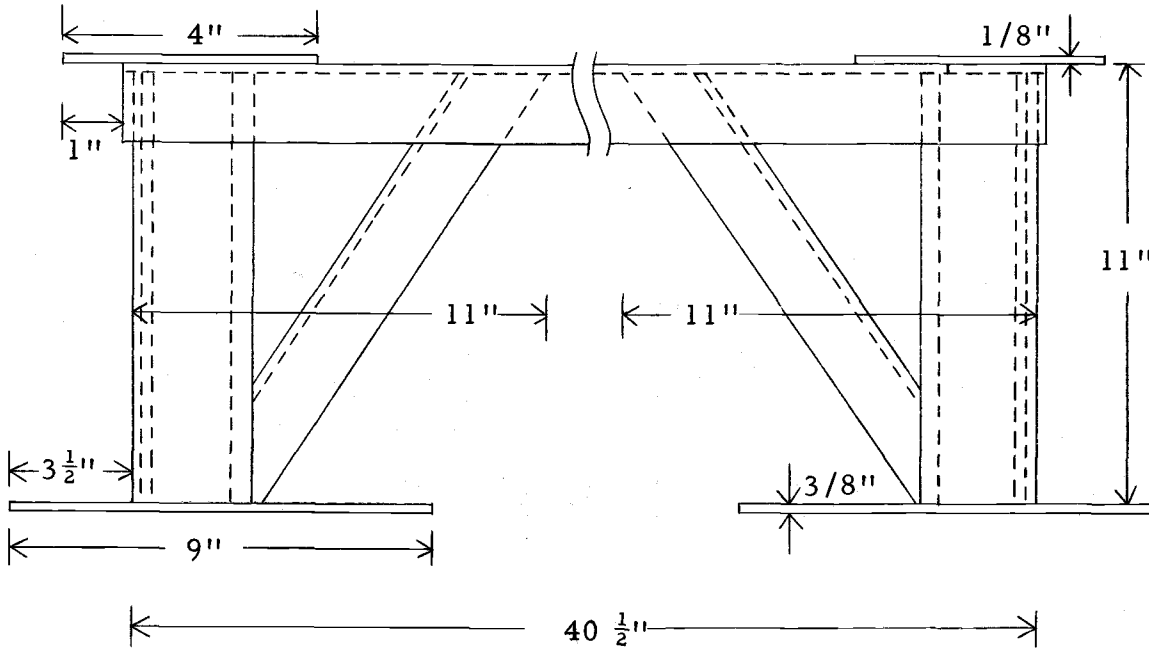

Legs: 2" x 2" x $\frac{1}{4}$" angle

All other angle: $1\frac{1}{2}$" x $1\frac{1}{2}$" x 1/8"

Figure 12. Base stand (side view).

used to tighten the top down. On the thermal column side of the box the angle has to be flanged in so that a neutron shutter can slide vertically between the box and thermal column without having a thick water layer to absorb the thermal neutrons supplied by the column. On this side of the box, a $\frac{1}{2}$" x 1" aluminum bar is welded to the underside of the angle. Five-sixteenth inch holes are tapped and the 5/16" bolts tightened into the bar. Also, a $\frac{1}{2}$" x 1" bar is used to sandwich the 1/8" top plate and gasket material to the angle.

Neoprene was first tried as a gasket material. However, neoprene is difficult to find. The type found at the local auto parts store has a cloth layer inside making it too stiff to seal. Next, latex tubing was tried, but was difficult to attach to the top cover. Finally, a truck inner tube cut into a strip $1\frac{1}{2}$" wide and 16 feet long was used and found to seal well and be able to be readily glued to the top cover with silicone rubber.

On the three sides where the angle flanges out, one $1\frac{1}{2}$" strip of the rubber is sufficient since the bolts do not protrude into the box. The strip is placed between the top cover and the angle as shown in Figure 13. For the side of the box where the angle flanges in, the bolt holes must be sealed since they protrude into the box. On this side, an extra rubber inner tube strip is put between the $\frac{1}{2}$" x 1" bar and the top plate to keep water from going underneath the bar and down through the bolt holes. Also, a neoprene washer under an

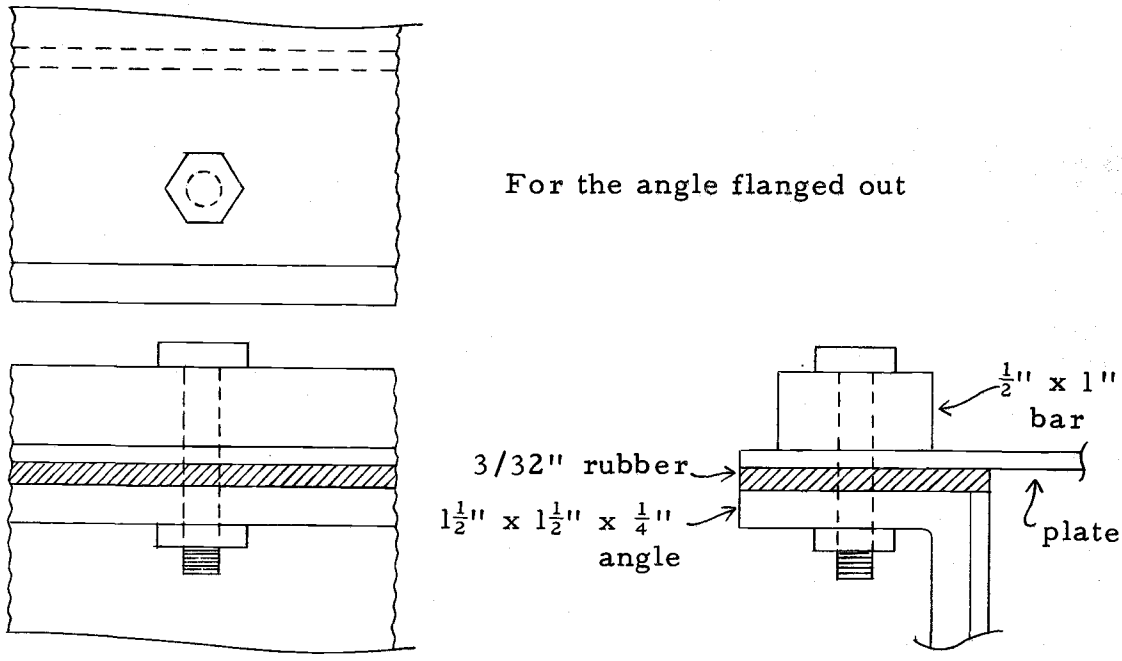

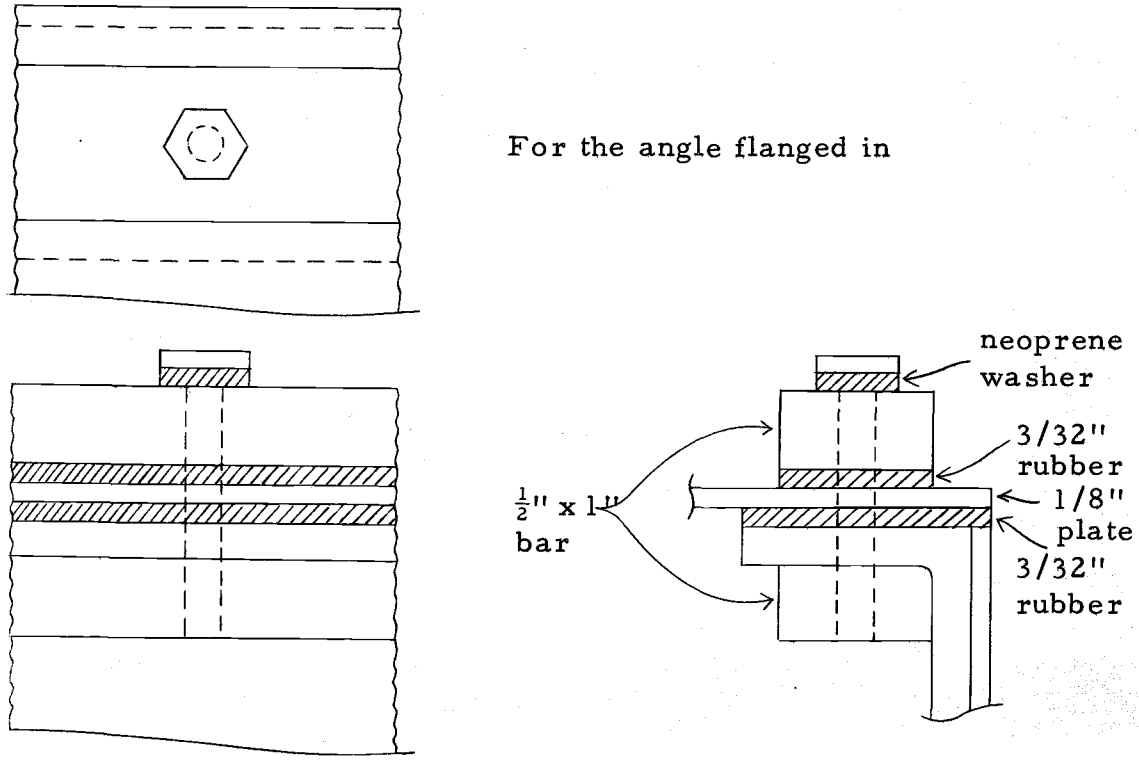

Figure 13. Gasket seal.

aluminum washer is used between the head of the bolt and the bar (see Figure 13).

Assembly Instructions

The procedure for putting the top of the box on is as follows. First, check the rubber gasket for signs of deterioration. A new gasket can easily be prepared if needed by cutting a long $1\frac{1}{2}$" strip around the circumference of a truck inner tube using tin snips. After punching out the holes for the bolts, rubber silicone can be used to fasten the gasket to the top cover. The air bubbles must be worked out from under the gasket before the rubber silicone dries. After allowing to dry overnight, the top then can be put on the box.

With the top plate resting on the box in approximately the correct position, put the square $\frac{1}{2}$" x 1" bar assembly over the top plate and line up the bolt holes. The bolts that go into the tapped holes must be started first. Since aluminum bolts tend to gall and are difficult to undo, the threads of the bolts should be coated with a moly-base lubricant. Make sure that all these bolts start by hand before putting a wrench on them or before proceeding to put the other bolts in. Before tightening these bolts, punch the rest of the bolts in around the box and put all of the nuts on finger tight. These bolts should also be coated with a lubricant. Now use a $\frac{1}{2}$" end wrench and a 3/8" ratchet with a $\frac{1}{2}$" socket (use no larger ratchet since aluminum bolts

strip very easily) to tighten the bolts down. Start with the bolts at the center of each side and work toward the corners. It is better to tighten partially the first time around the box and then repeat. If one of the bolts with a nut breaks, simply replace it. If one of the tapped holes strips out, the hole must be drilled out and tapped to 3/8" and a 3/8" bolt used.

Next, the snorkel assembly is attached. The 1" pipe is screwed into the 1" pipe coupler welded to the top of the box. Teflon tape is used to seal the pipe threads. The wires are attached through small holes on each corner of the box.

Now the entire fast spectrum facility is assembled and must be leak tested before submerging in the bulk shield tank. A 1" threaded pipe plug with a valve stem is screwed into a pipe coupler and attached to the top of the eight foot snorkel. Air is pumped into the box until a small pressure differential is evident. Do not over-pressurize since the box is designed to withstand pressure from the outside, not from the inside. Inside pressure could pop the plates away from the angles.

With a slight pressure differential inside the box, apply a solution of soapy water to the edges of the gasket, around the bolt holes and all along the $\frac{1}{2}$" x 1" bar. A leak will cause soap bubbles to form. If no leaks are found, the fast spectrum facility is ready to be placed into the bulk shield tank.

The above discussion has assumed that the graphite and internals were already in place. Let us now look at the graphite design and then end the design chapter with the designing of the uranium stand.

Graphite Liner

The fast spectrum facility assembly has a twelve inch thick graphite lining surrounding the central air cavity. Basic construction is with 6" x 6" x $20\frac{1}{2}$" graphite blocks. The blocks are stacked in such a manner as to minimize the amount of machining required and to reduce neutron streaming through voids. The blocks are used as cantilevers over the central cavity so that no braces will be needed. The corners of the cubic air cavity are filled with blocks cut so that the surface of each face is a plane whose normal passes through the centroid of the air cavity. The upper corner fill blocks are machined full sized blocks cantilevered over the cavity.

The graphite stack is composed of five layers beginning with the first layer on the bottom. Figure 14 shows the first two layers. The third layer is the walls of the air cavity and the cavity corner fills. Figure 15 shows the third layer as composed of two sets of identical groups of blocks, labeled set A and set B. A base diagram is presented and then each set is drawn. The blocks up through the third layer are held together with rubber silicone to prevent movement

First layer:

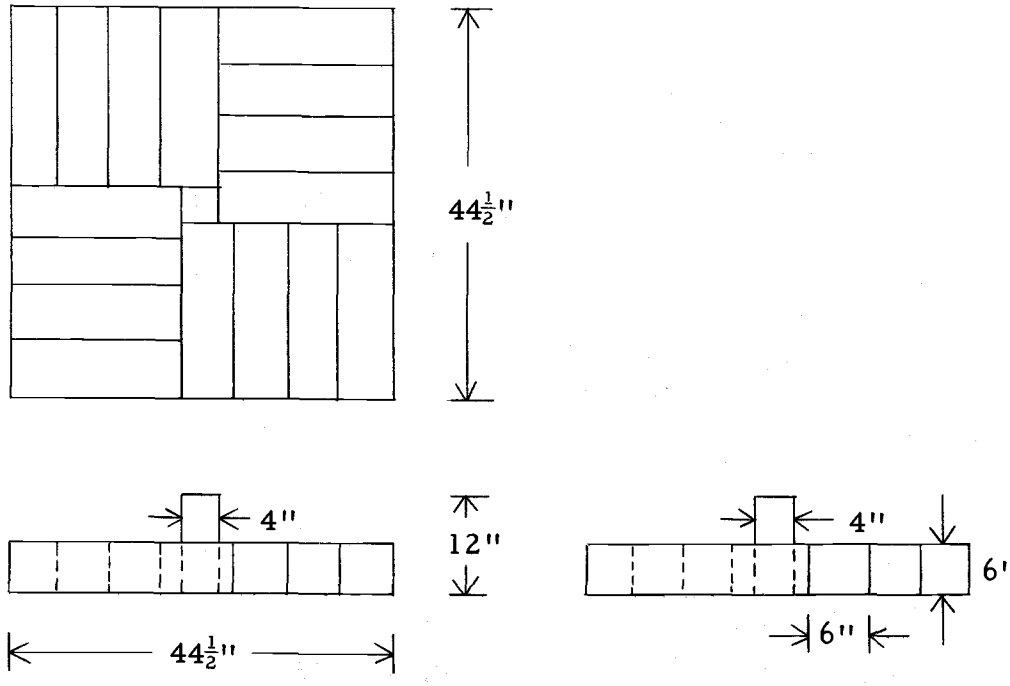

Second layer:

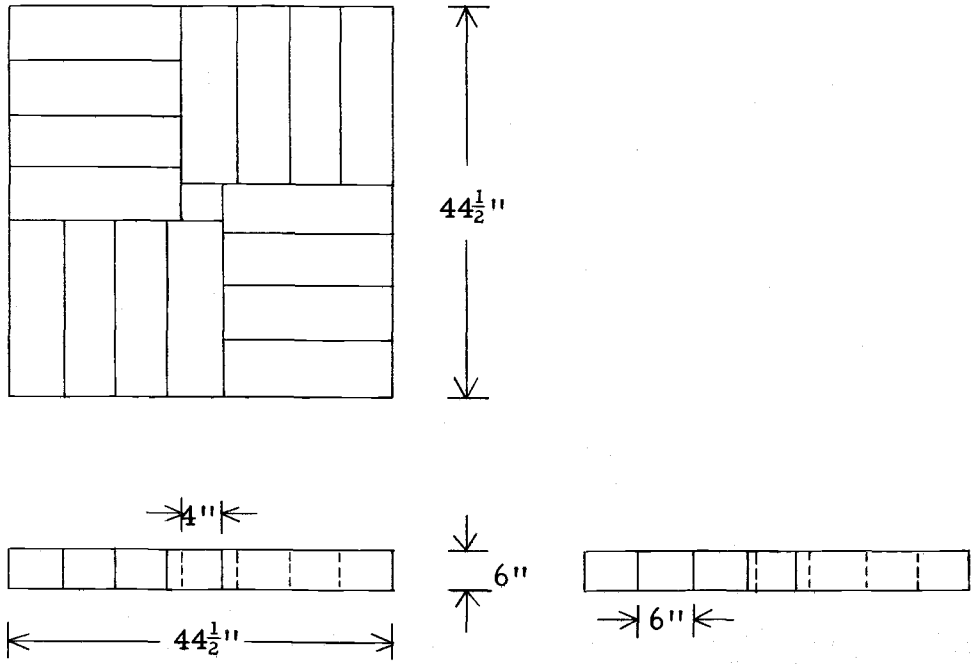

Figure 14. Graphite stack (first and second layers).

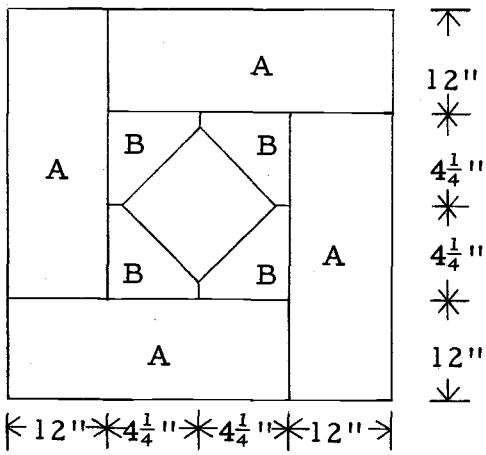

The bases of each set appear as in the diagram at the left.

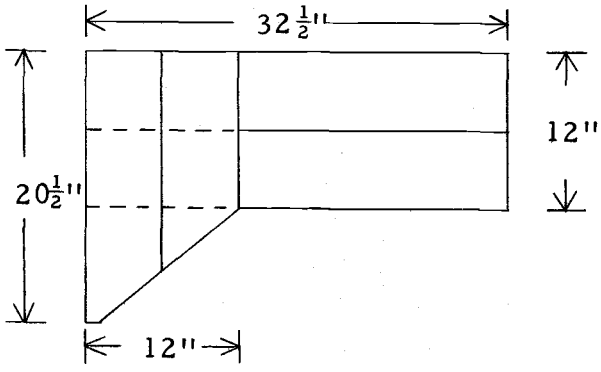

Set A (scale is different than in above diagram)

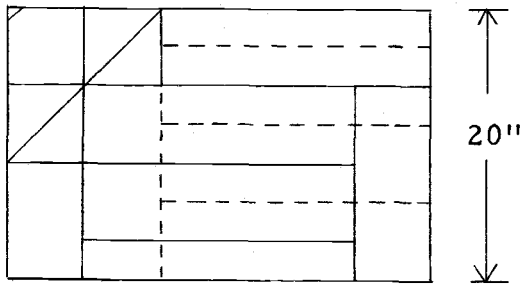

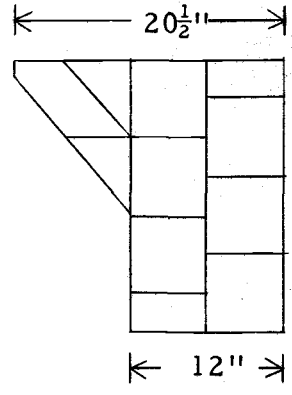

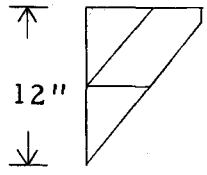

Set B

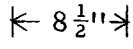

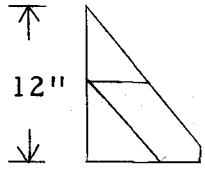

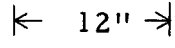

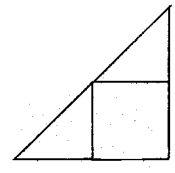

Figure 15. Graphite stack (third layer).

during transport. The top two layers, fourth and fifth, are stacked loosely with no glue. Figure 16 shows the fourth and fifth layers which are very similar to the first and second layers. The entire graphite stack was modeled with wood on a 1:4 scale. The wood stacked easily and permitted checking of the graphite cuts required.

Ring Stand and Glass Sphere

The ring stand is constructed from two sizes of aluminum tube as is shown in Figure 17. The uranium sphere radius to be supported is 12.25 cm (4.82 in). The ring stand is designed to hold the uranium shells, which will weigh 256 pounds, 10.25 inches above the floor of the air cavity. Since it is difficult to try to calculate the stress, strain, and deflection on the various members, the stand is assembled and then tested by stacking lead bricks on it. The stand holds 275 pounds without failure. The legs of the stand rest on two 10" x 2" x $\frac{1}{4}$" aluminum plates which distribute the uranium's weight evenly over a 40 square inch surface of the graphite. The plates are positioned horizontally by the head of a bolt which fits into a small indentation drilled into the graphite.

A 5000 ml Pyrex boiling flask is substituted for the uranium sphere for the initial thermal calibration of the facility. The flask is a borosilicate glass containing 13% boric oxide. Having a radius of 4.34", the flask will simulate the absorption of the uranium shells.

Fourth layer:

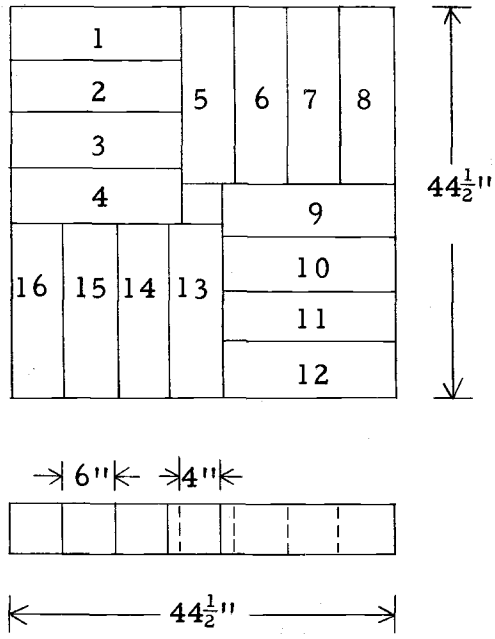

These layers are numbered since these layers must be removed to get to outer cavity.

Fifth layer:

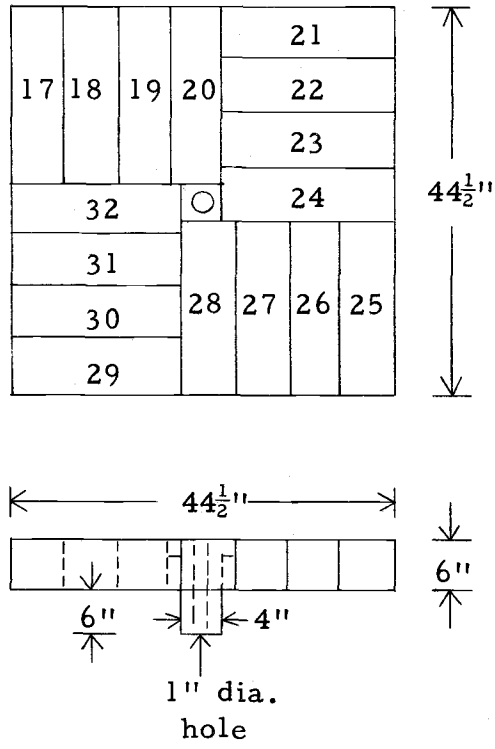

Figure 16. Graphite stack (fourth and fifth layers).

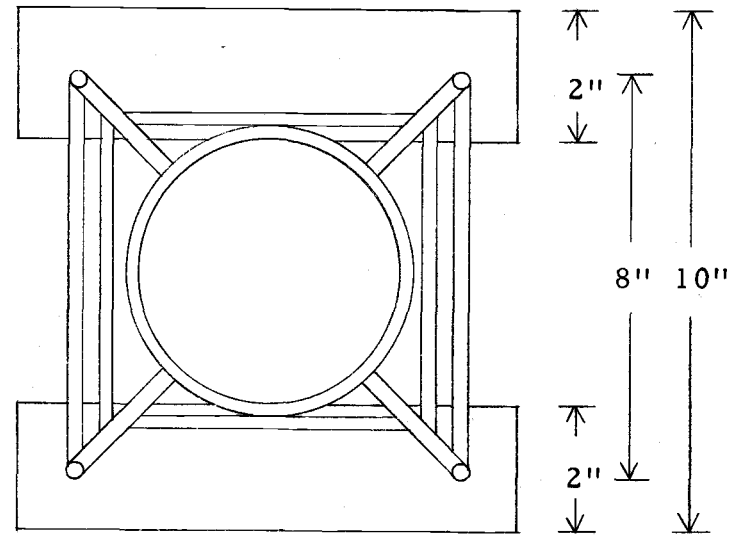

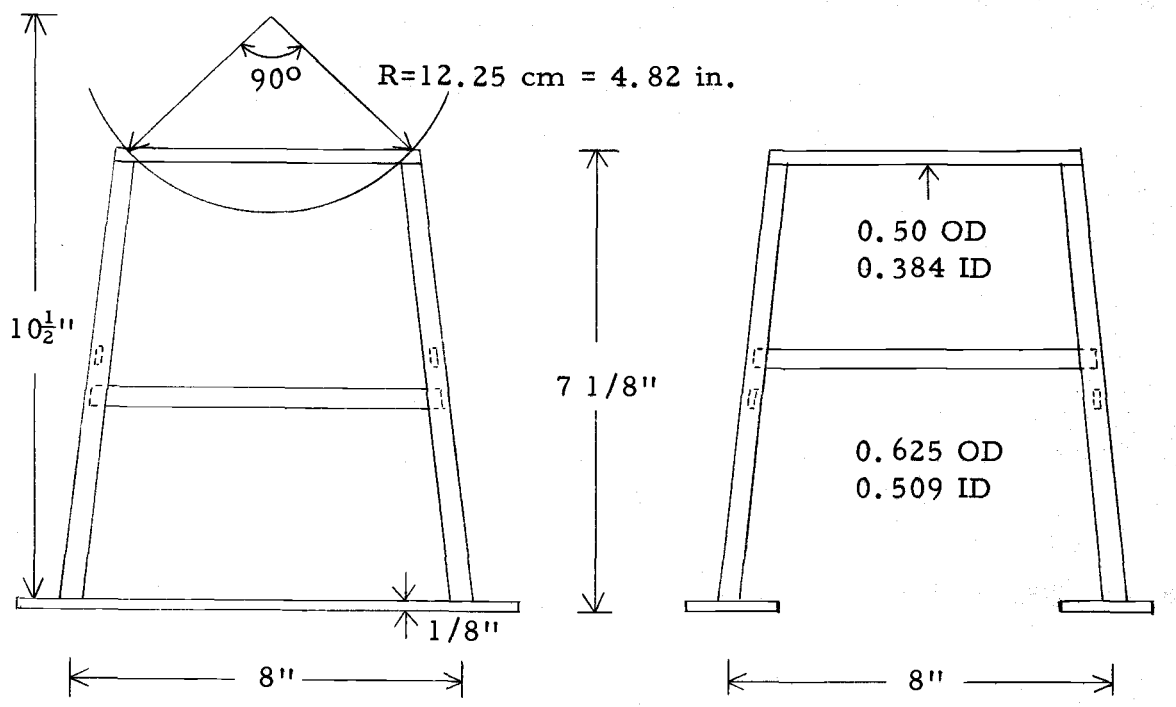

Figure 17. Ring stand.

The next chapter is the nuclear design of the facility. The justification of using one foot of graphite backed with water is presented along with a spherical geometry representation of the fast fluxes expected.

III. NUCLEAR DESIGN

The nuclear calculations of the fast spectrum facility must show that the design is capable of representing the spectrum found in a fast reactor. The simulated spectrum has two components: a direct component, which is the fission spectrum moderated by inelastic scattering in the uranium, and a return component, which consists of elastically scattered neutrons returned from the graphite surrounding the air cavity.

To obtain a characteristic fast reactor spectrum, the OSU fast spectrum facility will use the same size uranium shell and air cavity as Fabry's design (5) with graphite cavity walls backed with water instead of infinite graphite. So, we must determine how thick the graphite must be so that the wall return component is not affected by changes in the graphite thickness. Two computer codes are developed to insure that the OSU design will simulate a fast reactor spectrum. The nuclear design of the facility centers around these codes which will be presented in this chapter.

The OSU fast spectrum facility has a finite thickness of graphite backed with water in order to limit the size of the facility and the weight that must be transported in and out of the bulk shield tank. A first approximation code, called SLAB, was developed to determine what thickness of graphite is sufficient. SLAB is a six group

diffusion theory approximation which assumes two region plane geometry with a fission source at the center of a graphite slab which has water on both sides. The boundary conditions imposed are that the current is zero at the center of the graphite and the flux for each group is assumed to go to zero 15 cm into the water. This code represents the facility if the air cavity was collapsed so that the walls on both sides touched each other with the fission source sandwiched between the graphite walls.

The multigroup difference equations for slab geometry are developed in Appendix D. The difference equations are inserted into a tridiagonal matrix which is easily solved in a systematic form. Only downscatter is considered so that each group can be solved separately starting with the highest energy. Also, the neutrons are assumed to scatter only to the next group down in energy. The inputs to program SLAB are the removal cross section, Σ_R, the diffusion coefficient, D, and the fission fraction, $\hat{\chi}$, for each group. The removal and scattering cross sections are determined by the following equations where E_1 and E_2 are the energy limits of the group:

$$\Sigma_R = \frac{1}{\int_{E_1}^{E_2} \frac{dE}{\xi \Sigma_s E}} \qquad \Sigma_s = \frac{\ln(E_2/E_1)}{\int_{E_1}^{E_2} \frac{dE}{\Sigma_s E}} .$$

The diffusion coefficient is given by:

$$D = \frac{(1/3)\int_{E_1}^{E_2} \frac{dE}{\Sigma_s(\Sigma_a + \Sigma_s(1 - \bar{\mu}))E}}{\int_{E_1}^{E_2} \frac{dE}{\Sigma_s E}}, \quad \text{but,}$$

for this first approximation code, D is determined from:

$$D = \frac{1}{3(\Sigma_a + \Sigma_s(1 - \bar{\mu}))} \quad \text{where} \quad \bar{\mu} = \frac{2}{3(\text{atomic mass})} .$$

Values for the cross sections are taken from BNL 325. Σ_s is assumed to be equal to Σ_t, the total cross section, for groups one through five and $\Sigma_s = \Sigma_t - \Sigma_a$, where Σ_a is the absorption cross section, for group six. The values for the input data are listed in Appendix D after the listing of SLAB.

The groups are selected to allow the cross sections to be easily determined.

Group	Energy Range
1	1 MeV → ∞
2	0.1 MeV → 1 MeV
3	17 keV → 0.1 MeV
4	30 eV → 17 keV
5	0.4 eV → 30 eV
6	thermal → 0.4 eV

The change in the cross sections are small from 30 eV to 100 keV, so, only two groups are selected in this range. However, two groups were selected above and below this energy range since the cross

sections vary to a much greater extent. The fission neutrons are considered to be a source for the top two groups only.

The results of running SLAB for various thicknesses are presented in Appendix D. The purpose of SLAB is to determine the minimum thickness of graphite that can be used. Figure 18 is a plot of the fluxes of groups one through five at the center of the graphite for various graphite thicknesses. The thermal group, number six, is irrelevant to the determination of the fast fluxes and is not plotted. It is apparent that 12" (30.5 cm) of graphite is the desired thickness since the fluxes change very little with a thicker graphite wall. The results from SLAB indicate the size of the facility that is needed, but not whether the OSU facility will simulate the spectrum found in a fast reactor. So let us now look at the facility in more detail.

To predict the fast fluxes and the central fast spectrum of the OSU fast spectrum facility, a 16 group, four region computer code, called FASTSPEC is created (see Appendix E). A spherical shell of uranium is surrounded with three concentric shells of air, graphite, and water respectively. The thickness of each shell can be varied which allows the code to check the results of SLAB in more detail. This diffusion theory approximation code uses an isotropic spherical shell fission source on the outside surface of the uranium shell. The air gap is assumed to be filled with a hypothetical non-absorbing medium which is consistent with the diffusion theory approximation.

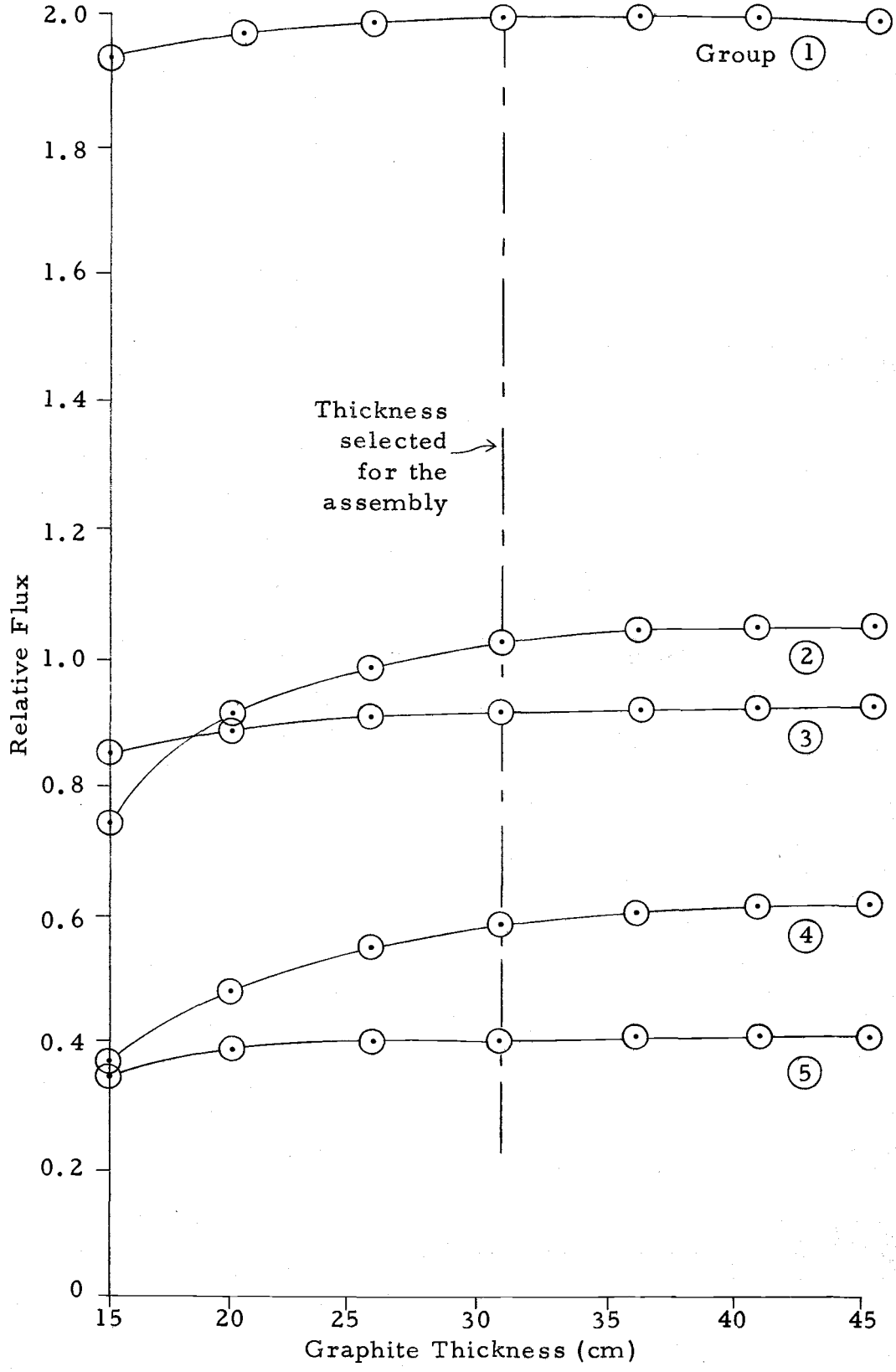

Figure 18. Group fluxes for varying thicknesses of graphite.

The boundary conditions imposed are that the current is zero for all radii less than the inside radius of the uranium and that the flux is zero at the farthest mesh point out in the water.

The formulation of the difference equations follows from the diffusion theory equation for spherical geometry and isotropic scatter. Appendix E shows the development of these equations to a form that can be solved by a tridiagonal matrix as were the equations for SLAB.

The cross sections for FASTSPEC are taken from the Los Alamos Scientific Laboratory (LASL) 16 group fast reactor group (15). The input data include the transport cross section, Σ_{tr}, the in-group scattering, $\Sigma_{i \rightarrow i}$, and the down-scattering, $\Sigma_{i \rightarrow j}$, where i is the group under consideration and j is another group lower in energy. No up-scatter is allowed and there is down-scatter to as many as five groups lower in energy for uranium and water. For graphite, however, only single group down-scattering is assumed. The diffusion coefficient, D, is considered as $1/3\ \Sigma_{tr}$ and the removal cross section, $\Sigma_R = \Sigma_{tr} - \Sigma_{i \rightarrow i}$.

The results for FASTSPEC are listed in Appendix E. FASTSPEC calculates the flux for each group at every space point. However, only the central spectrum produced by the system is desired. Therefore, the flux at the first space point, the inner surface of the uranium, is considered to be the central spectrum. FASTSPEC

prints $\int_{\Delta u} \phi \, du$ where Δu is the lethargy interval for a particular group. Table E.1 of Appendix E lists $\int_{\Delta u} \phi \, du$ for each group, normalizes each group so that $\int_{o}^{\infty} \phi \, du = 1$, and then lists the flux per unit lethargy for the graphite wall thickness of 30.5 cm of the OSU design. Table E.2 and E.3 repeats the results found in E.1 for graphite wall thicknesses of 35 and 45 cm respectively. The purpose of determining the central spectrum for the other graphite thicknesses is to check the results of SLAB and to show that when using a better approximation the central spectrum is still not significantly changed by increasing the graphite wall thickness. These thicknesses are chosen because the former is considered by Fabry to be "infinite graphite" (6), and the second is a much thicker wall which is used to check to see that the water has not changed the definition of "infinite graphite," which is the graphite needed so that changes in the graphite thickness do not significantly alter the central neutron spectrum.

The right-hand column in Tables E.2 and E.3 shows the change in the group fluxes due to a change in the graphite thickness. The changes are very small over most of the spectrum. Only in groups eight and nine (energy range 100 to 550 eV) is there a significant change. However, the magnitude of the numbers for these groups is small so a certain change represents a larger percentage than in a group with a larger flux. So, the results of FASTSPEC show that 30.5 cm of graphite backed with water is equivalent to within about

1% of "infinite graphite."

The flux per unit lethargy for each group is plotted in Figure 19 as a function of energy for FASTSPEC, Fabry's ΣΣ fast spectrum facility, and the Karlsruhe Na-2 project. (ΣΣ is the abbreviation for SISSIC, secondary intermediate standard spectrum in cavity.) The central spectrum produced by FASTSPEC seems somewhat softer than the measured ΣΣ spectrum (5). The difference between FAST-SPEC and ΣΣ is most probably caused by two factors. First, the small changes in the spectrum caused by introducing the water surrounding the graphite removes neutrons from the five highest groups and adds neutrons to the lower groups (see Tables E.2 and E.3). The water has a much greater ability to slow down the neutrons of these groups than does the graphite. Second, FASTSPEC assumes that all the fissioning occurs on the outside surface of the uranium shell. Actually, the fissioning occurs through a 1.5 cm shell decreasing as the distance from the outer surface increases. There is a fraction of the neutrons that actually do not travel the entire five centimeters from the outside surface of the uranium to the central cavity. These neutrons would appear in the upper energy groups.

It will be left to further work to determine how much each of the two factors affect the central spectrum. It is envisioned that FASTSPEC could be changed from a shell source to a distributed source which decreases as the distance from the outer surface

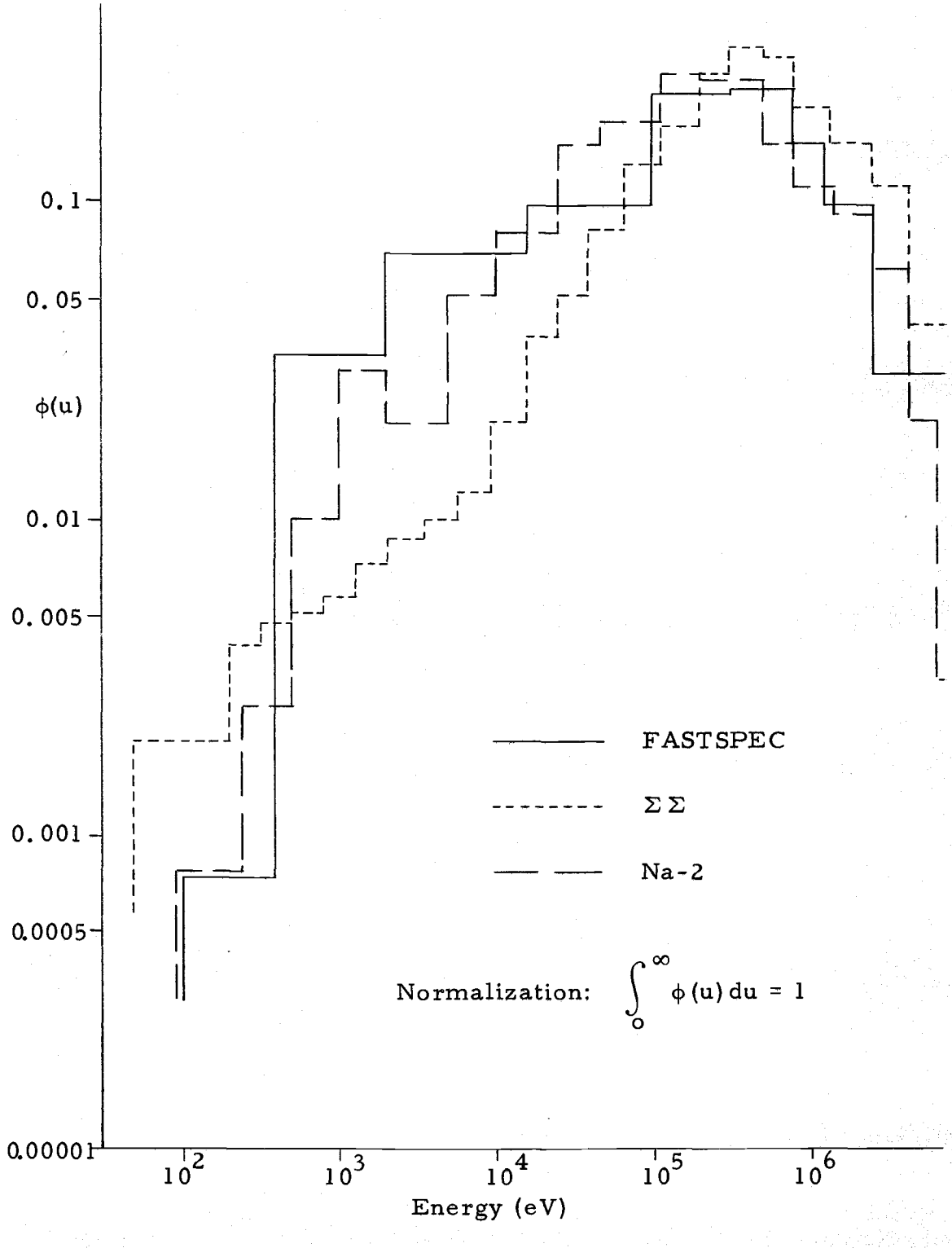

Figure 19. Comparison of the FASTSPEC central cavity spectrum with that of the ΣΣ source facility and Na-2 project.

increases. I suspect that the small changes caused by the water make up most of the difference.

Actually, the results obtained fit the spectrum of a fast reactor as well as does the $\Sigma\Sigma$ results. Using Karlsruhe's Na-2 spectrum as a reference (5), Figure 19 includes its spectrum along with FASTSPEC and $\Sigma\Sigma$. FASTSPEC appears to roughly fit the Na-2 spectrum. FASTSPEC suffers from too few energy groups, giving bars that are too wide. However, it certainly appears that the OSU fast spectrum facility produces a spectrum which simulates a fast sodium cooled reactor.

If the shell source approximation does change the spectrum, it would soften it. Then when a more accurate model is created, the spectrum will be harder and approach the $\Sigma\Sigma$ spectrum. So, the theoretical calculations show that Oregon State University has a workable simulator. The experimental central spectrum obtained will show whether the calculational model is valid. However, due to the inability to obtain an uranium shell in time for completion of this paper, only the thermal flux will be mapped. However, future work will prove the validity of the model.

IV. EXPERIMENTAL RESULTS

Three important sets of data are obtained from phase I operation of the fast spectrum facility. First, the test of the mechanical design determines whether the assembly can be transported and positioned safely and easily. Second, the health physics data shows whether the facility is radiologically safe to operate and how cautiously it must be handled. Third, a thermal neutron flux map of the surface of the glass absorber indicates whether the facility has any serious flux gradients which will hamper the production of a characteristic fast reactor spectrum.

Mechanical Data

The mechanical design of the facility proves to be workable. The transport rigging and box assembly is stable when lifted. The assembly clears the reactor stair and second floor railing as planned and the separator bar remains greater than one foot above the bulk shield tank water level when the box is in its final resting position. With the box in this position, the 12 foot long chains which lift the box can be connected and disconnected by maneuvering the ends of the chains above the water until the hooks 12 feet below slide into the eye bolts. The floor of the bulk shield tank seems to be very level because no leveling of the assembly is needed after the box is

lowered into position on top of the base stand. The bolts on the aluminum thermal column cover plate are longer than expected. The base stand must be pulled one inch away from the wall nearest the reactor core, and the bumpers on the aluminum box must be extended to allow a two-inch space between the reactor core wall and the box. The box then is easily set onto the base stand assembly.

The aluminum box construction proves satisfactory. The rubber gasket keeps the internals dry, but tends to break away from the top cover when the bolts are over-torqued. The neoprene washers on the bolts which fit into the tapped holes wear out and must be replaced every second time the box assembly is disassembled.

Health Physics Data

Phase I operation of the fast spectrum facility includes two reactor runs. For the first run, the snorkel assembly is left off and gold foils are used to map the thermal flux around the glass sphere when the reactor operates at one megawatt. Earlier, it was suspected that due to radiation streaming up through the snorkel, the reactor power might be limited. Since the foils need a two hour run at full power, the snorkel is left off. During this irradiation, an intensive radiation survey by the reactor operations personnel is made around the base of the bulk shield tank which faces the reactor bay and at the surface of the water above the tank. The second reactor run includes

the snorkel and the survey is repeated. In neither case does the survey show any significant increase in the radiation field over that present when the reactor is operating at one megawatt without the assembly present. Also, no streaming can be detected at the snorkel opening. A listing of the gamma and neutron dose equivalent rates is found in Appendix F. These numbers can be compared with those that will be obtained under phase II operation to determine how the uranium changes the radiation fields around the bulk shield tank.

After the two-hour irradiation, the box is allowed to cool in the bulk shield tank for 15 hours. After lifting it out of the water, the box is left hanging to drip dry while it is wiped down with wash cloths. A radiation survey shows very little activity for all parts of the box except at the center of the side nearest the thermalizing column where a dose equivalent rate of eight mrem per hour β-γ at contact with four mrem per hour β and four mrem per hour γ is detected. Smears on all sides of the box show no detectable contamination.

The assembly is lowered onto the floor in the southwest corner of the reactor bay. It is assumed that the graphite might be contaminated so the proper precautions are taken. The area is roped off and the floor covered with plastic. White absorbent laboratory bench paper is placed on top of the plastic so that any graphite dust is caught on the paper and does not become airborne. In case that some does become airborne, a plastic hood is suspended over this corner of the

reactor bay so that the exhaust fan, which is in this corner of the bay, removes the contamination before it spreads to other parts of the bay. A continuous air monitor continuously samples the air.

As the box is opened and the graphite blocks are removed, no detectable airborne activity is found. Smears of the graphite blocks show less than 200 counts per minute on a portable G-M detector, which is very little contamination. The foils are taped to the glass sphere using plastic tape. The tape shows hardly any activation while the glass registers four mrem per hour gross β - γ at contact, one mrem per hour of which is γ. Three people worked in the control area, two handling the graphite and one making the radiation survey.

Thermal Neutron Flux Data

The gold foils used to map the flux around the glass sphere (which simulates the absorption of the uranium) are coincidence counted to determine their absolute activity. They are counted so that 50,000 to 100,000 coincidence counts are obtained to give a statistical error of less than $\frac{1}{2}$%. Then from the absolute activities, the absolute neutron flux is determined (see Appendix F for a listing of the data and the flux calculations). Figure 20 shows the flux as a function of angle around the glass sphere. The purpose of the thermal neutron flux measurements is to determine the magnitude and

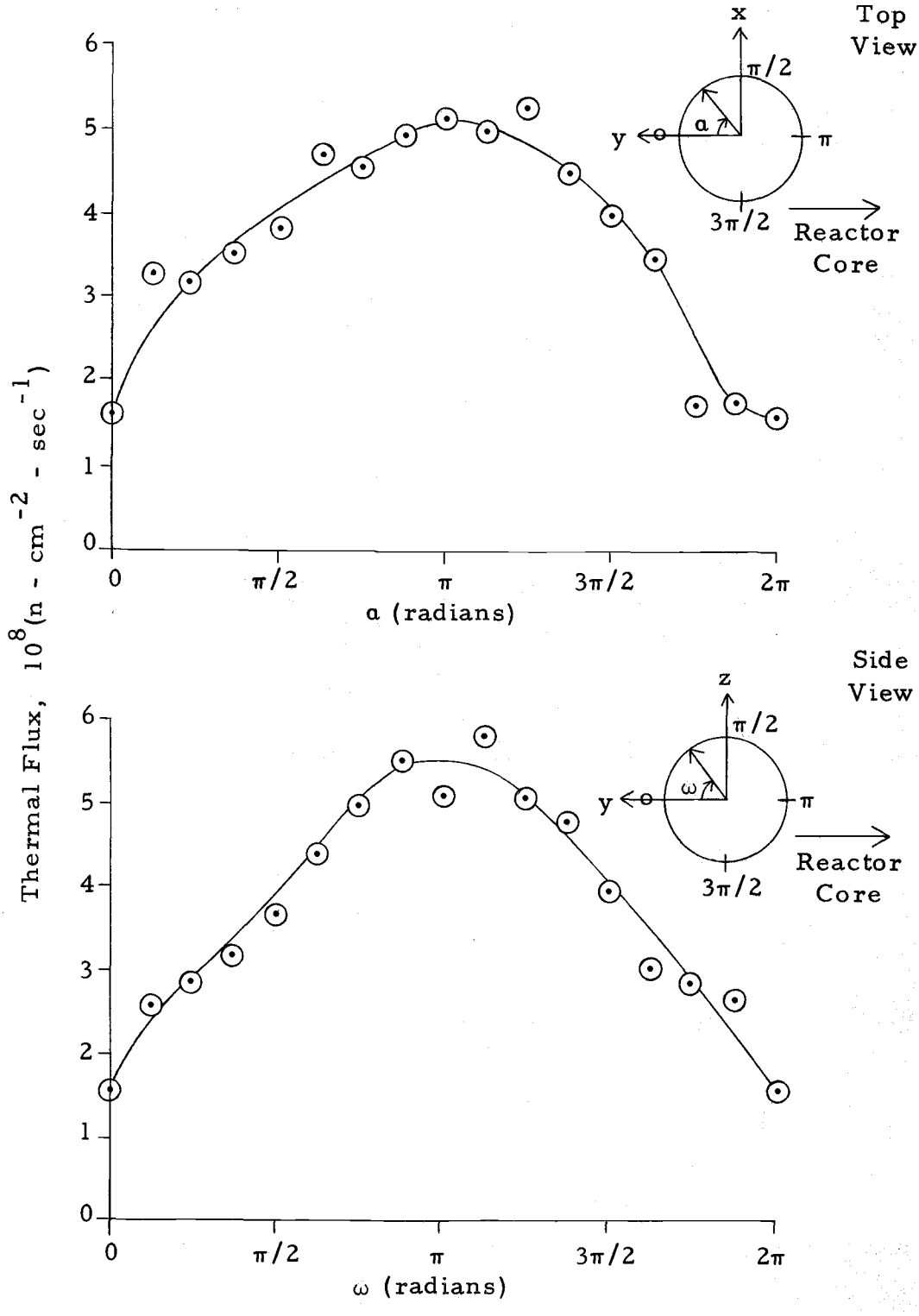

Figure 20. Thermal flux map of the surface of the glass absorber.

anisotropy of the thermal flux at the surface of the absorber. The gold foils are placed at $\pi/8$ radian intervals in two planes of the glass sphere. A right-handed orthogonal coordinate system is used to diagram the sphere where the y-axis coincides with the centerline of the thermalizing column. The x and z-axes are perpendicular to the column with the z-axis being vertical.

The results show that the flux is peaked towards the thermalizing column as expected (see Figure 20). The flux is nearly symmetric in the x and z directions with no gradients across the sphere in these directions. Therefore, the asymmetrical design features such as the aluminum ring stand and the steel base assembly do not significantly affect the thermal flux inside the air cavity. Also, having only one foot of water underneath the graphite does not affect the cavity thermal flux map. The flux gradient across the sphere in the y direction is certainly within acceptable limits. The flux on the side nearest the thermal column is 3.5 times greater than that on the farthest side. For the $\Sigma\Sigma$ facility this gradient is 2.4 to 1 (6). However, since the integrals of the currents tend to vanish at the center of the sphere due to the spherical geometry (16), the central spectrum will be disturbed very little due to this gradient. Also, in the OSU design, samples will be inserted into the central cavity vertically, so the gradient in the y direction is less important than in the $\Sigma\Sigma$ design where the samples are inserted horizontally (5).

The magnitude of the thermal flux ranges from 1.5 to 5.5 x 10^7 n-cm^{-2}-sec^{-1}. Total flux levels of 10^8 n-cm^{-2}-sec^{-1} are recommended for threshold detector work (2). For the NISUS system, this total flux requires a thermal flux of 10^8 n-$cm^{-2}sec^{-1}$ (2). The OSU values are less than this flux. However, the boron in the glass flask absorbs more neutrons than the uranium will. The 800 gram flask contains 13% B_2O_3, 19.8% of the boron, B^{10}, having a thermal absorption cross section of 3840 barns. The first 1.5 cm thickness of uranium, where the thermal absorption will take place, will have a mass of 4.73 x 10^4 grams with a thermal absorption cross section of 7.5 barns. It is expected that when the glass is replaced with the uranium, the thermal flux will increase. Therefore, the magnitude of the thermal flux is sufficiently large.

The cadmium ratio is determined from two samples, one bare and the other cadmium covered, placed at opposite ends of a TRIGA tube. The TRIGA tube is placed at the bottom of the outer air cavity on the side nearest the thermalizing column. A cadmium ratio of 187 is obtained. This value is less than the 500 required for the thermal neutron source (6) and is even less than the 350 obtained in an earlier flux mapping experiment in the water of the bulk shield tank without the fast spectrum facility. It seems that the graphite hohlraum assembly should increase the cadmium ratio over that in the water rather than decrease it. The problem is that since the

foils are at the bottom of the cavity near the aluminum ring stand, the thermal flux is depressed due to the thermal absorption in the aluminum in the stand. Therefore, this cadmium ratio is really not measuring the fraction of thermal to epithermal neutrons being supplied by the thermalizing column. The NISUS assembly has a cadmium ratio of 100 measured in the region of the uranium shells (2). The cadmium ratio that is measured for the OSU facility more probably represents the value that will be obtained in the region of the uranium shells since the bare foil measures a thermal flux equal in magnitude to the average flux on the glass absorber. Further work should include another cadmium ratio experiment to determine what cadmium ratio is actually being measured.

V. CONCLUSIONS

Phase I operation shows that the OSU fast spectrum facility is a workable design. The box assembly can be transported in and out of the bulk shield tank and easily positioned in front of the thermalizing column. The activation of the alloy elements of the aluminum and of the graphite impurities is minimal. The thermal flux measurements show that the magnitude of the flux is sufficiently large and the gradients are within acceptable bounds. The cadmium ratio is low, but it is suspected that the thermal flux is depressed due to the positioning of these foils near the aluminum ring stand. Further work is needed to determine the actual fraction of fast neutrons emerging from the thermalizing column.

The computer code, FASTSPEC, developed by this work, shows that the graphite backed with water produces a spectrum a little softer than the $\Sigma\Sigma$ facility, but one that looks very much like the Karlsruhe Na-2 fast reactor.

Phase II operation will replace the glass absorber with an uranium sphere. It is envisioned that one can quickly proceed to spectral index measurements and cross section determination with Doppler effects and microassemblies following. Time-of-flight measurements could be tried after more experimentation is done on extracting a neutron beam up through the snorkel.

BIBLIOGRAPHY

1. Aluminum Construction Manual, New York: the Aluminum Association, 1959.

2. Azad, Shala, C. B. Besant, J. Emmett, I. C. Richard, C. G. Campbell, T. C. Jones, M. Kerridge, J. Petr, and J. Williams, "NISUS--A neutron intermediate standard uranium source," Irradiation Facilities for Research Reactors, Vienna, Austria: International Atomic Energy Agency, 1973.

3. Bell, George I., and Samuel Glasstone, Nuclear Reactor Theory, New York: Van Nostrand Reinhold Company, 1970.

4. Besant, C. B., J. Emmett, C. G. Campbell, M. Kerridge, and T. Jones, "Design and construction of a fast reactor neutron spectrum generator--NISUS," Nuclear Engineering International, May 1973.

5. Fabry, A., J. C. Schepers, and P. Vandeplas, "Status of the work about the generation of intermediate standard neutron spectra at Mol," Memo to the European American Committee on reactor physics for submission at the London meeting, February, 1969.

6. Fabry, A., Mol, Belgium, Private information.

7. Fabry, A., and P. Vandeplas, "Generation of intermediate standard neutron spectra and their application in fast reactor physics," Fast Reactor Physics, Vienna, Austria: International Atomic Energy Agency, 1, 1968.

8. Glasstone, Samuel, and Alexander Sesonske, Nuclear Reactor Engineering, Princeton, New Jersey: D. Van Nostrand Co., Inc., 1967.

9. Greebler, P., B. A. Hutchins, and R. B. Linford, "Sensitivity of fast reactor economics to uncertainties in nuclear data," Nuclear Applications, 4, May 1968.

10. Hellstrand, E., and A. B. Atonenerge, "Comments about a facility for a standard fast spectrum," Sweden, April 2, 1969.

11. Higdon, Archie, Edward H. Ohlsen, William B. Stiles, and John A. Weese, Mechanics of Materials, New York: John Wiley and Sons, Inc., 1967.

12. Kuchle, M., and E. Wattecamps, "Proposal for a standard spectrum to check techniques of fast neutron spectrum measurements," Paper submitted for presentation at the eleventh EACRP meeting in London, February 10-14, 1969.

13. Lamarsh, John R., Introduction to Nuclear Reactor Theory, Reading, Massachusetts: Addison-Wesley Publishing Company, Inc., 1966.

14. NISUS, Winfrith Fast Reactor Physics Division, Atomic Energy Establishment, Dorchestor, Dorset, United Kingdom.

15. Reactor Physics Constants, Argonne National Laboratory, USAEC, Division of Technical Information, ANL 5800, 1963.

16. Spinrad, B. I., Oregon State University, Corvallis, Oregon, Private information.

17. Zartman, Ira F., "The future U. S. fast reactor physics program," ANL 7320, 1967.

APPENDICES

Appendix A

Calculations presented below show the effectiveness of the boral curtain for stopping thermal neutrons.

Overall composition (including B_4C core and Al clad):

Al = 77% by weight

B_4C = 23% by weight

Density = 2.5 gram/cm^3 (8)

Absorption cross sections (2200 m/sec):

σ_{Al} = 0.235 barns

σ_B = 759 barns (13)

Average cross sections:

$$\bar{\sigma}_{Al} = \frac{0.235}{1.128} = 0.208 \text{ barns}$$

$$\bar{\sigma}_B = \frac{759}{1.128} = 673 \text{ barns}$$

Atom densities:

$$N_{Al} = \frac{(0.77)(2.5)(0.6025 \times 10^{24})}{27} = 0.043 \times 10^{24}$$

$$N_B = \frac{4(0.23)(2.5)(0.6025 \times 10^{24})}{55.2} = 0.0251 \times 10^{24}$$

Macroscopic cross section for boral:

$$\Sigma_a = N_{Al}(\bar{\sigma}_{Al}) + N_B(\bar{\sigma}_B)$$

$$= (0.043)(0.2083) + (673)(0.0251) = 16.9 \text{ cm}^{-1}$$

Assume the thermal column is a uniform planar source, then the fraction of thermal neutron flux left after traveling through 1/8" of boral:

$$\frac{\phi}{\phi_o} = \frac{2e^{-\Sigma_a t}}{\Sigma_a t + 3} = \frac{2e^{-(16.9)(0.3175)}}{(16.9)(0.3175) + 3} = 1.12 \times 10^{-3} = 0.112\%$$

Appendix B

The following calculations are for the aluminum box design. Pressure on the box walls due to water at a depth of 12 feet corresponding to the bottom of the bulk shield tank is given below:

$$\text{Pressure} = (62.4\ \text{lb/ft}^3)(12\ \text{ft})(\text{ft}^2/144\ \text{in}^2) = 5.2\ \text{psi}.$$

The design pressure on each plate of the box will be 5.2 psi.

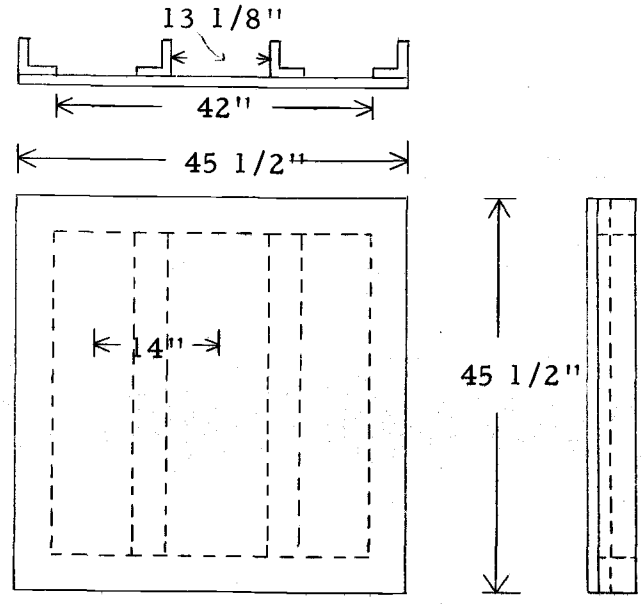

Each plate of the box is constructed as shown in the diagram above. Consider a $45\frac{1}{2}$" beam, 14" wide, composed of one of the angles and the surface of the plate that it supports. Pressure is assumed to be 5.2 psi from the outside only and constant over each plate. This assumption is conservative because the top plate is subject to less pressure, the pressure on each side varies according to depth, and the weight of the graphite opposes the water pressure on the bottom

plate. The weight of the graphite on the bottom plate during transport is considered in Appendix C.

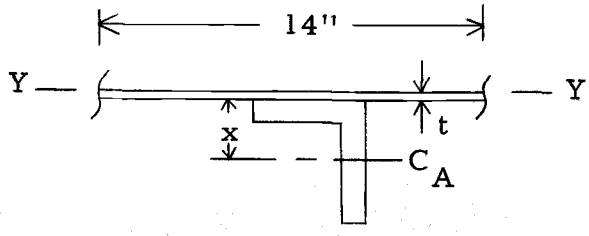

For the angle:

I_{C_A} = 0.31 in^4

area = 0.81 in^2

t = 0.125"

x = 0.66 in

C_A = centroid of 2" x $1\frac{1}{2}$" x $\frac{1}{4}$" angle

weight = 0.96 lb/ft

(1)

Centroid of the cross section of the beam:

$$C = \frac{\text{(area of plate)(distance from Y-Y) + (area of angle)(distance from Y-Y)}}{\text{(area of plate) + (area of angle)}}$$

$$= \frac{(0.125)(14)(0.0625) + (0.81)(0.785)}{(0.125)(14) + (0.81)}$$

$$= \frac{0.745}{2.56} = 0.291 \text{ in} \quad \text{from the top of beam}$$

Moment of inertia of the beam:

$$I = (1/12)(\text{base})(\text{height})^3 + (\text{area})(\text{distance from centroid})^2$$

$$= (1/12)(0.125)^3(14) + (0.125)(14)(0.229)^2 + 0.31 + (0.81)(0.494)^2$$

$$= 0.602 \text{ in}^4$$

Weight per unit length:

$$w = \frac{(14)(45.5)(5.2)}{45.5}$$

$$= 72.8 \text{ lb/in}$$

Now let us proceed to determine the maximum displacement of the beam. The beam is statically indeterminant since it is fixed at both ends.

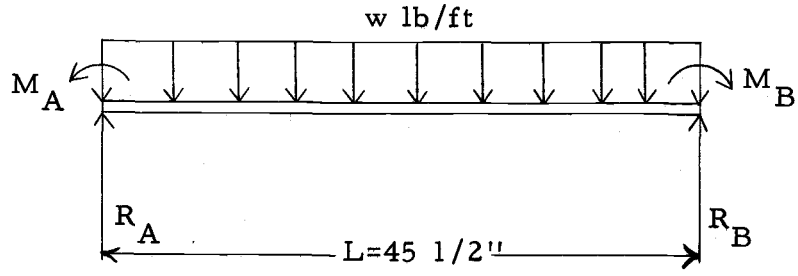

$$\sum \overset{+}{\curvearrowleft} M \text{ about } R_B = 0 = M_A - M_B + wL^2/2 - R_A L$$

$$R_A L = M_A - M_B + wL^2/2$$

$$R_A = (M_A - M_B)/L + wL/2$$

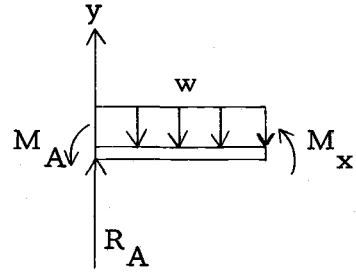

$$EId^2y/dx^2 = \overset{+}{\curvearrowleft} M_x = M_A - R_A x + wx(x/2)$$

$$= M_A - [(M_A - M_B)/L + wL/2]\, x + wx^2/2$$

$$EIdy/dx = M_A x - [(M_A - M_B)/L + wL/2]\, x^2/2 + wx^3/6 + C_1$$

$$EIy = M_A x^2/2 - [(M_A - M_B)/L + wL/2]\, x^3/6 + wx^4/24 + C_1 x + C_2$$

Evaluate M_A, M_B, C_1, C_2 from the four boundary conditions:

1. $dy/dx = 0$ at $x = 0$

$$C_1 = 0$$

2. $dy/dx = 0$ at $x = L$

$$0 = M_A L - [(M_A - M_B)/L + wL/2]\, L^2/2 + wL^3/6$$

$$0 = M_A L - M_A L/2 + M_B L/2 - wL^3/4 + wL^3/6$$

$$0 = M_A L/2 + M_B L/2 - 6wL^3/24 + 4wL^3/24$$

$$M_A L/2 = -M_B L/2 + wL^3/12$$

$$M_A = -M_B + wL^2/6$$

3. $y = 0$ at $x = 0$

$$C_2 = 0$$

4. $y = 0$ at $x = L$

$$0 = M_A L^2/2 - [(M_A - M_B)/L + wL/2]\, L^3/6 + wL^4/24$$

$$0 = L^2/2\,[-M_B + wL^2/6] - [(-M_B + wL^2/6 - M_B)/L + wL/2]\, L^3/6 + wL^4/24$$

$$0 = -M_B L^2/2 + wL^4/12 + 2M_B L^2/6 - wL^4/9 + wL^4/24$$

$$0 = -3M_B L^2/6 + 2wL^4/24 + 2M_B L^2/6 - wL^4/9 + wL^4/24$$

$$0 = -M_B L^2/6 - wL^4/9 + 3wL^4/24$$

$$M_B L^2/6 = -wL^4/9 + wL^4/8$$

$$M_B = -2wL^2/3 + 3wL^2/4$$

$$= -8wL^2/12 + 9wL^2/12$$

$$M_B = wL^2/12 \text{ lb-in clockwise}$$

$$M_A = -M_B + wL^2/6$$

$$= -wL^2/12 + wL^2/6$$

$$M_A = wL^2/12 \text{ lb-in counterclockwise}$$

Now, $$EIy = (wL^2/12)x^2/2 - wL/2(x^3/6) + wx^4/24$$

$$= wL^2x^2/24 - wLx^3/12 + wx^4/24$$

From symmetry we know that y_{max} occurs at L/2:

$$EIy_{max} = wL^4/96 - wL^4/96 + wL^4/384$$

$$= wL^4/384$$

$$y_{max} = wL^4/384EI = \frac{(72.8)(45.5)^4}{(384)(0.602)(10^7)} = 0.135 \text{ in}$$

which is the deflection in the angles.

$$R_A = (M_A - M_B)/L + wL/2 = (72.8)(45.5)/2 = 1656 \text{ lb}$$

Shear stress is maximum at the reaction, so

$$\tau_{max} = 1656 \text{ lb}/2.56 \text{ in}^2 = 647 \text{ psi}$$

Moment at the center of the beam:

$$M_x = M_A - R_A x + wx^2/2$$

$$= wL^2/12 - 1656L/2 + wL^2/8$$

$$= (72.8)(45.5)^2/12 - (1656)(45.5)/2 + (72.8)(45.5)^2/8$$

$$= 6275 \text{ lb-in clockwise}$$

Maximum fiber stress occurs at the center, so

$\sigma_{max} = My/I$ where y is the distance from the neutral surface to the farthest point away on the cross section at the center of the beam (y = 1.84 in).

$$\sigma_{max} = (6275 \text{ lb-in})(1.84 \text{ in})/0.602 \text{ in}^4$$

$$= 19,100 \text{ psi T (tension)}$$

Determine the deflection in the plate between the two angle stiffeners.

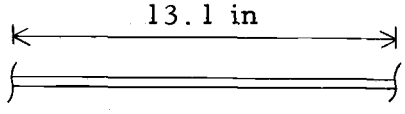

centroid = 0.0625"

thickness = 0.125"

Looking at an one inch strip,

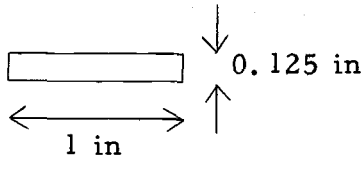

$$I = (1/12)(\text{base})(\text{height})^3$$

$$= (1/12)(1)(0.125)^3$$

$$= 1.63 \times 10^{-4} \text{ in}^4$$

the maximum deflection will probably occur about one foot from the bottom since the plate is fixed to the angle at the bottom and the maximum pressure occurs at the bottom. So, the pressure on the strip is the water pressure at 11 feet which is 4.77 psi.

The distributed load, w:

$$w = (13.1)(1)(4.77)/13.1 = 4.77 \text{ lb/in}$$

This beam is again indeterminant as the previous beams were, so y_{max} is given by:

$$y_{max} = wL^4/(384)EI = \frac{(4.77)(13.1)^4}{(384)(10^7)(1.63 \times 10^{-4})}$$

$$= 0.224 \text{ in} \quad \text{which is the deflection in the plate}$$

$$R_A = wL/2 = (4.77 \text{ lb/in})(6.5 \text{ in}) = 31 \text{ lb}$$

The shear stress is maximum at the reaction:

$$\tau_{max} = 31 \text{ in}/0.125 \text{ in}^2 = 284 \text{ psi}$$

The moment at the center of the beam:

$$M_x = M_A - R_A x + wx^2/2$$

$$M_{L/2} = wL^2/12 - R_A L/2 + wL^2/8$$

$$= (4.77)(13.1)^2/12 - (31)(13.1)/2 + (4.77)(13.1)^2/8$$

$$= 32.5 \text{ lb-in clockwise}$$

The maximum fiber stress:

$$\sigma_{max} = My/I$$

$$= (32.5)(0.0625)/(1.63 \times 10^{-4})$$

$$= 1.25 \times 10^4 \text{ psi}$$

Appendix C

The base and transport assembly design calculations appear on the following pages.

Weight of aluminum box:

5 $45\frac{1}{2}$" x $45\frac{1}{2}$" x 1/8" plates, vol. = 259 in^3, ρ = 0.098 lb/in^3

weight = 126.8 lb

1 49" x $47\frac{1}{4}$" x 1/8" plate, vol. = 289 in^3, ρ = 0.098 lb/in^3

weight = 28.4 lb

12 2" x $1\frac{1}{2}$" x $\frac{1}{4}$" angles $45\frac{1}{2}$" long @ 0.96 lb/ft each

weight = 43.7 lb

9 $1\frac{1}{2}$" x $1\frac{1}{2}$" x $\frac{1}{4}$" angles $45\frac{1}{2}$" long @ 0.81 lb/ft each

weight = 27.6 lbs

3 $1\frac{1}{2}$" x $1\frac{1}{2}$" x $\frac{1}{4}$" angles 49" long @ 0.81 lb/ft each

weight = 12.3 lb

Total weight of aluminum = 238.8 lb

Weight of graphite:

Assume spherical hole in $44\frac{1}{2}$" cube (113 cm)

Volume = $(113)^3 - (4\pi/3)(26)^3 = 1.37 \times 10^6\ cm^3$

Weight = $(1.37 \times 10^6\ cm^3)(1.7\ gram/cm^3)(lb/454\ grams)$

= 5136 lb

Weight of uranium sphere:

$$\text{Weight} = (18.95)(4\pi/3)[(12.25)^3 - (7.25)^3] = 116 \text{ Kg} = 254 \text{ lb}$$

Contents of sphere, stand, and snorkel (estimate): 18 lb

Weight of base:

7" channel, 108" @ 12.25 lb/ft = 110.2 lbs

3" channel, 126" @ 4.1 lb/ft = 43 lbs

Total weight which must be lifted = 5800 lbs

Channel base design calculations:

See the mechanical design chapter (Figures 8 and 9) for the diagrams of the base assembly. Each 7" channel has 2900 lbs distributed as shown below:

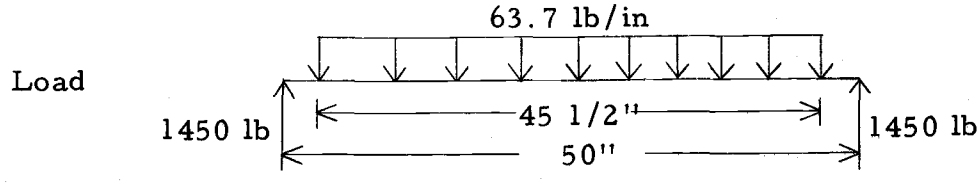

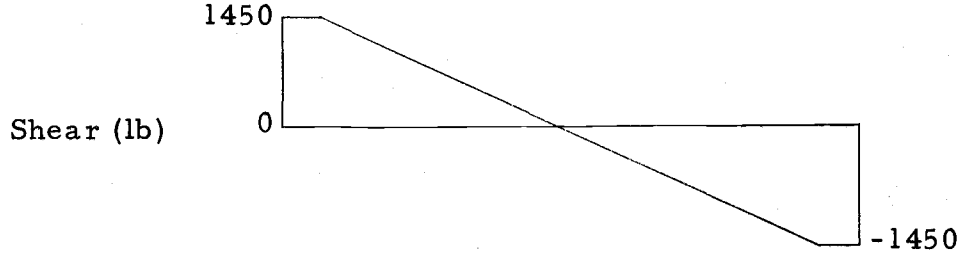

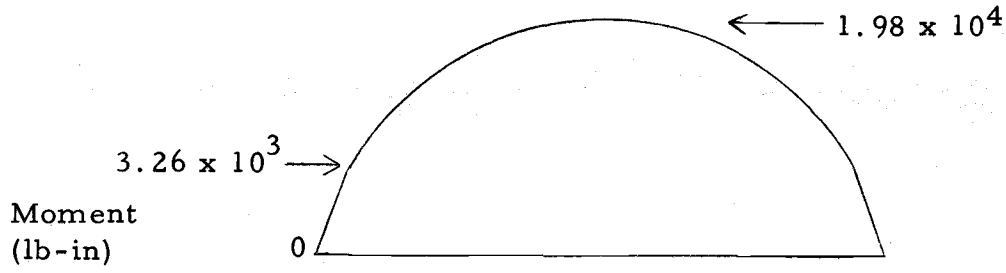

The elastic and ultimate strength for structural steel are 36 and 66 ksi respectively.

Maximum fiber stress: (For 7", 12.25 lb channel, $z = 0.71\ in^3$ and the cross sectional area = $3.58\ in^2$) (11)

$$\sigma_{max} = M_{max}(y)/I$$

$$= M_{max}/z = 1.98 \times 10^4\ lb\text{-}in/0.71\ in^3 = 2.79 \times 10^4\ psi$$

Maximum vertical shear stress:

$$\tau_{max} = 1450\ lb/3.58\ in^2 = 405\ psi$$

Maximum deflection: ($E = 2.9 \times 10^7$ psi for structural steel)

$$y_{max} = 5(w)(L^4)/(384)(E)(I)$$

for a simply supported beam and uniform loading (11); consider only the deflection for the length of the beam that the box sits on.

$L = 45.5"$, $w = 63.7\ lb/in$, $I = 1.2\ in^4$ (11)

$$y_{max} = \frac{(5)(63.7)(45.5)^4}{(384)(2.9)(10^7)(1.2)} = 0.102\ in$$

The fiber stress, shear stress, and deflection show that the load on the 7" channels is safe. A conservative estimate for the 3" channels is that each channel must support an area of 14" x 31.5" = 441 in^2. There is a load of 5700 lbs (everything except the 7" channels) distributed on the floor of the box. The pressure would then be 5700 lbs/2070 in^2 = 2.75 psi. So the load on the 3" channel is:

$$w = (441)(2.75)/31.5$$

$$= 38.5 \text{ lb/in.}$$

Load

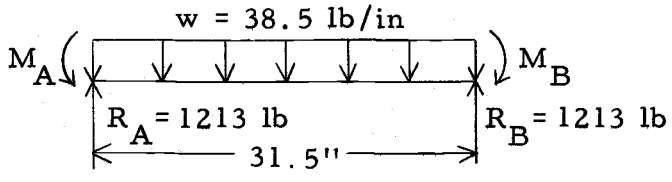

3" x 1½" channel:

w = 4.1 lb/ft

$I = 0.20 \text{ in}^4$

$z = 0.21 \text{ in}^3$

$\text{area} = 1.19 \text{ in}^2$

Shear (lb)

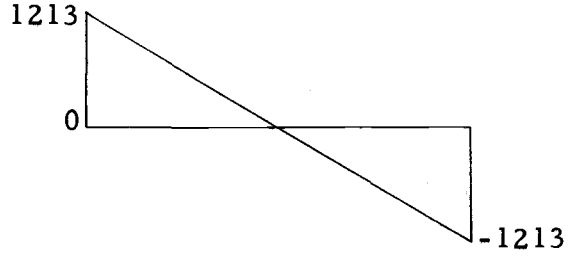

(11)

Moment (lb-in)

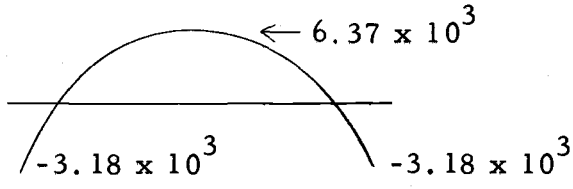

From Appendix B:

$$M_A = M_B = wL^2/12 = (38.5)(31.5)^2/12 = 3.18 \times 10^3 \text{ lb-in}$$

Checking the stresses and deflection:

$$\sigma_{max} = M_{max}/z = 6.37 \times 10^3/0.21 = 3.03 \times 10^4 \text{ lb-in}$$

$$\tau_{max} = \text{Max shear/area} = 1213/1.19 = 1019 \text{ psi}$$

$$y_{max} = wL^4/(384)EI = \frac{(38.5)(31.5)^4}{(384)(2.9)(10^7)(0.20)} = 0.017 \text{ in}$$

All three above show that the load on the 3" channels is safe.

Now let us consider the I-beam separator bar.

4" x 2 5/8" I-beam:

$$w = 9.5 \text{ lb/ft}$$

$$\text{area} = 2.76 \text{ in}^2$$

$$I = 6.4 \text{ in}^4$$

$$z = 3.3 \text{ in}^3 \qquad (11)$$

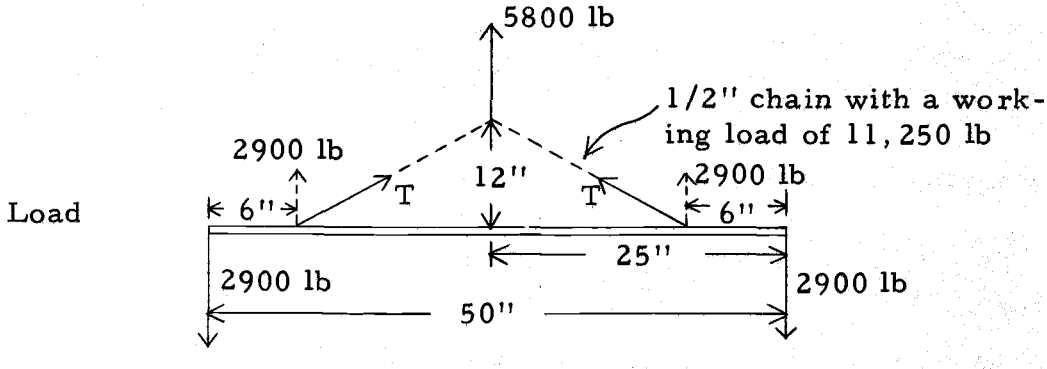

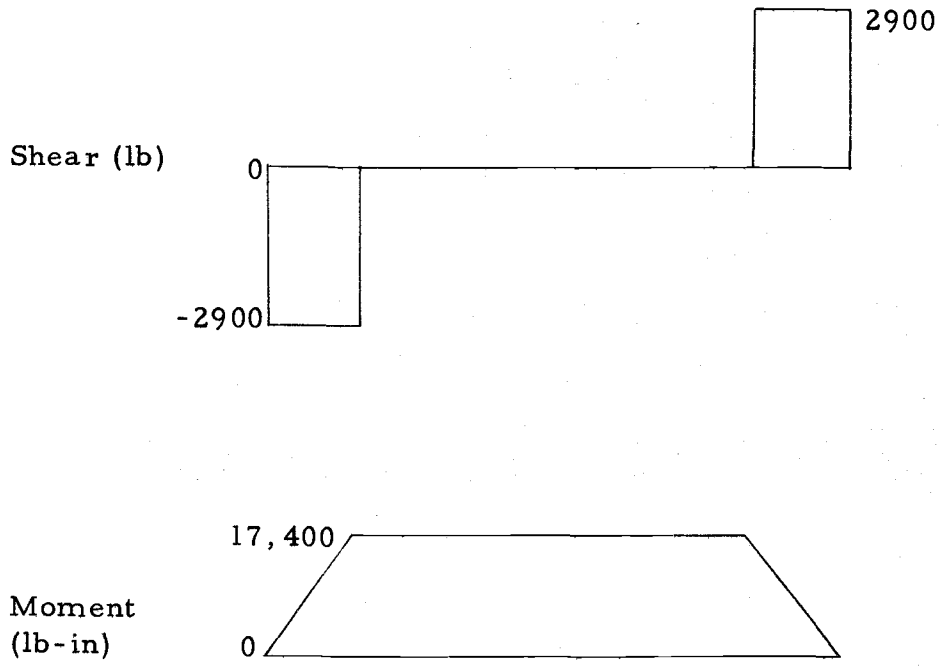

$$\sigma_{max} = M_{max}/z = 17,400/3.3 = 5272 \text{ lb-in}$$

$$\tau_{max} = \text{Max shear/area} = 2900/2.76 = 1051 \text{ psi}$$

$$T = 2900/\cos\theta = 5438 \text{ lb}$$

To determine whether the base stand will fail, we must first determine the actual weight on it after allowing for the buoyancy of the water. Assume the volume displaced is $45\frac{1}{2}'' \times 45\frac{1}{2}'' \times 45\frac{1}{2}''$ and that the materials have weight equal to 5800 pounds. First, if the box does not leak, the net force on the stand is:

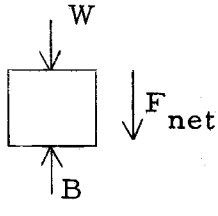

$$B = (45\tfrac{1}{2}'' \times 45\tfrac{1}{2}'' \times 45\tfrac{1}{2}'')(\text{ft}/12'')^3(62.4 \text{ lb/ft}^3)$$

$$= 3400 \text{ lb}$$

$$F_{net} = 5800 - 3400 = 2400 \text{ lb}$$

Second, if the box leaks then the $20\frac{1}{2}$" diameter air cavity in the center will fill with water, so, the B force will decrease:

$$B = (45\tfrac{1}{2}\text{" x } 45\tfrac{1}{2}\text{" x } 45\tfrac{1}{2}\text{")}(\text{ft}/12\text{"})^3(62.4\ \text{lb}/\text{ft}^3)$$
$$- (20\tfrac{1}{2}\text{" x } 20\tfrac{1}{2}\text{" x } 20\tfrac{1}{2}\text{")}(\text{ft}/12\text{"})^3(62.4\ \text{lb}/\text{ft}^3)$$
$$= 3400 - 311 = 3089\ \text{lbs}$$
$$F_{net} = 5800 - 3089 = 2711\ \text{lb}$$

So the worst case would be if the box should fill with water, then the force on the stand would be about 2700 pounds. On each leg of the stand will be 675 pounds. To determine how to treat each to see if it will fail, the slenderness ratio of the leg as a column is found.

2" x 2" x 1/8" angle

area = $0.48\ \text{in}^2$

L = length = 11 in

r = radius of gyration = 0.4 in

slenderness ratio = L/r = 11/0.4 = 27.5

This value can be considered in the compression block range where the material would fail under compressive fiber stress (11).

$$\sigma_{max} = 675\ \text{lb}/0.48\ \text{in}^2 = 1406\ \text{psi}$$

This fiber stress is much less than the 36,000 psi yield strength of structural steel.

The design for the pads of the base stand is considered next. The design pressure on the floor of the bulk shield tank is 2000 lb/ft^2 (13.89 psi), while the pressure due to 12 feet of water is 5.2 psi. The maximum weight which the assembly could exert on the floor is 2700 pounds.

$$P_{max} = 13.89 \text{ psi} - 5.2 \text{ psi} = 8.69 \text{ psi}$$

$$\text{Required area, } A = 2700 \text{ lb}/8.69 \text{ psi} = 310.7 \text{ in}^2$$

The weight is distributed on four legs, so the area per leg:

$$A_{each} = 310.7 \text{ in}^2/4 = 77.7 \text{ in}^2$$

Each pad is 10" x 9" which gives a sufficient area.

Appendix D

Consider the following problem where an infinite slab of graphite with a planar fission source at its midplane is immersed in an infinite pool of water.

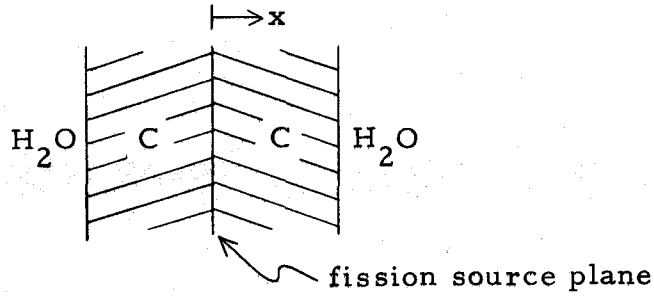

Multigroup equation for slab geometry:

$$-\frac{d}{dx} D(E) \frac{d}{dx} \phi(E) + \Sigma_t(E)\phi(E) = \int_0^\infty \Sigma_s(E' \rightarrow E)\phi(E')dE' + FS$$

where D = diffusion coefficient

ϕ = neutron flux

Σ_t = total cross section

Σ_s = scattering cross section

FS = fission source

$$-\frac{d}{dx} D_i \frac{d}{dx} \phi_i + \Sigma_{t_i} \phi_i = \sum_{j=1}^{N} \Sigma_s(j \rightarrow i)\phi_j + FS$$

$$-\frac{d}{dx} D_i \frac{d}{dx} \phi_i + \Sigma_{t_i} \phi_i = \sum_{j=1}^{i-1} \Sigma_s(j \rightarrow i)\phi_j + \Sigma_s(i \rightarrow i)\phi_i + \sum_{j=i+1}^{N} \Sigma_s(j \rightarrow i)\phi_i + FS$$

The last term is zero because there is no up-scatter.

$$- \frac{d}{dx} D_i \frac{d}{dx} \phi_i + \Sigma_{t_i} \phi_i - \Sigma_s(i \rightarrow i) \phi_i = \sum_{j=1}^{i-1} \Sigma_s(j \rightarrow i) \phi_j + FS = s_i$$

$$\Sigma_{t_i} - \Sigma_s(i \rightarrow i) = \Sigma_{R_i}$$

Now derive the difference equation. Δk is constant for each region.

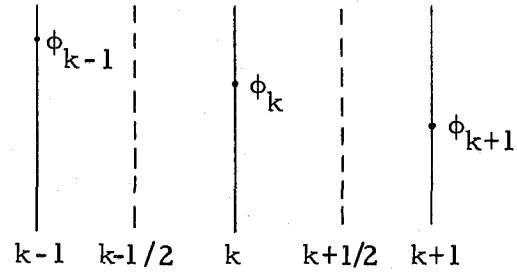

$$\int_{k-\frac{1}{2}}^{k+\frac{1}{2}} - \frac{d}{dx} D_i \frac{d}{dx} \phi_i \, dx = - D_i \frac{d}{dx} \phi_i \Big|_{k-\frac{1}{2}}^{k+\frac{1}{2}} = -D_{i,k+\frac{1}{2}} \frac{d}{dx} \phi_{,} + D_{i,k-\frac{1}{2}} \frac{d}{dx} \phi_i$$

$$\int_{k-\frac{1}{2}}^{k+\frac{1}{2}} \Sigma_{R_i} \phi_i \, dx = \phi_{i,k} (\Sigma_{R_{i,k+\frac{1}{2}}} \Delta k + \Sigma_{R_{i,k-\frac{1}{2}}} \Delta k)/2$$

$$\int_{k-\frac{1}{2}}^{k+\frac{1}{2}} s_i \, dx = k s_{i,k} = S_{i,k}$$

$$-D_{i,k+\frac{1}{2}}(\phi_{i,k+1} - \phi_{i,k})/\Delta k + D_{i,k-\frac{1}{2}}(\phi_{i,k} - \phi_{i,k-1})/\Delta k$$

$$+ (\Sigma_{R_{i,k+\frac{1}{2}}} \Delta k + \Sigma_{R_{i,k-\frac{1}{2}}} \Delta k) \phi_{i,k}/2 = S_{i,k}$$

The source is just the fission source for the first group since there are no higher groups from which the neutrons can scatter. So, the above equation can be put into a tridiagonal matrix and the fluxes solved. Then for the second group, the flux at each point is used to find the source at each point, k. Then the tridiagonal matrix is used to again solve for the fluxes in the second group. This procedure is continued for six groups.

The last equation is now prepared for insertion into a tridiagonal matrix. First, define the values of D and Σ to be the values of the material to the left of the mesh point. That is, $D_{k-\frac{1}{2}} \rightarrow D_k$ and $D_{k+\frac{1}{2}} \rightarrow D_{k+1}$ and likewise with Σ. Then the equation becomes: (let h be the mesh spacing)

$$-D_{i,k+1}(\phi_{i,k+1}-\phi_{i,k})/h + D_{i,k}(\phi_{i,k}-\phi_{i,k-1})/h$$

$$+ (\Sigma_{R_{i,k+1}} h + \Sigma_{R_{i,k}} h)\phi_{i,k}/2 = S_{i,k}$$

$$-(D_{i,k+1}/h)\phi_{i,k+1} + (D_{i,k+1}/h + D_{i,k}/h + \Sigma_{R_{i,k+1}} h/2$$

$$+ \Sigma_{R_{i,k}} h/2)\phi_{i,k} - (D_{i,k}/h)\phi_{i,k-1} = S_{i,k}$$

Now, α, β, and γ are defined such that the above equation can be written as follows:

$$-\alpha_k \phi_{i,k+1} + \beta_k \phi_{i,k} - \gamma_k \phi_{i,k-1} = S_{i,k}$$

The two boundary conditions are that the current is zero at $k=1$ and that the flux is zero at $k=N$.

For $k=1$:

$$-\alpha_1 \phi_{i,2} + \beta_1 \phi_{i,1} - \gamma_1 \phi_{i,2} = S_{i,1}$$

For $k=N$:

$$\beta_N \phi_{i,N} - \gamma_N \phi_{i,N-1} = S_{i,N}$$

So, there are N equations in N unknowns which are to be solved, where N is the number of mesh points. These equations are placed in the following matrix:

$$\begin{bmatrix} \beta_1 & (-\alpha_1-\gamma_1) & & & & & \\ -\gamma_2 & \beta_2 & -\alpha_2 & & & & \\ & -\gamma_3 & \beta_3 & -\alpha_3 & & & \\ & & \ddots & \ddots & \ddots & & \\ & & & & & & \\ & & & -\gamma_{n-1} & \beta_{n-1} & -\alpha_{n-1} & \\ & & & & -\gamma_n & \beta_n & \end{bmatrix} \begin{bmatrix} \phi_{i,1} \\ \phi_{i,2} \\ \phi_{i,3} \\ \vdots \\ \phi_{i,N-2} \\ \phi_{i,N-1} \\ \phi_{i,N} \end{bmatrix} = \begin{bmatrix} S_{i,1} \\ S_{i,2} \\ S_{i,3} \\ \vdots \\ S_{i,N-2} \\ S_{i,N-1} \\ S_{i,N} \end{bmatrix}$$

The above matrix could be solved using Gaussian elimination, but the tridiagonal matrix lends itself to a quicker solution. A matrix, $\bar{\bar{A}}$, can be factored into two matrices, $\bar{\bar{C}}$ and $\bar{\bar{B}}$, if $\bar{\bar{A}}$ is of the following form:

$$\bar{\bar{A}} = \begin{bmatrix} a_{11} & a_{12} & & & & & & \\ a_{21} & a_{22} & a_{23} & & & & & \\ & a_{32} & a_{33} & a_{34} & & & & \\ & & & \ddots & & & & \\ & & & & \ddots & & & \\ & & & & & a_{n-1,n-2} & a_{n-1,n-1} & a_{n-1,n} \\ & & & & & & a_{n,n-1} & a_{n,n} \end{bmatrix}$$

Note that in these matrices the elements not shown are zero. The following matrix equation solution is taken from the class notes of Professor Alan Robinson's computational methods in nuclear engineering.

$$\bar{\bar{C}} = \begin{bmatrix} 1 & & & & & & \\ c_{21} & 1 & & & & & \\ & c_{32} & 1 & & & & \\ & & \ddots & \ddots & & & \\ & & & & c_{n-1,n-2} & 1 & \\ & & & & & c_{n,n-1} & 1 \end{bmatrix}$$

$$\bar{\bar{B}} = \begin{bmatrix} b_{11} & b_{12} & & & & \\ & b_{22} & b_{23} & & & \\ & & b_{33} & b_{34} & & \\ & & & \ddots & \ddots & \\ & & & & b_{n-1,n-1} & b_{n-1,n} \\ & & & & & b_{n,n} \end{bmatrix}$$

Since, $\bar{\bar{A}} = \bar{\bar{C}} \cdot \bar{\bar{B}}$, then the following relationships hold:

$$b_{11} = a_{11} \qquad c_{21}b_{11} = a_{21} \qquad c_{21}b_{12} + b_{22} = a_{22}$$

$$b_{12} = a_{12} \qquad c_{21} = a_{21}/b_{11} \qquad b_{22} = a_{22} - c_{21}b_{12}$$

or, in general:

$$c_{p,p-1} = a_{p,p-1}/b_{p-1,p-1}$$

$$b_{p,p+1} = a_{p,p+1}$$

$$b_{p,p} = a_{p,p} - c_{p,p-1}b_{p-1,p}$$

The equations are now in the form: $(\bar{\bar{C}} \cdot \bar{\bar{B}})\bar{x} = \bar{y}$

Let $\bar{z} = \bar{\bar{B}}\,\bar{x}$ so $\bar{\bar{C}}\,\bar{z} = \bar{y}$

$$\begin{bmatrix} 1 & 0 & 0 \\ c_{21} & 1 & 0 \\ 0 & c_{32} & 1 \end{bmatrix} \quad \begin{bmatrix} z_1 \\ z_2 \\ z_3 \end{bmatrix} = \begin{bmatrix} y_1 \\ y_2 \\ y_3 \end{bmatrix}$$

$$z_1 = y_1$$

$$c_{21}z_1 + z_2 = y_2 \quad \text{then} \quad z_2 = y_2 - c_{21}z_1$$

$$c_{32}z_2 + z_3 = y_3 \quad \text{then} \quad z_3 = y_3 - c_{32}z_2$$

In general: $z_p = y_p - c_{p,p-1}z_{p-1}$ Equation (A)

Next, solve $\bar{\bar{B}}\,\bar{x} = \bar{z}$ where $\bar{x}$ is the unknown.

$$\begin{bmatrix} b_{11} & b_{12} & 0 \\ 0 & b_{22} & b_{23} \\ 0 & 0 & b_{33} \end{bmatrix} \quad \begin{bmatrix} x_1 \\ x_2 \\ x_3 \end{bmatrix} = \begin{bmatrix} z_1 \\ z_2 \\ z_3 \end{bmatrix}$$

$b_{11}x_1 + b_{12}x_2 = z_1$ then $x_1 = (z_1 - b_{12}x_2)/b_{11}$

$b_{22}x_2 + b_{23}x_3 = z_2$ then $x_2 = (z_2 - b_{23}x_3)/b_{22}$

$b_{33}x_3 = z_3$ then $x_3 = z_3/b_{33}$

In general: $x_p = z_p/b_{pp}$ Equation (B)

$x_{p-1} = (z_{p-1} - b_{p-1,p}x_p)/b_{p-1,p-1}$ Equation (C)

Use equation (A) to calculate all the z_p's, then use equations (B) and (C) to solve for the x_p's.

Now, the general notation is ready to be converted into the specific notation of the original matrix equation.

$$y_p = S_{i,k} \qquad k = 1 \text{ to } N$$

$$c_{p,p-1} = a_{p,p-1}/b_{p-1,p-1} = -\gamma_{i,k}/\beta_{i,k-1} \qquad k = 2 \text{ to } N$$

$$b_{p-1,p} = -\alpha_{i,k-1} \qquad k = 3 \text{ to } N$$

$$b_{p-1,p-1} = \beta_{i,k-1} \qquad k = 2 \text{ to } N$$

$$x_p = \phi_{i,k} \qquad k = 1 \text{ to } N$$

Equation (A) now becomes:

$$z_{i,1} = S_{i,1}$$

$$z_{i,k} = S_{i,k} + (\gamma_{i,k}/\beta_{i,k-1})\, z_{i,k-1} \qquad k = 2 \text{ to } N$$

For the set of (B) and (C) equations:

$$\phi_{i,N} = z_{i,N}/\beta_{i,N}$$

$$\phi_{i,k} = (z_{i,k} + a_{i,k}\phi_{i,k+1})/\beta_{i,k} \qquad k = N-1 \text{ to } 2$$

$$\phi_{i,1} = (z_{i,1} + (a_{i,1} + \gamma_{i,1})\phi_{i,2})/\beta_{i,1}$$

$S_{i,k}$ is determined from integrating the source from $x = k - \frac{1}{2}$ to $k + \frac{1}{2}$ for each space point as is done on page 78.

$$S_{i,k} = FS + \sum_{j=1}^{i-1} (\Sigma_s(j \rightarrow i)_{k+1} h + \Sigma_s(j \rightarrow i)_k h)\phi_{j,k}/2$$

Program SLAB is listed on the next several pages preceded by its data file called DATA. DATA includes three columns. Column one is the removal cross section where the first six values are for the graphite and the last six for the water. Column two is the diffusion coefficient for the graphite and water, six values for each, respectively. The last column is the fission fraction for groups one through six.

0.0095	0.73	0.6667
0.02166	1.512	0.3333
0.0353	0.891	0
0.010	0.880	0
0.01468	0.879	0
0.00028	0.84	0
0.05966	1.005	

0.2203	1.238
0.5855	0.740
0.2079	0.6029
0.3292	0.561
0.0197	0.150

```
      PROGRAM SLAB
C     SIX GROUP DIFFUSION THEORY REPRESENTATION OF NEUTRON
C          SPECTRUM OF GRAPHITE HOHLRAUM BACKED WITH WATER
C          (TWO REGIONS; 200 MESH POINTS MAXIMUM)
      DIMENSION ALPHA(6,200), BETA(6,200), GAMMA(6,200),
     1     S(200), Z(200), CSRC(6), CSRW(6), FX(6),
     2     DC(6),DW(6),B(200),C(200),PHI(6,200)
   10 X=TTYIN(4HGRAP,4HHITE,4H THI,4HCKNE,4HSS(C,4HM)= )
      NC=TTYIN(4HNUMB,4HER O,4HF ME,4HSH P,4HOINT,4HS IN,
     1     4H CAR,4HBON=)
      FS=TTYIN(4HFISS,4HION ,4HSOUR,4HCE(N,4HEUTR,4HONS/,
     1     4HCM2-,4HSEC),4H=    )
C     MESH POINTS IN CARBON INCLUDES CENTERLINE AND
C          BOUNDARY
      NM=NC-1
      NCM=NC-1
      NM3=NC-2
      ANC=NM
      HX=X/ANC
      HX2=HX*HX
      HW=.2*HX
      ANW=15.0/HW
      NPW=ANW
      NW=NC+NPW
      NCP=NC+1
      NWM=NW-1
C     DATA INPUT
      REWIND 30
      READ(30,101)(CSRC(I),DC(I),FX(I),I=1,6)
      READ(30,102)(CSRW(I),DW(I),I=1,6)
  101 FORMAT(3F10.5)
  102 FORMAT(2F10.5)
C    CALCULATION OF CONSTANTS
      S(1)=FS*FX(1)/2.0
      DO 11 I=2,NW
   11 S(I)=0.0
      DO 14 J=1,6
      DO 13 K=1,NM
      ALPHA(J,K)=DC(J)/HX
      BETA(J,K)=2.0*(DC(J)/HX)+CSRC(J)*HX
   13 GAMMA(J,K)=DC(J)/HX
      ALPHA(J,NC)=DW(J)/HW
      BETA(J,NC)=(DW(J)/HW)+(DC(J)/HX)+0.5*CSRW(J)*HW+
     1     0.5*CSRC(J)*HX
      GAMMA(J,NC)=DC(J)/HX
      DO 15 K=NCP,NWM
      ALPHA(J,K)=DW(J)/HW
      BETA(J,K)=2.0*(DW(J)/HW)+CSRW(J)*HW
   15 GAMMA(J,K)=DW(J)/HW
      ALPHA(J,NW)=0.0
      BETA(J,NW)=2.0*(DW(J)/HW)
     1     +CSRW(J)*HW
   14 GAMMA(J,NW)=DW(J)/HW
```

```
C     CALCULATION OF FLUXES
      DO 60 J=1,6
      JP=J+1
      B(1)=BETA(J,1)
      C(2)=-GAMMA(J,2)/B(1)
      B(2)=BETA(J,2)-C(2)*(-ALPHA(J,1)-GAMMA(J,1))
      DO 80 I=3,NW
      IM=I-1
      C(I)=-GAMMA(J,I)/B(IM)
      B(I)=BETA(J,I)-C(I)*(-ALPHA(J,IM))
   80 CONTINUE
      Z(1)=S(1)
      DO 50 K=2,NW
      KM=K-1
   50 Z(K)=S(K)-C(K)*Z(KM)
      PHI(J,NW)=Z(NW)/B(NW)
      DO 55 K=1,NWM
      KM=NW-K
      KP=KM+1
   55 PHI(J,KM)=(Z(KM)+ALPHA(J,KM)*PHI(J,KP))/B(KM)
      PHI(J,1)=(Z(1)+(ALPHA(J,1)+GAMMA(J,1))*PHI(J,2))/B(1)
      IF(J.EQ.6) GO TO 60
C     CALCULATION OF SOURCES FOR NEXT ENERGY GROUP
      S(1)=FS*FX(JP)/2.0+CSRC(J)*HX*PHI(J,1)
      DO 45 M=2,NCM
   45 S(M)=CSRC(J)*HX*PHI(J,M)
       S(NC)=(.5*CSRC(J)*HX+.5*CSRW(J)*HW)*PHI(J,NC)
      DO 46 M=NCP,NW
   46 S(M)=CSRW(J)*HW*PHI(J,M)
   60 CONTINUE
      WRITE(61,302)
  302 FORMAT(1HO,'FLUX PRINTED EVERY FIFTH SPACE POINT')
      WRITE(61,303)HX,HW
  303 FORMAT(1HO,'SPACING IN CARBON (CM)',F10.5,3X,
     1      'SPACING IN WATER(CM)',F10.5)
      WRITE(61,299)(KK,KK=1,6)
  299 FORMAT(1HO,'GROUP',1X,I2,7X,I2,9X,I2,9X,I2,9X,I2,
     1      9X,I2)
      WRITE(61,301)((PHI(J,K),J=1,6),K=1,NW,5)
  301 FORMAT(6E11.4)
      WRITE(61,202)
  202 FORMAT(1HO,'TRY NEW THICKNESS OR SPACING?')
      READ(60,203)JJJ
  203 FORMAT(A3)
      IF(JJJ.EQ.3HYES)GO TO 10
      END
```

Table D.1. SLAB central spectrum group fluxes for various graphite thicknesses.

Fluxes normalized to $\int_0^\infty \phi \, du = 1$ for various graphite thicknesses in inches (cm).

Group	6 (15.24)	8 (20.32)	10 (25.40)	12 (30.48)	14 (35.56)	16 (40.64)	18 (45.72)
1	0.2653	0.2270	0.1996	0.1802	0.1664	0.1561	0.1483
2	0.1165	0.1028	0.0915	0.0831	0.0823	0.0721	0.0685
3	0.0489	0.0448	0.0406	0.0370	0.0343	0.0322	0.0307
4	0.1020	0.1040	0.0993	0.0930	0.0872	0.0823	0.0784
5	0.0507	0.0555	0.0554	0.0532	0.0505	0.0480	0.0459
6	0.4166	0.4659	0.5137	0.5534	0.5848	0.6094	0.6282

Appendix E

The diffusion equation for spherical geometry:

$$-\frac{1}{r^2}\frac{d}{dr}\left[r^2 D\ \frac{d\phi(r)}{dr}\right] + \Sigma_R(r)\,\phi(r) = Q$$

Multiply by $4\pi r^2$ and integrate from $r_{k-\frac{1}{2}}$ to $r_{k+\frac{1}{2}}$:

$$-4\pi \int_{r_{k-\frac{1}{2}}}^{r_{k+\frac{1}{2}}} \frac{d}{dr}\left[r^2 D\ \frac{d\phi(r)}{dr}\right] dr + 4\pi \int_{r_{k-\frac{1}{2}}}^{r_{k+\frac{1}{2}}} r^2 \Sigma_R\,\phi(r)\,dr$$

$$= 4\pi \int_{r_{k-\frac{1}{2}}}^{r_{k+\frac{1}{2}}} r^2 Q\,dr$$

The above equation transforms into the difference equation:

$$-4\pi r^2_{k+\frac{1}{2}} D_{k+\frac{1}{2}}(\phi_{k+1} - \phi_k)/k+\tfrac{1}{2} \;+\; 4\pi r^2_{k-\frac{1}{2}} D_{k-\frac{1}{2}}(\phi_k - \phi_{k-\frac{1}{2}})/k-\tfrac{1}{2}$$

$$+ (4\pi\phi_k/3)(\Sigma_{R_{k+\frac{1}{2}}}(r^3_{k+\frac{1}{2}} - r^3_k) + \Sigma_{R_{k-\frac{1}{2}}}(r^3_k - r^3_{k-\frac{1}{2}})) =$$

$$= (4\pi/3)(r^3_{k+\frac{1}{2}} - r^3_k)\,Q_{k+\frac{1}{2}} + (4\pi/3)(r^3_k - r^3_{k-\frac{1}{2}})\,Q_{k-\frac{1}{2}} + FS = S_k(2)$$

where

$$Q_{k+\frac{1}{2}} = \sum_{j=i-5}^{i} \phi_{j,k}\,\Sigma_{s_{j,k+\frac{1}{2}}}$$

$$Q_{k-\frac{1}{2}} = \sum_{j=i-5}^{i} \phi_{j,k}\,\Sigma_{s_{j,k-\frac{1}{2}}}$$

$$FS = 4\pi(RB)^2 \text{(fission fraction)} \qquad \text{for } k = NU \text{ only}$$

The equation can be rewritten to account for several energy groups (for group i):

$$-4\pi r^2_{k+\frac{1}{2}} D_{i,k+\frac{1}{2}} (\phi_{i,k+1} - \phi_{i,k})/k+\tfrac{1}{2} + 4\pi r^2_{k-\frac{1}{2}} D_{i,k-\frac{1}{2}} (\phi_{i,k} - \phi_{i,k-1})/k-\tfrac{1}{2}$$

$$+ (4\pi \phi_{i,k}/3)(\Sigma_{R_{i,k+\frac{1}{2}}} (r^3_{k+\frac{1}{2}} - r^3_k) + \Sigma_{R_{i,k-\frac{1}{2}}} (r^3_k - r^3_{k-\frac{1}{2}})) = S_{i,k}$$

Collect terms containing the same flux:

$$(-4\pi r^2_{k+\frac{1}{2}} D_{i,k+\frac{1}{2}}/k+\tfrac{1}{2})\,\phi_{i,k+1} + (4\pi r^2_{k+\frac{1}{2}} D_{k+\frac{1}{2}}/k+\tfrac{1}{2} + 4\pi r^2_{k-\frac{1}{2}} D_{k-\frac{1}{2}}/k-\tfrac{1}{2}$$

$$+ (4\pi/3)\,\Sigma_{R_{i,k+\frac{1}{2}}} (r^3_{k+\frac{1}{2}} - r^3_k) + (4\pi/3)\,\Sigma_{R_{i,k-\frac{1}{2}}} (r^3_k - r^3_{k-\frac{1}{2}}))\,\phi_{i,k}$$

$$+ (-4\pi r^2_{k-\frac{1}{2}} D_{i,k-\frac{1}{2}}/k-\tfrac{1}{2})\,\phi_{i,k-\frac{1}{2}} = S_{i,k}$$

The fast spectrum facility has five regions:

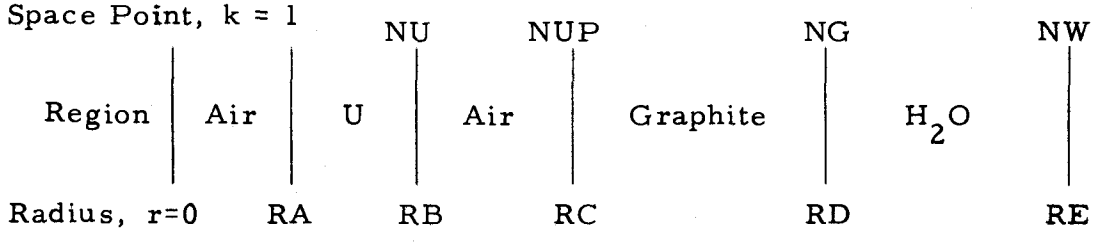

The boundary conditions are that the current is zero at $k = 1$ and that the flux is zero at $k = NW$. Let the values of the constants be for the region to the left of the mesh point as follows:

$$D_{i,k+\frac{1}{2}} = D_{i,k+1} \qquad D_{i,k-\frac{1}{2}} = D_{i,k}$$

$$\Sigma_{R_{i,k+\frac{1}{2}}} = \Sigma_{R_{i,k+1}} \qquad \Sigma_{R_{k,k-\frac{1}{2}}} = \Sigma_{R_{i,k}}$$

$$k+\tfrac{1}{2} = h_{k+1} \qquad k-\tfrac{1}{2} = h_{k}$$

$$(-4\pi r^2_{k+\frac{1}{2}} D_{i,k+1}/h_{k+1})\,\phi_{i,k+1} + (4\pi r^2_{k+\frac{1}{2}} D_{i,k+1}/h_{k+1}$$

$$+ 4\pi r^2_{k-\frac{1}{2}} D_{i,k}/h_k + (4\pi/3)\Sigma_{R_{i,k+1}} (r^3_{k+\frac{1}{2}} - r^3_k)$$

$$+ 4\pi/3)\Sigma_{R_{i,k}} (r^3_k - r^3_{k-\frac{1}{2}}))\,\phi_{i,k} + (-4\pi r^2_{k-\frac{1}{2}} D_{i,k}/h_k)\,\phi_{i,k-1} = S_{i,k}$$

Let:

$$\alpha_{i,k} = 4\pi r^2_{k+\frac{1}{2}} D_{i,k+1}/h_{k+1}$$

$$\beta_{i,k} = 4\pi r^2_{k+\frac{1}{2}} D_{i,k+1}/h_{k+1} + 4\pi r^2_{k-\frac{1}{2}} D_{i,k}/h_k$$

$$+ (4\pi/3)(\Sigma_{R_{i,k+1}} (r^3_{k+1} - r^3_k) + \Sigma_{R_{i,k}} (r^3_k - r^3_{k-\frac{1}{2}}))$$

$$\gamma_{i,k} = 4\pi r^2_{k-\frac{1}{2}} D_{i,k}/h_k$$

Then in general:

$$-\alpha_{i,k}\phi_{i,k+1} + \beta_{i,k}\phi_{i,k} - \gamma_{i,k}\phi_{i,k-1} = S_{i,k}$$

Applying the first boundary condition, $\phi_{i,NW} = 0$, the N-1 equation is:

$$\beta_{i,N-1}\phi_{i,N-1} - \gamma_{i,N-1}\phi_{i,N-2} = S_{i,N-1}$$

To apply the second boundary condition that the current at $r = RA$ is zero, the diffusion equation is integrated from $r = RA$ to $r = RA+h/2$ and the current is set equal to zero at $r = RA$.

$$-4\pi \int_{RA}^{RA+h/2} \frac{d}{dr}\left(r^2 D \frac{d\phi(r)}{dr}\right) dr + 4\pi \int_{RA}^{RA+h/2} r^2 \Sigma_R \phi(r)\, dr + 4\pi \int_{RA}^{RA+h/2} r^2 Q\, dr$$

$$-4\pi r^2 D \left.\frac{d\phi}{dr}\right|_{RA}^{RA+h/2} + 4\pi \int_{RA}^{RA+h/2} r^2 \Sigma_R \phi(r)\, dr = 4\pi \int_{RA}^{RA+h/2} r^2 Q\, dr$$

but, $D \left.\frac{d\phi}{dr}\right|_{RA} = 0$, so the difference equations then become:

$$-4\pi D_{i,2}(RA^2/h + RA + h/4)(\phi_{i,2} - \phi_{i,1})$$
$$+ (4\pi\phi_{i,1}/3)(\Sigma_{R_{i,2}}((R_A + h/2)^3 - RA^3)) = S_{i,1}$$

Collect the terms containing the same flux:

$$-4\pi D_{i,2}(RA^2/h + RA + h/4)\phi_{i,2} + (4\pi/3)(\Sigma_{R_{i,2}}((RA+h/2)^3 - RA^3)$$
$$+ 4\pi D_{i,2}(2RA^2/h + 4RA + 2h))\phi_{i,1} = S_{i,1}$$

Let:

$$\alpha_{i,1} = 4\pi D_{i,2}(RA^2/h + RA + h/4)$$

$$\beta_{i,1} = (4\pi/3)(\Sigma_{R_{i,2}}((RA + h/2)^3 - RA^3)) + 4\pi D_{i,2}(RA^2/h + RA + h/4)$$

So for $k = 1$:

$$-\alpha_{i,1}\phi_{i,2} + \beta_{i,1}\phi_{i,1} = S_{i,1}$$

where $S_{i,1} = \sum_{j=i-5}^{i-1} ((4\pi\phi_{j,1}/3)(\Sigma_{s,j}((RA + h/2)^3 - RA^3))$

The α's, β's, and γ's are in a form that can be put into the matrix equation on page 80. Program FASTSPEC, which solves this matrix equation for the fluxes at the mesh points, is listed on the next several pages.

```
      PROGRAM FASTSPEC
C     SIXTEEN GROUP DIFFUSION THEORY REPRESENTATION OF
C          NEUTRON SPECTRUM OF URANIUM SPHERE INSIDE
C          GRAPHITE HOHLRAUM BACKED WITH WATER
C          (200 MESH POINTS MAXIMUM)
      DIMENSION ALPHA(16,200), BETA(16,200), GAMMA(16,200),
     1     B(200), C(200), DU(16), DG(16), DW(16), URS(16),
     2     USS(5,16), GRS(16), GSS(16), WRS(16), WSS(5,16),
     3     S(200), Z(200), PHI(16,200),FX(16)
   10 WRITE(61,100)
  100 FORMAT(1HO,'RADII OF MATERIALS & NUMBER OF MESH PTS')
      RA=TTYIN(4HURAN,4HIUM ,4HINNE,4HR RA,4HDIUS,4H=    )
      RB=TTYIN(4HOUTE,4HR RA,4HDIUS,4H=    )
      NHU=TTYIN(4H# OF,4HMESH,4H PTS,4H=    )
      RC=TTYIN(4HGRAP,4HHITE,4H INN,4HER R,4HADIU,4HS=   )
      RD=TTYIN(4HOUTE,4HR RA,4HDIUS,4H=    )
      NHG=TTYIN(4H# OF,4HMESH,4H PTS,4H=    )
      RE=TTYIN(4HWATE,4HR OU,4HTER ,4HRADI,4HUS= )
      NHW=TTYIN(4H# OF,4HMESH,4H PTS,4H=    )
      WRITE(61,101)
  101 FORMAT(1HO,'FISSION SOURCE NORMALIZED TO '
     1     '1 NEUT/CM2-SEC')
      NHUM=NHU-1
      ANHU=NHUM
      HU=(RB-RA)/ANHU
      NHGM=NHG-1
      ANHG=NHGM
      HG=(RD-RC)/ANHG
      ANHW=NHW
      HW=(RE-RD)/ANHW
      NU=NHU
      NG=NU+NHG
      NW=NG+NHW
      NUM=NU-1
      NUP=NU+1
      FOP=4.*3.141
      NUP2=NU+2
      NGM=NG-1
      NWM=NW-1
      NWM2=NW-2
      NGP=NG+1
      ND=NW-NUP
      NDP2=ND+2
C     DATA INPUT
      REWIND 30
      READ(30,102)(DU(I),DG(I), DW(I),I=1,16)
      READ(30,103)(URS(I),USS(1,I),USS(2,I),USS(3,I),
     1    USS(4,I),USS(5,I),I=1,16)
      READ(30,104)(GRS(I),GSS(I),I=1,16)
      READ(30,105)(WRS(I),WSS(1,I),WSS(2,I),WSS(3,I),
     1     WSS(4,I),WSS(5,I),I=1,16)
      READ(30,106)(FX(I), I=1,16)
  102 FORMAT(3F10.5)
```

```
  103 FORMAT(6F10.5)
  104 FORMAT(2F10.5)
  105 FORMAT(6F10.5)
  106 FORMAT(F10.5)
      DA=(4./9.)*(RC**3-RB**3)/(RC*RC+RB*RB)
C     CALCULATION OF CONSTANTS
      DO 11 I=1,NUM
   11 S(I)=0.0
      S(NU)=FOP*RB*RB*FX(1)
      DO 12 I=NUP,NW
   12 S(I)=0.0
      DO 20 J=1,16
      ALPHA(J,1)=FOP*DU(J)*(RA*RA/HU+RA+.25*HU)
      BETA(J,1)=(FOP/3)*(URS(J)*((RA+HU/2)**3-RA**3))
     1      +FOP*DU(J)*(RA*RA/HU+RA+.25*HU)
      RM=RA+0.5*HU
      RP=RA+1.5*HU
      DO 13 K=2,NUM
      ALPHA(J,K)=FOP*RP*RP*DU(J)/HU
      BETA(J,K)=(FOP*DU(J)/HU)*(RP*RP+RM*RM)+(FOP/3)*(RP**3
     1      -RM**3)*URS(J)
      GAMMA(J,K)=FOP*RM*RM*DU(J)/HU
      RM=RM+HU
   13 RP=RP+HU
      HA=(RC-RB)
      RH=(RC+RB)*.5
      ALPHA(J,NU)=FOP*RH*RH*DA/HA
      BETA(J,NU)=(FOP*DA/HA)*(RH*RH)+(FOP*DU(J)/HU)*(RM*RM)
     1      +(FOP/3)*(URS(J)*(RB**3-RM**3))
      GAMMA(J,NU)=FOP*RM*RM*DU(J)/HU
      RP=RC+.5*HG
      ALPHA(J,NUP)=FOP*RP*RP*DG(J)/HG
      BETA(J,NUP)=(FOP*DG(J)/HG)*(RP*RP)+(FOP*DA/HA)*(RH*RH)
     1      +(FOP/3)*(GRS(J)*(RP**3-RC**3))
      GAMMA(J,NUP)=FOP*DA*RH*RH/HA
      RM=RC+.5*HG
      RP=RC+1.5*HG
      DO 14 K=NUP2,NGM
      ALPHA(J,K)=FOP*RP*RP*DG(J)/HG
      BETA(J,K)=(FOP*DG(J)/HG)*(RP*RP+RM*RM)+(FOP/3)*(RP**3
     1      -RM**3)*GRS(J)
      GAMMA(J,K)=FOP*RM*RM*DG(J)/HG
      RM=RM+HG
   14 RP=RP+HG
      RM=RD-.5*HG
      RP=RD+.5*HW
      ALPHA(J,NG)=FOP*RP*RP*DW(J)/HW
      BETA(J,NG)=(FOP*DW(J)/HW)*(RP*RP)+(FOP*DG(J)/HG)*(RM*
     1      RM)+(FOP/3)*(WRS(J)*(RP**3-RD**3)+GRS(J)*(RD**3
     1      -RM**3))
      GAMMA(J,NG)=FOP*DG(J)*RM*RM/HG
      RM=RD+.5*HW
      RP=RD+1.5*HW
```

```
      DO 15 K=NGP,NWM
      ALPHA(J,K)=FOP*RP*RP*DW(J)/HW
      BETA(J,K)=(FOP*DW(J)/HW)*(RP*RP+RM*RM)+(FOP/3)*(RP**3-
     1      RM**3)*WRS(J)
      GAMMA(J,K)=FOP*RM*RM*DW(J)/HW
      RM=RM+HW
   15 RP=RP+HW
   20 CONTINUE
C     CALCULATION OF FLUXES
      DO 60 J=1,16
      JP=J+1
      B(1)=BETA(J,1)
      DO 30 I=2,NWM
      IM=I-1
      C(I)=-GAMMA(J,I)/B(IM)
      B(I)=BETA(J,I)-C(I)*(-ALPHA(J,IM))
   30 CONTINUE
      Z(1)=S(1)
      DO 50 K=2,NWM
      KM=K-1
   50 Z(K)=S(K)-C(K)*Z(KM)
      PHI(J,NWM)=Z(NWM)/B(NWM)
      DO 55 K=1,NWM2
      KM=NWM-K
      KP=KM+1
   55 PHI(J,KM)=(Z(KM)+ALPHA(J,KM)*PHI(J,KP))/B(KM)
      IF(J.EQ.16) GO TO 60
C     CALCULATION OF SOURCES FOR NEXT ENERGY GROUP
      S(1)=0.0
      DO 38 KM=1,5
      KK=KM-1
      KL=J-KK
      IF(KL.EQ.0)GO TO 39
   38 S(1)=S(1)+(FOP/3)*PHI(KL,1)*USS(KM,KL)*((RA+HU/2)**3
     1      -RA**3)
   39 RM=RA+.5*HU
      RP=RA+1.5*HU
      DO 40 K=2,NUM
      S(K)=.0
      DO 41 KM=1,5
      KK=KM-1
      KL=J-KK
      IF(KL.EQ.0) GO TO 42
   41 S(K)=S(K)+(FOP/3)*PHI(KL,K)*USS(KM,KL)*(RP**3-RM**3)
   42 RM=RM+HU
   40 RP=RP+HU
      A=0.0
      DO 43 KM=1,5
      KK=KM-1
      KL=J-KK
      IF(KL.EQ.0) GO TO 44
   43 A=A+(FOP/3)*PHI(KL,NU)*USS(KM,KL)*(RB**3-RM**3)
   44 S(NU)=A+FX(JP)*FOP*RB*RB
```

```
      RM=RC
      RP=RC+.5*HG
      A=0.0
      DO 45 KM=1,5
      KK=KM-1
      KL=J-KK
      IF(KL.EQ.0) GO TO 46
   45 A=A+(FOP/3)*PHI(KL,NUP)*USS(KM,KL)*(RP**3-RC**3)
   46 S(NUP)=A
      RM=RC+.5*HG
      RP=RP+1.5*HG
      DO 47 K=NUP2,NGM
      S(K)=(FOP/3)*(PHI(J,K)*GSS(J)*(RP**3-RM**3))
      RM=RM+HG
   47 RP=RP+HG
      RM=RD-.5*HG
      RP=RD+.5*HW
      A=(FOP/3)*(PHI(J,NG)*GSS(J)*(RD**3-RM**3))
      B=0.0
      DO 48 KM=1,5
      KK=KM-1
      KL=J-KK
      IF(KL.EQ.0) GO TO 49
   48 B=B+(FOP/3)*PHI(KL,NG)*(WSS(KM,KL)*(RP**3-RD**3))
   49 S(NG)=A+B
      RM=RD+.5*HW
      RP=RD+1.5*HW
      DO 59 K=NGP,NW
      S(K)=.0
      DO 52 KM=1,5
      KK=KM-1
      KL=J-KK
      IF(KL.EQ.0) GO TO 53
   52 S(K)=S(K)+(FOP/3)*PHI(KL,K)*WSS(KM,KL)*(RP**3-RM**3)
   53 RM=RM+HW
   59 RP=RP+HW
   60 CONTINUE
      DO 309 J=1,16
      WRITE(61,304)J
  304 FORMAT(1HO,'GROUP ',I3)
      WRITE(61,305)(PHI(J,KK),KK=1,NW,5)
  305 FORMAT(1H ,4E12.4)
  309 CONTINUE
      WRITE(61,310)
  310 FORMAT(1HO,'TRY NEW THICKNESS OR SPACING?')
      READ(60,311) MMM
  311 FORMAT(A3)
      IF(MMM.EQ.3HYES) GO TO 10
      END
```

The data for FASTSPEC is input using a data file called DATA2, which is listed on pages 100 and 101. The data is taken from the LASL 16-group cross section set (15). The energy groups are:

Group	Energy Range	Lethargy Interval
1	3--10 MeV	1.204
2	1.4--3 MeV	0.762
3	0.9--1.4 MeV	0.442
4	0.4--0.9 MeV	0.811
5	0.1--0.4 MeV	1.386
6	17--100 keV	1.772
7	3--17 keV	1.735
8	0.55--3 keV	1.696
9	100--550 eV	1.705
10	30--100 eV	1.204
11	10--30 eV	1.099
12	3--10 eV	1.204
13	1--3 eV	1.099
14	0.4--1 eV	0.916
15	0.1--0.4 eV	1.386
16	Thermal	

DATA2 lists five sets of 16 rows. Each set lists the values for energy groups one through sixteen, one group to a row. The first set has three columns with the diffusion coefficients of uranium, graphite, and water respectively. The second set lists for uranium and the fourth set for water the removal cross section in the first column with columns two through six containing respectively the down-scattering cross sections from one to five groups lower in energy. Column one of the third set contains the removal and the second column the down-scatter cross sections for graphite. The

last set of rows contains the fission fractions.

Starting on page 102 is a sample output from FASTSPEC. The flux is printed for every fifth mesh point starting with the first.

```
FIN,DATA2
]TTP
```

1.736	3.17	3.94			
1.58	2.75	3.21			
1.53	1.73	1.69			
1.33	1.33	1.37			
.848	1.09	1.03			
.579	.918	.729			
.496	.88	.614			
.462	.898	.587			
.314	.898	.586			
.118	.898	.586			
.107	.898	.586			
.0585	.88	.576			
.718	.88	.575			
.686	.88	.574			
.600	.88	.569			
.44	.88	.558			
.132	.0158	.022	.0379	.0254	.00335
.123	.0168	.046	.0306	.00431	.0
.077	.0383	.0263	.00479	.0	.0
.035	.0239	.00384	.0	.0	.0
.012	.00384	.0	.0	.0	.0
.027	.00478	.0	.0	.0	.0
.038	.00287	.0	.0	.0	.0
.102	.00287	.0	.0	.0	.0
.536	.0024	.0	.0	.0	.0
2.404	.00287	.0	.0	.0	.0
2.701	.00287	.0	.0	.0	.0
5.271	.00287	.0	.0	.0	.0
.035	.00287	.0	.0	.0	.0
.057	.00287	.0	.0	.0	.0
.126	.0024	.0	.0	.0	.0
.325	.0	.0	.0	.0	.0

.0439	.044				
.0266	.0268				
.073	.0731				
.051	.0516				
.037	.037				
.034	.0342				
.036	.0366				
.037	.0366				
.037	.0366				
.052	.0515				
.057	.0565				
.052	.0526				
.058	.0578				
.069	.0694				
.046	.0458				
.000273	.0				
.112	.0657	.016	.016	.00964	.00328
.135	.0526	.0462	.0278	.00777	.00134
.247	.150	.0720	.0201	.00348	.000803
.271	.208	.0523	.00884	.00147	.000368
.337	.282	.0458	.00783	.00145	.000301
.496	.411	.070	.0125	.00198	.000837
.613	.502	.0903	.014	.00407	.00204
.654	.537	.0817	.0241	.00817	.00348
.653	.459	.129	.0455	.0129	.00643
.793	.532	.182	.0522	.0155	.0104
.826	.582	.162	.0481	.0241	.00803
.808	.542	.158	.0791	.0259	.0
.844	.51	.247	.0831	.0	.0
.914	.685	.223	.0	.0	.0
.759	.749	.0	.0	.0	.0
.019	.0	.0	.0	.0	.0
.204					
.344					
.168					
.180					
.090					
.014					
.0					
.0					
.0					
.0					
.0					
.0					
.0					
.0					
.0					
.0					

```
#EQUIP,30=DATA2
#FORTRAN,I=FASTSPEC,R


 NO ERRORS FOR FASTSPEC
RUN



RADII OF MATERIALS & NUMBER OF MESH PTS
URANIUM INNER RADIUS=   7.25
OUTER RADIUS=   12.25
# OFMESH PTS=   41
GRAPHITE INNER RADIUS=  26.0
OUTER RADIUS=   56.5
# OFMESH PTS=   30
WATER OUTER RADIUS= 71.5
# OFMESH PTS=   75

FISSION SOURCE NORMALIZED TO 1 NEUT/CM2-SEC

GROUP   1
  9.3273E-02  9.4588E-02  9.8319E-02  1.0427E-01
  1.1236E-01  1.2261E-01  1.3515E-01  1.5015E-01
  1.6785E-01  3.5368E-02  1.6208E-02  7.5662E-03
  3.5464E-03  1.6079E-03  6.0592E-04  5.0172E-04
  4.1513E-04  3.4308E-04  2.8303E-04  2.3286E-04
  1.9082E-04  1.5547E-04  1.2556E-04  1.0010E-04
  7.8205E-05  5.9157E-05  4.2326E-05  2.7168E-05
  1.3203E-05       0E 00

GROUP   2
  2.0199E-01  2.0474E-01  2.1251E-01  2.2490E-01
  2.4174E-01  2.6305E-01  2.8905E-01  3.2009E-01
  3.5667E-01  1.2762E-01  7.4380E-02  4.2573E-02
  2.3599E-02  1.2055E-02  4.6176E-03  3.7180E-03
  2.9932E-03  2.4085E-03  1.9361E-03  1.5538E-03
  1.2435E-03  9.9076E-04  7.8386E-04  6.1330E-04
  4.7134E-04  3.5159E-04  2.4875E-04  1.5837E-04
  7.6580E-05       0E 00
```

```
GROUP    3
  1.8168E-01   1.8271E-01   1.8561E-01   1.9015E-01
  1.9616E-01   2.0350E-01   2.1206E-01   2.2176E-01
  2.3250E-01   8.5142E-02   4.8067E-02   2.7372E-02
  1.5209E-02   7.7210E-03   2.6970E-03   1.9970E-03
  1.4909E-03   1.1218E-03   8.4991E-04   6.4767E-04
  4.9565E-04   3.8009E-04   2.9117E-04   2.2179E-04
  1.6678E-04   1.2228E-04   8.5395E-05   5.3874E-05
  2.5912E-05        0E 00

GROUP    4
  4.9839E-01   4.9806E-01   4.9707E-01   4.9532E-01
  4.9262E-01   4.8868E-01   4.8310E-01   4.7543E-01
  4.6511E-01   2.1025E-01   1.2083E-01   6.9219E-02
  3.8490E-02   1.9250E-02   5.9782E-03   4.2271E-03
  3.0195E-03   2.1790E-03   1.5881E-03   1.1680E-03
  8.6575E-04   6.4546E-04   4.8253E-04   3.6002E-04
  2.6612E-04   1.9247E-04   1.3302E-04   8.3307E-05
  3.9895E-05        0E 00

GROUP    5
  8.2764E-01   8.2430E-01   8.1482E-01   7.9977E-01
  7.7941E-01   7.5376E-01   7.2270E-01   6.8592E-01
  6.4301E-01   4.1086E-01   2.6464E-01   1.6084E-01
  9.1956E-02   4.5893E-02   1.2785E-02   8.1994E-03
  5.3598E-03   3.5732E-03   2.4293E-03   1.6829E-03
  1.1860E-03   8.4803E-04   6.1279E-04   4.4500E-04
  3.2208E-04   2.2924E-04   1.5661E-04   9.7310E-05
  4.6390E-05        0E 00

GROUP    6
  4.6165E-01   4.6335E-01   4.6816E-01   4.7574E-01
  4.8593E-01   4.9861E-01   5.1379E-01   5.3151E-01
  5.5187E-01   5.3442E-01   4.0127E-01   2.6565E-01
  1.5908E-01   8.0357E-02   2.0366E-02   1.1168E-02
  6.4080E-03   3.8468E-03   2.4099E-03   1.5688E-03
  1.0555E-03   7.2926E-04   5.1391E-04   3.6643E-04
  2.6171E-04   1.8451E-04   1.2520E-04   7.7456E-05
  3.6832E-05        0E 00

GROUP    7
  3.3389E-01   3.3781E-01   3.4892E-01   3.6661E-01
  3.9064E-01   4.2107E-01   4.5818E-01   5.0247E-01
  5.5463E-01   6.1517E-01   5.1097E-01   3.6351E-01
  2.2796E-01   1.1784E-01   3.0045E-02   1.5178E-02
  8.0187E-03   4.4505E-03   2.5994E-03   1.5950E-03
  1.0233E-03   6.8151E-04   4.6718E-04   3.2639E-04
  2.2968E-04   1.6022E-04   1.0792E-04   6.6440E-05
  3.1507E-05        0E 00
```

GROUP 8

1.5379E-01	1.5973E-01	1.7688E-01	2.0519E-01
2.4571E-01	3.0050E-01	3.7271E-01	4.6671E-01
5.8841E-01	7.4232E-01	6.6394E-01	5.0089E-01
3.2775E-01	1.7426E-01	4.6299E-02	2.2889E-02
1.1625E-02	6.1241E-03	3.3732E-03	1.9520E-03
1.1873E-03	7.5615E-04	5.0031E-04	3.4032E-04
2.3486E-04	1.6158E-04	1.0781E-04	6.5965E-05
3.1175E-05	0E 00		

GROUP 9

3.4436E-03	4.3142E-03	7.3061E-03	1.4049E-02
2.8442E-02	5.9018E-02	1.2418E-01	2.6361E-01
5.6300E-01	8.8578E-01	8.4944E-01	6.7396E-01
4.5797E-01	2.5042E-01	6.9611E-02	3.5229E-02
1.7923E-02	9.2734E-03	4.9339E-03	2.7261E-03
1.5750E-03	9.5385E-04	6.0376E-04	3.9617E-04
2.6600E-04	1.7941E-04	1.1808E-04	7.1620E-05
3.3682E-05	0E 00		

GROUP 10

3.6767E-06	4.6243E-06	7.9079E-06	1.5724E-05
3.8709E-05	1.8348E-04	1.9580E-03	2.8225E-02
4.3005E-01	7.9616E-01	8.0260E-01	6.5850E-01
4.5852E-01	2.5472E-01	7.0023E-02	3.4978E-02
1.7628E-02	9.0051E-03	4.6986E-03	2.5262E-03
1.4113E-03	8.2401E-04	5.0331E-04	3.2005E-04
2.0950E-04	1.3863E-04	9.0018E-05	5.4121E-05
2.5328E-05	0E 00		

GROUP 11

4.1563E-09	5.5211E-09	1.5352E-08	1.4841E-07
2.7194E-06	5.5315E-05	1.1424E-03	2.3715E-02
4.9408E-01	9.4242E-01	9.8172E-01	8.2667E-01
5.8687E-01	3.2976E-01	8.9366E-02	4.3893E-02
2.1819E-02	1.0998E-02	5.6474E-03	2.9744E-03
1.6195E-03	9.1799E-04	5.4366E-04	3.3579E-04
2.1440E-04	1.3911E-04	8.9060E-05	5.3044E-05
2.4693E-05	0E 00		

GROUP 12

2.3036E-12	3.1184E-12	9.8011E-12	1.0915E-10
2.1834E-09	7.7372E-08	1.0219E-05	2.4855E-03
6.5316E-01	1.3377E 00	1.4320E 00	1.2333E 00
8.9079E-01	5.0543E-01	1.3531E-01	6.5419E-02
3.2040E-02	1.5914E-02	8.0411E-03	4.1544E-03
2.2095E-03	1.2183E-03	7.0008E-04	4.1962E-04
2.6076E-04	1.6547E-04	1.0418E-04	6.1353E-05
2.8377E-05	0E 00		

```
GROUP  13
  9.0647E-01  9.1466E-01  9.3781E-01  9.7444E-01
  1.0238E 00  1.0855E 00  1.1597E 00  1.2469E 00
  1.3478E 00  1.7139E 00  1.7871E 00  1.5510E 00
  1.1323E 00  6.4684E-01  1.7219E-01  8.2482E-02
  3.9946E-02  1.9592E-02  9.7585E-03  4.9565E-03
  2.5821E-03  1.3889E-03  7.7610E-04  4.5178E-04
  2.7306E-04  1.6919E-04  1.0456E-04  6.0782E-05
  2.7903E-05       0E 00

GROUP  14
  8.4196E-01  8.5424E-01  8.8907E-01  9.4465E-01
  1.0204E 00  1.1166E 00  1.2345E 00  1.3759E 00
  1.5434E 00  2.0372E 00  2.1033E 00  1.8289E 00
  1.3426E 00  7.6915E-01  1.9963E-01  9.3190E-02
  4.4253E-02  2.1354E-02  1.0477E-02  5.2397E-03
  2.6828E-03  1.4144E-03  7.7253E-04  4.3880E-04
  2.5886E-04  1.5693E-04  9.5294E-05  5.4707E-05
  2.4928E-05       0E 00

GROUP  15
  7.9031E-01  8.2047E-01  9.0747E-01  1.0508E 00
  1.2553E 00  1.5307E 00  1.8921E 00  2.3602E 00
  2.9630E 00  4.1746E 00  4.3053E 00  3.7516E 00
  2.7681E 00  1.5942E 00  4.2526E-01  2.0092E-01
  9.5379E-02  4.5671E-02  2.2129E-02  1.0887E-02
  5.4625E-03  2.8103E-03  1.4914E-03  8.2046E-04
  4.6832E-04  2.7530E-04  1.6290E-04  9.1753E-05
  4.1331E-05       0E 00

GROUP  16
  1.6465E 00  1.8760E 00  2.5831E 00  3.9020E 00
  6.1278E 00  9.7829E 00  1.5744E 01  2.5458E 01
  4.1309E 01  6.1927E 01  6.5511E 01  6.0555E 01
  5.0020E 01  3.6673E 01  2.2977E 01  1.9210E 01
  1.5885E 01  1.3047E 01  1.0665E 01  8.6817E 00
  7.0357E 00  5.6689E 00  4.5303E 00  3.5762E 00
  2.7697E 00  2.0795E 00  1.4789E 00  9.4507E-01
  4.5805E-01       0E 00
TRY NEW THICKNESS OR SPACING?
NO



END OF FORTRAN EXECUTION
```

Table E.1. Central neutron spectrum calculated from FASTSPEC for a graphite thickness of 30.5 cm.

Group	$\int_{\Delta u} \phi \, du$	Flux Normalized to $\int_0^\infty \phi \, du = 1$	Normalized Flux Per Unit Lethargy
1	0.09327	0.03384	0.02811
2	0.2020	0.07330	0.09619
3	0.1817	0.06593	0.1492
4	0.4984	0.1809	0.2231
5	0.8276	0.3003	0.2167
6	0.4617	0.1675	0.09453
7	0.3339	0.1212	0.06986
8	0.1538	0.05581	0.03291
9	0.003444	0.00125	0.00073

Table E.2. Central neutron spectrum calculated from FASTSPEC for a graphite thickness of 35 cm.

Group	$\int_{\Delta u} \phi \, du$	Flux Normalized to $\int_0^\infty \phi \, du = 1$	Normalized Flux Per Unit Lethargy	% Change from 30.5 cm
1	0.09328	0.03366	0.02796	0.534
2	0.2022	0.07296	0.09575	0.457
3	0.1819	0.06564	0.14851	0.462
4	0.4991	0.1801	0.2221	0.448
5	0.8300	0.2995	0.2161	0.277
6	0.4653	0.1679	0.09475	0.233
7	0.3388	0.1223	0.07049	0.902
8	0.1572	0.05672	0.03344	1.61
9	0.003542	0.000128	0.00075	2.7

Table E.3. Central neutron spectrum calculated from FASTSPEC for a graphite thickness of 45 cm.

Group	$\int_{\Delta u} \phi \, du$	Flux Normalized to $\int_{o}^{\infty} \phi \, du = 1$	Normalized Flux Per Unit Lethargy	% Change from 30.5 cm
1	0.09329	0.03355	0.02787	0.854
2	0.2023	0.07275	0.09547	0.749
3	0.1820	0.06545	0.1481	0.737
4	0.4995	0.1796	0.2214	0.762
5	0.8314	0.2990	0.2157	0.461
6	0.4675	0.1681	0.09486	0.349
7	0.3418	0.1229	0.07084	1.40
8	0.1593	0.05729	0.03378	2.64
9	0.00361	0.00130	0.00076	4.11

Appendix F

The gold-197 foils taped to the glass flask were irradiated on June 25, 1974 for two hours at a reactor power of one megawatt. Let T = time since irradiation and t = duration of irradiation. The data from the coincidence count is listed below.

Sample	Mass (gm)	T (hr)	Count (min)	β Counts	Coin. Counts	γ Counts
1	0.0912	28.00	5	834,496	96,364	674,794
2	0.0913	28.08	5	827,123	98,727	680,095
3	0.240	28.17	5	973,986	90,701	1,432,711
4	0.2436	28.33	5	796,029	72,314	1,158,856
5	0.3066	29.08	5	709,325	59,631	1,203,877
6	0.305	29.17	5	650,101	53,925	1,047,904
7	0.3239	29.33	10	1,221,252	101,820	1,059,552
8	0.6110	29.58	10	1,520,740	90,690	1,402,607
9	0.6054	30.33	10	1,547,757	88,751	1,213,810
10	0.3212	30.50	10	1,177,868	93,426	1,997,922
11	0.3215	30.75	10	1,297,243	105,738	2,014,798
12	0.250	31.08	5	610,634	52,581	896,043
13	0.2459	31.25	5	747,016	67,475	1,017,488
14	0.2430	31.33	5	796,625	69,693	1,187,040
15	0.0875	31.42	5	713,615	83,829	562,647
16	0.0850	31.58	5	780,101	89,750	590,056
17	0.1750	31.67	5	647,634	65,290	767,594
18	0.1824	31.83	5	775,470	76,868	922,717
19	0.1850	31.92	5	925,150	93,155	1,101,691
20	0.1723	32.00	5	929,264	94,212	1,148,419
21	0.1729	33.75	10	651,260	61,734	829,413
22	0.1707	32.17	5	1,009,231	102,981	1,175,429
23	0.1710	32.25	5	876,364	88,233	1,026,487
24	0.2392	32.33	5	838,023	74,838	1,169,471
25	0.2388	32.50	5	566,688	46,574	881,691
26	0.1810	32.67	5	546,448	53,068	622,556
27	0.1720	32.75	5	503,561	50,263	591,988
28	0.1733	32.83	5	500,518	50,911	560,047
29	0.1684	34.00	10	203,776	19,971	264,616

Appendix F Table (continued)

Sample	Mass (gm)	T (hr)	Count (min)	β Counts	Coin. Counts	γ Counts
30	0.1651	32.92	5	463,828	47,159	535,396
31	0.1736	33.08	10	902,440	86,118	1,129,802
32	0.1823	33.25	5	560,124	55,696	670,740
33	0.6011	33.42	5	973,884	54,465	1,075,192
34	0.610	33.5	12	203,334	11,550	431,800
35	0.6092	34.17	5	1,639,624	92,846	1,418,196
36	0.6076	34.25	120	126,444	8,283	436,732
Background Count			120	18,765	1,194	226,489

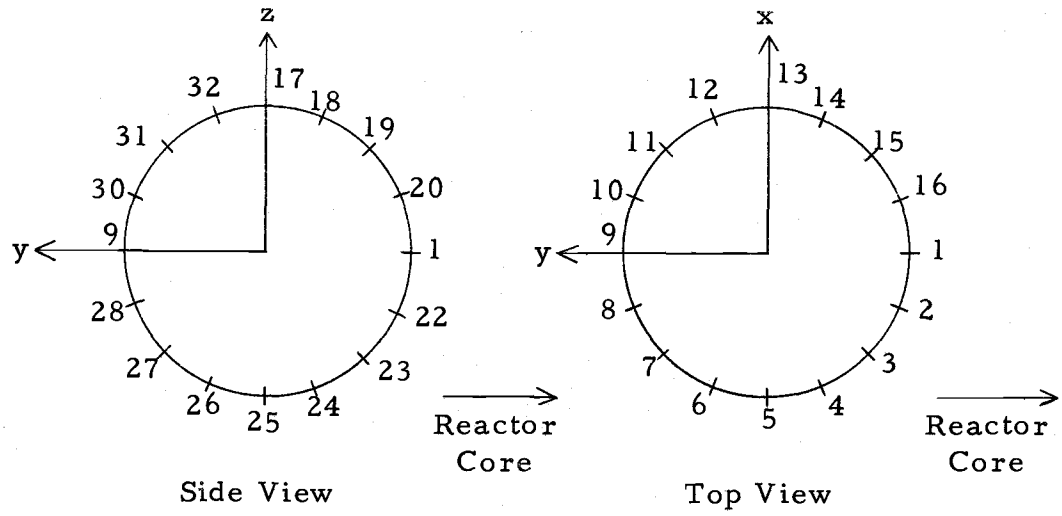

The diagrams above show the positions of the gold foils around the glass sphere. A right-handed, orthogonal coordinate system is used to identify the foil positions. The y-axis is parallel to the thermal column and directed out from the reactor core while the x and z axes are perpendicular to it. The x-axis is horizontal while the z-axis is directed vertically up. Foils numbered 21, 29, 33, and 34 are positioned on top of the graphite stack as is shown below. These foils determine the thermal neutron flux at various positions on the aluminum box.

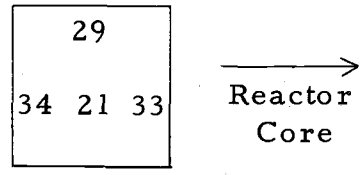

Numbers 35 and 36 are the bare and cadmium covered foils, respectively, for the cadmium ratio experiment. The position of these foils is on the floor of the hohlraum next to the wall nearest the thermal column.

$$\text{Absolute activity, } A = \frac{(\text{net } \beta \text{ counts})(\text{net } \gamma \text{ counts})}{\text{net coin. counts}}$$

Absolute activity corrected for the decay since the end of irradiation, $A_o = Ae^{\lambda T}$

$$\text{Absolute neutron flux, } \phi = \frac{(A_o)(\text{atomic mass})(1.128)(f)}{(N_o)(\text{foil mass})(\sigma)(1 - e^{-\lambda t})}$$

where $f = (1/N\sigma s)(1 - e^{-N\sigma s})$

and s is the thickness of the foil, N is the atom density and f is the foil self shielding factor.

A listing of the activities and fluxes of the various foils are given below.

Sample	$A \times 10^4$ (dis./sec)	$A_o \times 10^4$ (dis./sec)	$\phi \times 10^7$ (neutrons/cm^2-sec)
1	1.920	2.591	5.083
2	1.872	2.529	4.960
3	5.093	6.887	5.264
4	4.216	5.710	4.304
5	4.735	6.465	3.911
6	4.172	5.702	3.467
7	2.080	2.848	1.635
8	3.867	5.308	1.695
9	3.474	4.807	1.548
10	4.157	5.763	3.336

Sample	$A \times 10^4$ (dis./sec)	$A_o \times 10^4$ (dis./sec)	$\phi \times 10^7$ (neutrons/cm^2-sec)
11	4.080	5.671	3.281
12	3.431	4.786	3.517
13	3.719	5.197	3.881
14	4.486	6.275	4.739
15	1.569	2.197	4.488
16	1.681	2.358	4.957
17	2.506	3.518	3.648
18	3.070	4.317	4.300
19	3.615	5.088	4.999
20	3.744	5.274	5.552
21	1.423	2.043	2.143
22	3.808	5.374	5.709
23	3.366	4.755	5.042
24	4.329	6.120	4.693
25	3.537	5.010	3.848
26	2.103	2.984	2.994
27	1.944	2.761	2.911
28	1.803	2.563	2.682
29	0.4168	0.5999	0.6457
30	1.723	2.451	2.690
31	1.939	2.763	2.888
32	2.184	3.118	3.103
33	6.353	9.087	2.945
34	1.034	1.480	0.4734
35	8.296	11.96	3.830
36	0.0443	0.0639	0.0205

The radiation survey of the bulk shield tank for both reactor runs is tabulated on the next page. Then on the next page are the positions where the measurements are taken. The measurements over the top are at the water level and those around the sides are in the reactor bay at a four-foot height next to the concrete shielding around the bulk shield tank.

Position	Without Snorkel		With Snorkel[1]	
	γ mrem/hr	Neutron mrem/hr	γ mrem/hr	Neutron mrem/hr
1	19	4.9		
2	110	44	100	29
3	170	48	185	44
4	110	32	85	30
5	16	4.5		
6	80	29	85	29
7	100	37	115	35
8	70	26	75	30
9	29	14	40	15
10	31	19	50	17
11	30	15	45	14
12	3	0.78		
13	2	0.75		
14	0.8	0.35		
15	1	0.35		
16	0.8	0.18		
17	0.5	0.12		
18	0.6	0.16		
19	0.8	0.35		
20	0.9	0.4		
21	1	2.2		
22	0.75	0.55		
23	0.5	0.36		
24	0.5	0.4		

[1] The survey for the snorkel run included measurements for only the top of the tank since the snorkel should not affect the radiation fields around the sides.

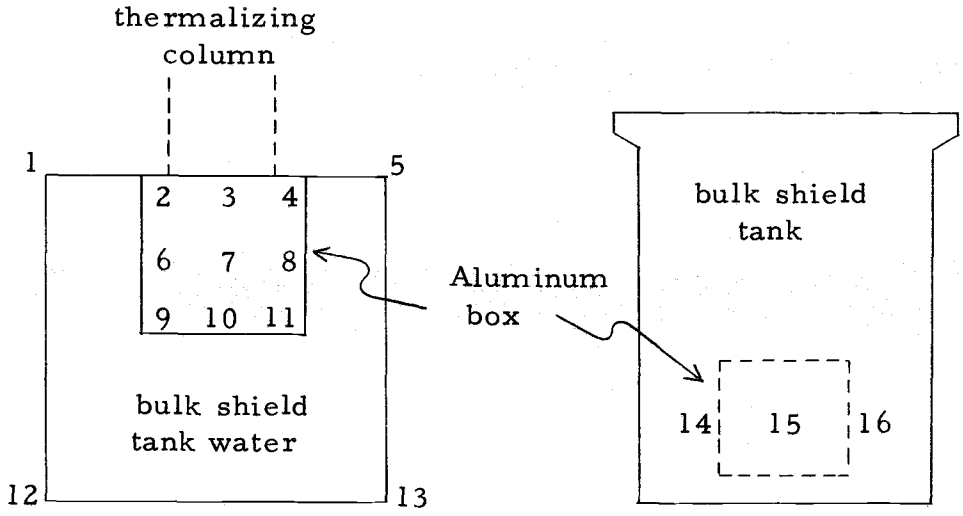

Top View

West Side

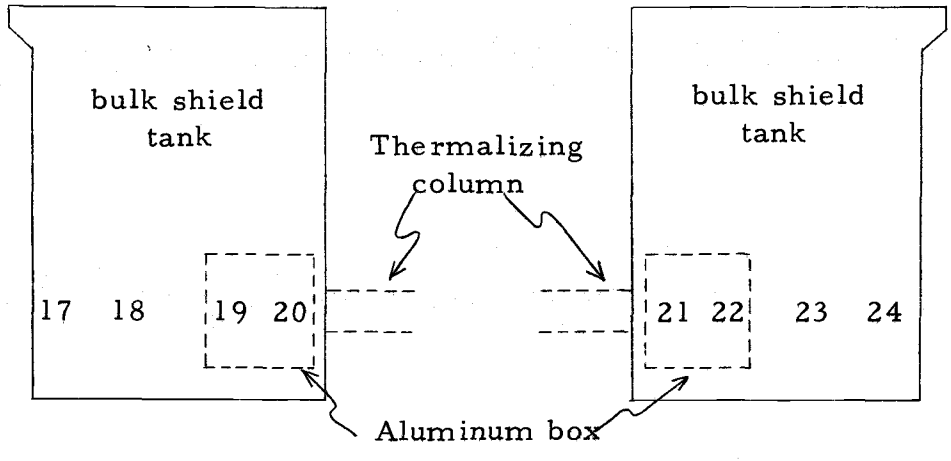

South Side

North Side